

Standardized Evaluation of Chondrocyte Inflammation Model with TNF alpha

Doctoral thesis
to obtain a doctorate (Dr. med.)
from the Faculty of Medicine
of the University of Bonn

Su Wang
Shandong/China
2025

Written with authorization of
the Faculty of Medicine of the University of Bonn

First reviewer: Prof. Frank A. Schildberg

Second reviewer: PD Dr. Matthias Stope

Day of oral examination: 17.12.2025

From the Clinic and Polyclinic for Orthopaedics and Trauma Surgery, University Hospital
Bonn

Table of contents

List of abbreviations	5
1. Introduction	7
2. Materials and methods	14
2.1 Materials	14
2.1.1 Instruments	14
2.1.2 Reagents	15
2.1.3 Buffers and solutions	17
2.2 Experimental design	18
2.3 Chondrocyte isolation	21
2.4 Passaging of chondrocytes	22
2.5 Establishment of a 3d chondrocyte inflammation pellets model	23
2.6 Analysis	24
2.6.1 RNA extraction, reverse transcription and real-time PCR	24
2.6.2 Histology: safranin-o fast green staining	25
2.6.3 Enzyme-linked immunosorbent assay (ELISA) of pellet medium	26
2.6.4 Biochemistry analysis	26
2.7 Statistics	27
3. Results	28
3.1 Results of experiment one	28
3.1.1 Gene expression	28
3.1.2 Analysis of glycosaminoglycans and ELISA	35
3.2 Results of experiment two	36
3.2.1 Gene expression	37
3.2.2 Medium analysis of IL-6, nitric oxide and MCP-1	45
3.2.3 Histology analysis: safranin-o fast green staining	46
4. Discussion	51
4.1 TNF α concentration dependent effect and stimulation duration	51
4.2 TNF α effects on chondrocyte 3D model	55
4.2.1 Anabolic aspect	55

4.2.2	Catabolic aspect	57
4.2.3	Inflammation	58
4.2.4	Histology	60
4.3	Passage	60
4.4	Clinical relevance	61
4.4.1	Cartilage regenerative therapy	61
4.4.2	Osteoarthritis	62
4.4.3	Rheumatoid arthritis	63
4.4.4	Origin of chondrocyte	65
4.5	Limitations	67
4.6	Conclusion and future Perspective	68
5.	Summary	69
6.	List of figures	70
7.	List of tables	72
8.	References	73
9.	Statement on personal contributions	90
10.	Publications	91
11.	Acknowledgments	92

List of abbreviations

2D, 3D	2 dimensional, 3 dimensional
ACI	autologous chondrocyte implantation
ACL	anterior cruciate ligament
AGN	aggrecan
cm, mm, μ m	centimeter, millimeter, micrometer
Col1	collagen 1, collagen I
Col2	collagen 2, collagen II
COMP	cartilage oligomeric matrix protein
COX2	cyclooxygenase-2
CT	threshold cycle
Da	dalton (atomic mass)
ECM	extracellular matrix
ELISA	enzyme-Linked Immunosorbent Assay
GAG, GAGs, sGAG	glycosaminoglycan, glycosaminoglycans, sulfated glycosaminoglycans
h, min, s	hour, minute, second
HA	hyaluronic acid
Hz	hertz
IFN- γ	interferon- γ
IL-1 β	interleukin-1 β
IL-6	interleukin-6
IL-8	interleukin-8
MCP-1	monocyte chemoattractant protein-1

MMP3	matrix metalloproteinase 3
MMP13	matrix metalloproteinase 13
MSC	mesenchymal stromal cell
NFkb1	nuclear factor kappa-light-chain-enhancer of activated b cells 1
NO	nitric oxide
NSAIDs	non-steroidal anti-inflammatory drugs
OA	osteoarthritis
OATs	osteochondral autograft transplantation
P1, P2, P3	passage 1, passage 2, passage 3
PBS	phosphate buffered saline
PCR	polymerase chain reaction
PRG4	proteoglycan 4
PTGES2	prostaglandin E synthase 2
RA	rheumatoid arthritis
RPM	revolutions per Minute
SE	standard error
sTNF α	soluble tumor necrosis factor alpha
tm-TNF α	transmembrane form-tumor necrosis factor alpha
TNFR	tumor necrosis factor receptor
TNF- α	tumornecrosis factor- α
VEGF-A	vascular endothelial growth factor-a

1. Introduction

Osteoarthritis (OA) is a major cause of disability, imposing a heavy social burden. Research related to cartilage holds significant economic and social benefits (Chen et al., 2021).

There are three types of cartilage in the human body, and the articular cartilage is a type of hyaline cartilage, which has unique smooth and resilient characteristics that allow low-friction daily movement of the joints (Athanasou et al., 2017; Carballo et al., 2017; Sophia Fox et al., 2009). Based on functional and compositional variations, articular cartilage could spatially be divided into four zones: superficial zone, middle zone, deep zone and calcified zone (Fig. 1) (Athanasou et al., 2017; Carballo et al., 2017). The superficial zone, the outermost layer, contains relatively high levels of collagen, with collagen fibers and chondrocytes arranged parallel to the articular surface (Carballo et al., 2017; Sophia Fox et al., 2009). That arrangement could provide the zone with low friction and protect the deeper zone during movement (Sophia Fox et al., 2009). In this zone chondrocytes express a specialized protein called proteoglycan 4 (PRG4) or lubricin, which is related to the lubricating function of the cartilage (Alquraini et al., 2017; Athanasou et al., 2017). The middle zone is rich in proteoglycan, water and thick fibres, it takes the largest volume of extracellular matrix (ECM) (around 50 % in wet weight) (Athanasou et al., 2017; Carballo et al., 2017; Sophia Fox et al., 2009). Collagen in this zone is arranged at a relatively oblique angle, and the chondrocytes in this zone are round or olive-shaped and sparsely distributed (Athanasou et al., 2017; Sophia Fox et al., 2009). The main function of this zone is to absorb compressive forces (Athanasou et al., 2017; Carballo et al., 2017; Sophia Fox et al., 2009). The tidemark is a line separated uncalcified zone and calcified zone (Carballo et al., 2017). In the deep zone, the collagen is arranged horizontally to the surface, and the chondrocytes are arranged horizontally as well, this arrangement could provide the cartilage with resilience and transfer force to the calcified zone (Sophia Fox et al., 2009). The deepest zone is the calcified zone, the main character of this zone is that the ECM is calcified and this zone forms the connection between cartilage and subchondral bone (Athanasou et al., 2017; Sophia Fox et al., 2009).

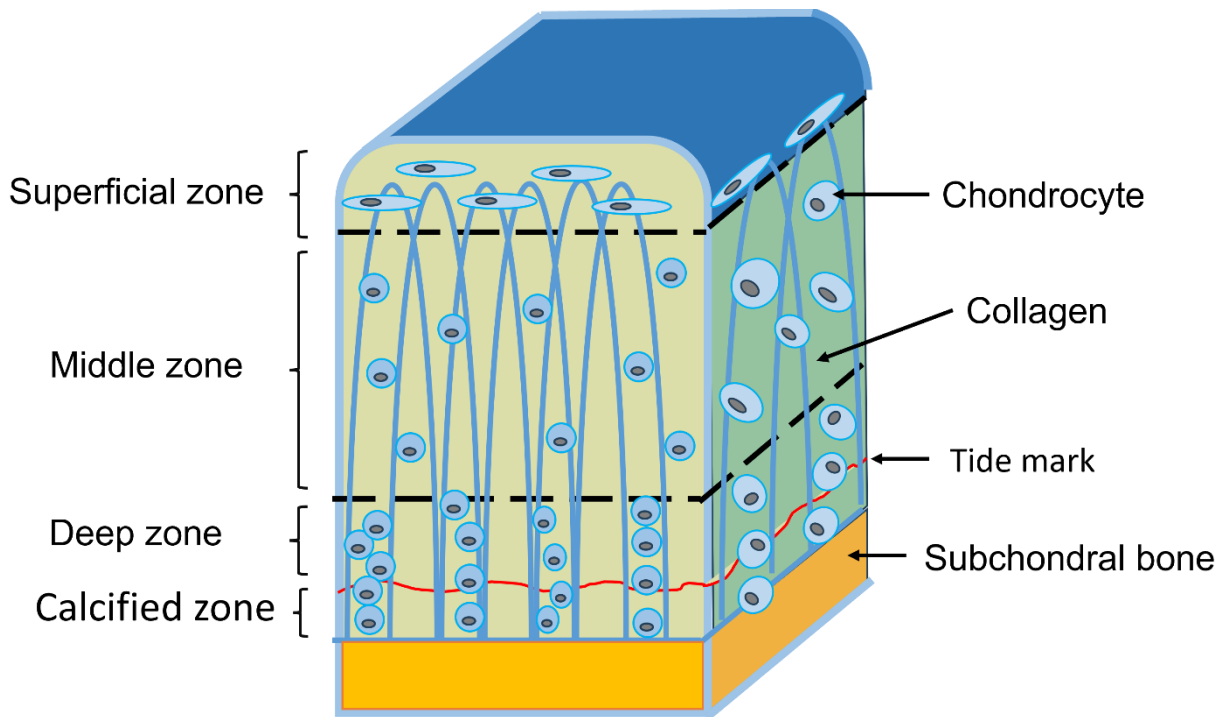


Fig. 1: A schematic illustration of the four zones of articular cartilage, the distribution and morphology of chondrocytes, and the arrangement of collagen. Adapted from (Sophia Fox et al., 2009).

Chondrocytes are the only cell type found in adult normal cartilage and are derived from mesenchymal stem cells (Buckwalter et al., 2005; Goldring and Otero, 2011). They are embedded within ECM that they produce and are responsible for maintaining cartilage homeostasis by regulating ECM synthesis and degradation (Carballo et al., 2017; Eschweiler et al., 2021; Goldring and Otero, 2011). Despite their crucial role, chondrocytes occupy only a small percentage of the total volume of cartilage. Chondrocytes have a very limited ability to repair cartilage tissue (Carballo et al., 2017). Adult normal cartilage is an avascular tissue, all its nutrient supplementation and the removal of metabolic waste are provided by joint fluid, especially during movement (Carballo et al., 2017).

Because articular cartilage is hyaline cartilage, the most abundant collagen is collagen 2, which is a typical marker of cartilage differentiation (Athanasou et al., 2017). Hyaline cartilage matrix also contains other collagens such as collagen 1 which is rich in fibrocartilage but is very little content in hyaline cartilage (Athanasou et al., 2017). Additionally, other collagen types also play important roles in reinforcing the structural

network of hyaline cartilage (Athanasou et al., 2017; Carballo et al., 2017; Eschweiler et al., 2021). The interaction between collagen and proteoglycan is vital to cartilage matrix stability (Carballo et al., 2017; Hecht et al., 2005; Roughley and Lee, 1994).

Proteoglycan is another important macromolecule which is vital to ECM structure and physical properties (Athanasou et al., 2017; Carballo et al., 2017). Aggrecan is a representative proteoglycan because it is abundant in articular cartilage (Athanasou et al., 2017). It is composed of a core protein and many glycosaminoglycans (GAGs) (Fig. 2). GAGs are long, unbranched polysaccharide chains made of repeating disaccharide units (Athanasou et al., 2017; Carballo et al., 2017). A lot of GAGs (many repeated chondroitin sulphates and keratan sulphates) attach to a core protein to form proteoglycans such as aggrecan. Since proteoglycans contain many GAGs, and GAGs carry negative electric charges, these negative charges repel each other, forming a brush-like structure that helps retain water within the matrix (Carballo et al., 2017). This hydration is crucial for the physical properties of cartilage, including resilience and shock absorption (Carballo et al., 2017). There are also other proteins in cartilage that contain short, branched carbohydrate chains, one of which is cartilage oligomeric matrix protein (COMP), which plays a crucial role in the stability of the cartilage matrix (Cui and Zhang, 2022; Koelling et al., 2006).

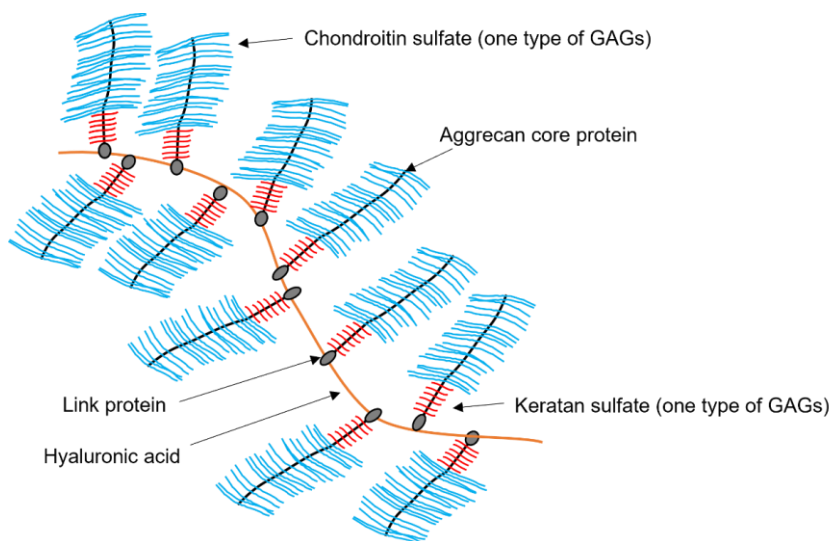


Fig. 2: A schematic illustration of the basic components of aggrecan monomer and how they connect to form a macromolecular structure. GAGs: glycosaminoglycans. Adapted from (Athanasou et al., 2017; Eschweiler et al., 2021).

Water makes up a large volume of cartilage and interacts with other components of the ECM, combined with proteoglycans and collagen to provides cartilage with unique properties that enable it to resist and distribute compressive and shear forces during movement (Carballo et al., 2017; Eschweiler et al., 2021; Sophia Fox et al., 2009). Besides that water also plays a crucial role in chondrocytes metabolism and ECM turnover (Carballo et al., 2017; Sophia Fox et al., 2009). The water content of cartilage varies from region to region, and is related to the content of protein. In general, the middle and surface layers of cartilage tissue contain more water, while the deeper layers contain less (Sophia Fox et al., 2009).

Adult healthy cartilage is an avascular tissue, all its nutrients are provided by joint fluid, which also removes metabolic waste (Carballo et al., 2017). Chondrocytes have a limited ability of self-repair after injury (Carballo et al., 2017; Darling and Athanasiou, 2003). And once cartilage got injured or is affected by abnormal wear and tear, osteoarthritis (OA) is the most common result. It is now widely accepted that OA is a dynamic and complex process, involving inflammatory, mechanical, and metabolic factors (Allen et al., 2022; Blasioli and Kaplan, 2014; Fernandes et al., 2002; Goldring and Otero, 2011). OA can affect the knees, hips, spine, and fingers and other joints (Oliveria et al., 1995). OA affects all the tissues in and around the joint, this includes degradation of the articular cartilage; thickening of the subchondral bone; osteophyte formation; variable degrees of synovial inflammation; hypertrophy of the joint capsule; and changes in periarticular muscles, nerves, bursa, and local fat pads (Blasioli and Kaplan, 2014; Di Chen et al., 2017; Fernandes et al., 2002; Kleemann et al., 2005; Loeser, 2006; Loeser et al., 2012; Martin et al., 2004). Among these, cartilage degradation in persistent inflammatory surroundings is considered to be the central feature (Di Chen et al., 2017; Loeser et al., 2012; Martin et al., 2004; Kleemann et al., 2005).

Pro-inflammatory cytokines, play a vital role in induce and maintain the inflammation process in cartilage (Fernandes et al., 2002). Tumor necrosis factor alpha (TNF α) and interleukin-1 beta (IL-1 β) are the most extensively studied for their pivotal roles in OA pathophysiology (Kapoor et al., 2011). These cytokines disturb the cartilage normal turnover balance by enhancing the activity of matrix metalloproteinases (MMPs) and aggrecanases which degrade ECM components such as collagens and proteoglycans

and suppress anabolic activities, like collagen II formation. Furthermore, studies proved that these cytokines can also induce apoptosis during cartilage inflammation (Fernandes et al., 2002).

To better understand the mechanism in chondrocyte inflammation, models are crucial for understanding disease mechanisms and exploring new therapeutic agents (Bendele, 2001; Johnson et al., 2016).

Research related to the development and improvement of models of inflammation has been conducted for many years (Bendele, 2001; Chu et al., 2010; Teeple et al., 2013). The general method to induce inflammation is the use of proinflammatory cytokines (TNF α or IL-1 β , alone or combined) to stimulate chondrocytes (Liu et al., 2022; Wojdasiewicz et al., 2014). TNF α related inflammation model could be divided into *in vivo* and *in vitro* categories (Bendele, 2001; Cope et al., 2019; Johnson et al., 2016). Considering the economy and the varying ease of model construction, *in vitro* models are relatively simple and more reproducible. Additionally, *in vitro* models are often used as the first step in assessing new drugs or therapies, which is why they have been adopted by numerous researchers (Cope et al., 2019).

There are several ways to construct an *in-vitro* TNF α inflammation model. The models of chondrocyte inflammation used in more than 90 % of studies can be summarized in the following three categories (Fig. 3): 1. direct chondrocytes when cultured; 2. use of artificial or natural materials as scaffolds for chondrocytes; 3. direct use of cartilage tissue explants as experimental models (Wang et al., 2024). Each model has their own advantages and disadvantages. Growing chondrocytes in a monolayer then induce inflammation by cytokine and perform experiments on these cells is a easiest one, and because chondrocytes are not abundant in cartilage, expanding them in a monolayer can be a necessary step to obtain enough experimental material, especially when the chondrocytes are derived from small animals like mice or rats (Chu et al., 2010; Cope et al., 2019).

There are more than 48 % studies choose 3D model (Fig. 3) (Wang et al., 2024). Since chondrocytes are highly specialized cells, they will lose their phenotype (collagen 2 expression) and undergo dedifferentiation, adopting a fibroblast-like phenotype, so a 3D environment is essential for chondrocyte development (Caron et al., 2012).

Cartilage explant could simulate a natural-like environment for chondrocytes, but it may encounter the difficult to ensure homogeneity of explant, and chondrocytes in the edge of the explant may react differently compared to those of the center area (Bartolotti et al., 2021; Darling and Athanasiou, 2003; Freed et al., 1993). Another method is using artificial material as a scaffold to provide chondrocytes a 3D environment. In this approach, it is necessary to consider whether the artificial material will affect the activity of chondrocytes and the ratio of chondrocytes to the artificial material to promote chondrocyte differentiation (Darling and Athanasiou, 2003; Freed et al., 1993; Johnson et al., 2016). In our study group has used chondrocytes without scaffold to build a 3D environment by making cells into a micro pellet (Ossendorff et al., 2023). This method is relatively simple and inexpensive compared to other methods, is reproducible, does not require the consideration of artificial materials, and also allows for adequate experimental materials obtained through *in vitro* chondrocyte expansion.

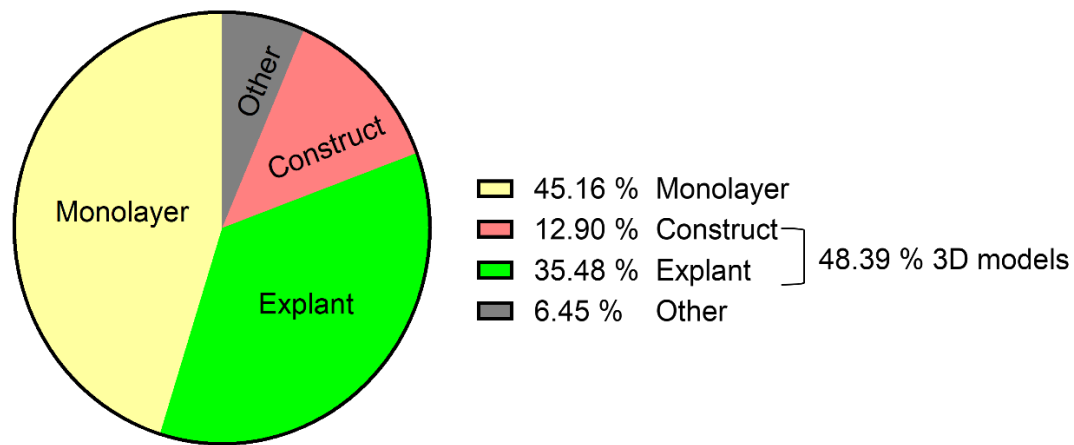


Fig. 3: TNF α inflammation models categories (*in vitro*). Adapted from (Wang et al., 2024)

In addition to the differences in the methods used to construct the models, the concentrations of TNF α used in the same model varied considerably (Wang et al., 2024). Some models use TNF α at concentrations that can even reach 100 ng/mL (Wang et al., 2024). There are no systematic studies to explore the relationship between concentration and model construction, and how much cytokine concentration is needed to effectively mimic the inflammatory response.

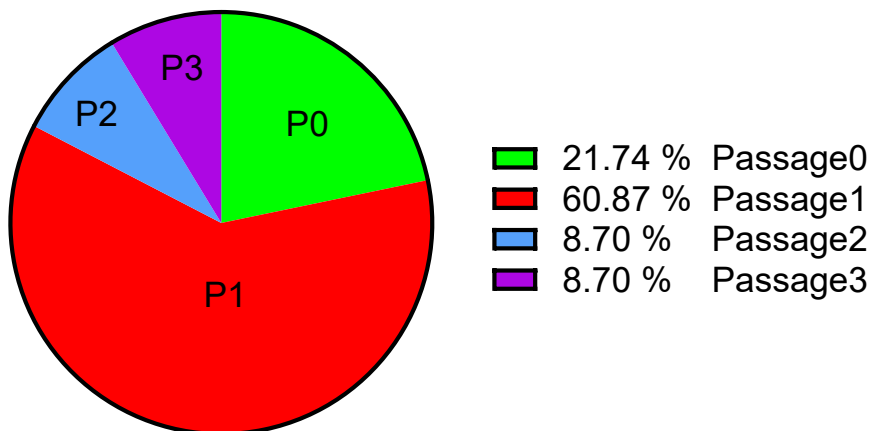


Fig. 4: Summary pie chart showing the utilization of chondrocytes at different passages in inflammation model construction. Adapted from (Wang et al., 2024).

Wang et al. reported that the used passages of chondrocytes which are supposed to construct inflammation model are also different (Fig. 4) and passage 1 is the most common used (Wang et al., 2024). Vanlauwe et al. demonstrated that chondrocytes can still maintain their phenotype when expanded in vitro up to passage 3 (Vanlauwe et al., 2011). Given that changes in chondrocyte phenotype may influence their response to inflammation, this factor should be considered when constructing models. However, there are still few studies focused on this aspect.

Due to the lack of uniformity in the existing TNF α induced chondrocytes inflammation models, and the fact that there are many variations in the conditions under which the same model is constructed, without a standardized inflammation model to serve as a research platform, it is not possible to effectively compare the results of different studies, and at the same time the interpretation of the results of a particular study is likely to be biased. In addition, current inflammation models are fixed and cannot accurately replicate the inflammatory environment of cartilage tissue (Wang et al., 2024). As an effective tool for researchers seeking to further investigate the mechanisms behind inflammation and develop new drugs, there is a need for not only a standardized 3D inflammation model as a research platform but also a model that can dynamically simulate the disease from its onset to its progression.

The aim of this study is: (1) to establish a standardized chondrocyte inflammation model by examining the effects of cytokine concentration (TNF α) and chondrocyte passage on the construction of an inflammation model; and (2) to use this model as a foundation for developing a dynamic inflammation model that more accurately simulates the inflammatory process of chondrocytes under pathological conditions.

2. Materials and Methods

2.1 Materials

2.1.1 Instruments

384 well plate	Greiner BIO-ONE, Kremsmünster, Austria
96well v bottom plate	Greiner BIO-ONE, Kremsmünster, Austria
96well normal bottom plate	Greiner BIO-ONE, Kremsmünster, Austria
Autoclave machine	Systemtechnik, Wettenberg, Germany
BioTek plate washer	BioTek Instruments, Winooski, Vermont, USA
Cell strainer 40 μ m	Greiner BIO-ONE, Kremsmünster, Austria
CO2-Incubator	Memmert, Schwabach, Germany
Culture flask(T175)	Greiner BIO-ONE, Kremsmünster, Austria
Eppendorf centrifuge 5430/5430R (PCR)	Eppendorf, Hamburg, Germany
Eppendorf centrifuge 5810/5810 R (cell culture)	Eppendorf, Hamburg, Germany
Falcon tubes	Carl Roth, Karlsruhe, Germany
FlexMap 3D instrument	Luminex, Austin, Texas, USA
Hemocytometer/cell counter	NanoEnTek, Seoul, South Korea.
Laminar safety cabinet	ScanLab, Puchheim, Germany

Magnetic stirrers	Velp Scientifica, Brianz, Italy
Microscope	Olympus, Tokyo, Japan
MILLIPLEX® Bovine	
Cytokine/Chemokine Magnetic Bead	Merck, Darmstadt, Germany
Panel 1	
NanoDrop 1000 spectrophotometer	IMPLEN, Munich, Germany
ProFlex PCR system	Applied biosystem, Foster City, California, USA
Quant Studio 5 real-time PCR systems	Thermo Fisher scientific, Waltham, Massachusetts, USA
Syringe-filter (0.22µm)	Sartorius AG, Göttingen, Germany
2.1.2 Reagents	
18S rRNA Control MIX	Applied biosystems, Foster City, California, USA
0.5 % Trypsin-EDTA (10X),	Life Technologies, Carlsbad, California, USA
1-Bromo-3-chloropropane	Sigma-Aldrich, St. Louis, Missouri, USA
4-(Dimethylamino)benzaldehyde	Sigma Aldrich, St. Louis, Missouri, USA
Ascorbic-Acid-Phosphate	Sigma-Aldrich, St. Louis, Missouri, USA
Blyscan™ assay kit	BiColor, Belfast, United Kingdom
Bovine-Serum-Albumine	Sigma-Aldrich, St. Louis, Missouri, USA
Cell Death Detection ELISA kit	Roche, Basel, Switzerland
Chondroitinase ABC from <i>Proteus vulgaris</i>	Merck, Darmstadt, Germany
Collagenase, Type II, powder	Thermo Sientific, Waltham, Massachusetts, USA

DEPC-Treated Water	Invitrogen, Massachusetts, USA
Di-Sodium hydrogen phosphate dihydrate	Carl Roth, Karlsruhe, Germany
DMEM, high glucose, no glutamine, no calcium	Thermo Fisher Scientific, Waltham, Massachusetts, USA
DPBS	Thermo Fisher Scientific, Waltham, Massachusetts, USA
Ethanol	Sigma-Aldrich, St. Louis, Missouri, USA
Fast-Green-	Sigma Aldrich, St. Louis, Missouri, USA
Fetal calf serum	Bio&SELL GmbH, Kleinmachnow, Germany
Goat anti-Rabbit IgG (H+L) biotinylated	Vector laboratories, Newark, CA, USA
Griess reagent system	Promega, Minneapolis, Minnesota, USA
HEPES	Carl Roth, Karlsruhe, Germany
Horse anti-Mouse IgG (H+L) Biotinylated	Vector laboratories, Newark, CA, USA
Horse serum liquid	Sigma Aldrich, St. Louis, Missouri, USA
Hyaluronidase	Sigma Aldrich, St. Louis, Missouri, USA
Hydrogen peroxide 30 %	Carl Roth, Karlsruhe, Germany
ImmPACT™ DAB from Vector Laboratories	BIOZOL, Eching, Germany
L-Glutamin (200 mM)	Thermo Fisher Scientific, Waltham, Massachusetts, USA
Mayers Haemalaum	Carl Roth, Karlsruhe, Germany
MEM Non-Essential Amino Acids Solution (100X)	Thermo Fisher Scientific, Waltham, Massachusetts, USA
Methanol	Sigma-Aldrich, St. Louis, Missouri, USA

Milliplex Bovine Cytokine/Chemokine Magnetic Beads Panel 1 kit	Millipore, Darmstadt, Germany
NORMAL GOAT SERUM 20 ml	BIOZOL, Eching, Germany
Penicillin/Streptomycin	Gibco, Waltham, Massachusetts, USA
Polyacryl Carrier	MRC, Cincinnati, USA
Pronase E (from Streptomyces griseus)	Merck, Darmstadt, Germany
Proteinase K, recombinant, PCR grade	Thermo Fisher Scientific, Waltham, Massachusetts, USA
RNeasy MINI kit	Qigen, Hilden, Germany
Safranin-O	Sigma Aldrich, St. Louis, Missouri, USA
Sodium chloride ≥99,5 %, p.a., ACS, ISO	Carl Roth, Karlsruhe, Germany
Sodium dihydrogen phosphate monohydrate	Carl Roth, Karlsruhe, Germany
TaqMan™ Reverse Transcription Reagents	Thermo Fisher Scientific, Waltham, Massachusetts, USA
TaqMan™ Universal PCR Master Mix	Thermo Fisher Scientific, Waltham, Massachusetts, USA
TE Buffer	Sigma Aldrich, St. Louis, Missouri, USA
Trans-4-Hydroxy-L-prolin	Sigma Aldrich, St. Louis, Missouri, USA
Tumor-necrosis-factor-alpha-(TNF α)	R&D Systems, Minneapolis, USA
Xylene	Carl Roth, Karlsruhe, Germany
2.1.3 Buffers and Solutions	
Cartilage Digestion Solution	DMEM (high glucose), supplemented with 10 % fetal calf serum (FCS), 1 % L-

	glutamine, 1 % penicillin/streptomycin, and 600 U/mL collagenase II
Cartilage Wash Solution	PBS supplemented with 10 % penicillin/streptomycin
Chondrocyte Growth Medium (for Monolayer Culture)	DMEM (high glucose) supplemented with 10 % FCS, 1 % L-glutamine, 1 % penicillin/streptomycin
Chondrogenic Growth Medium (for Pellet Culture)	DMEM (high glucose) supplemented with 10 % FCS, 1 % L-glutamine, 1 % penicillin/streptomycin, 60 µg/mL L-ascorbic acid phosphate, 40 µg/mL L-proline, 1 % non-essential amino acids
PBS Wash Solution	PBS supplemented with 1 % penicillin/streptomycin
PBS-Tween	1 mL of Tween 20 to 1 Liter of PBS

2.2 Experimental Design

The entire study was divided into two parts, designated as experiment one and experiment two. Experiment one: Investigation of the effects of different concentrations of TNF α and chondrocyte expansion (passage) on a standard chondrocyte pellet inflammation model. This will hereafter be referred to as 'experiment one'. Experiment two: Investigation and development of a standard chondrocyte pellet inflammation model with dynamic TNF α concentrations. This will hereafter be referred to as 'experiment two'. The following represents the experimental workflow. The bovine biomaterials (cartilage) employed in this study were obtained from biological waste discarded at a slaughterhouse, and therefore, ethical approval from a committee was not required.

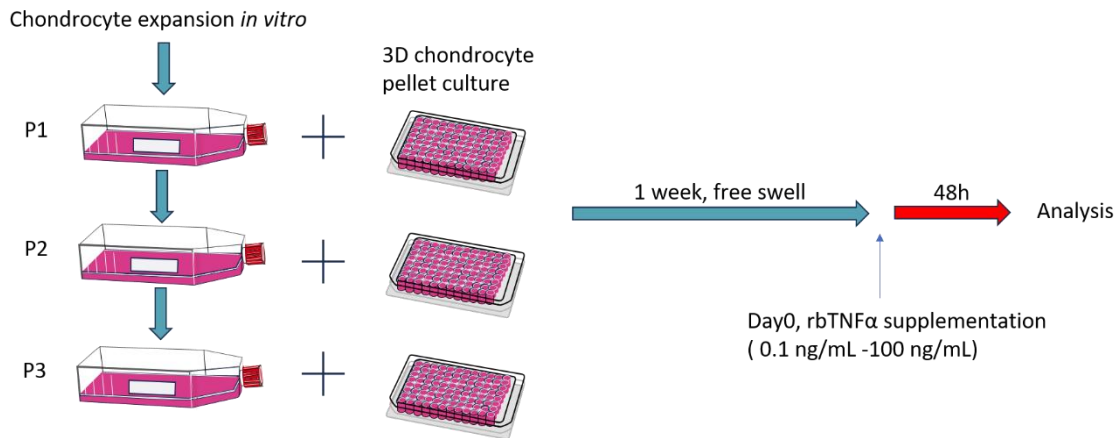


Fig. 5: Flowchart of the design of Experiment One. In experiment one: Bovine chondrocytes isolated from bovine articular cartilage digestion were initially expanded *in vitro*. Once the cells approached confluence, they were passaged and cultured until reaching passage 3. 3D chondrocyte pellet models were constructed using chondrocytes from each passage. After one week of culture, varying concentrations of bovine recombinant TNF α were introduced to induce an inflammatory response in the chondrocyte pellets. The pellets and their cultures were then collected and analyzed for further investigation. P1-3 refer to passages 1 to 3, from which chondrocytes were harvested to form a pellet. 'Day0' marked the beginning of TNF α supplement (Ossendorff et al., 2024c).

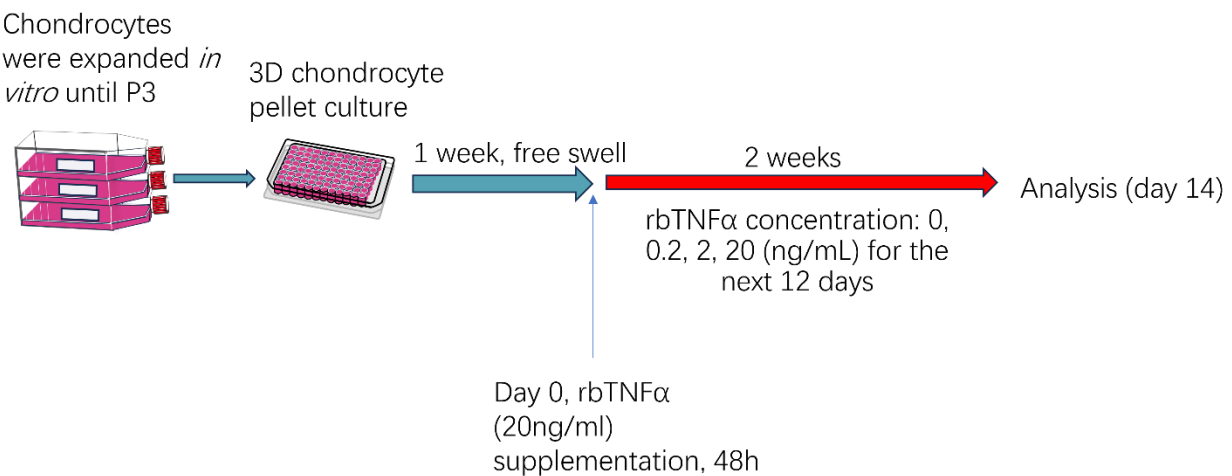


Fig. 6: Flowchart of the design of Experiment Two. In experiment two: Bovine chondrocytes were expanded to passage 3, after which pellets of chondrocytes were constructed. Following one week of culture, these pellets were stimulated with 20 ng/mL of recombinant bovine TNF α . After 2 days, recombinant bovine TNF α at different concentrations was used to continue stimulating the chondrocyte pellets for an additional 12 days. The pellets and cultures were subsequently collected. P3: passage 3. 'Day0' marked the beginning of TNF α supplement.

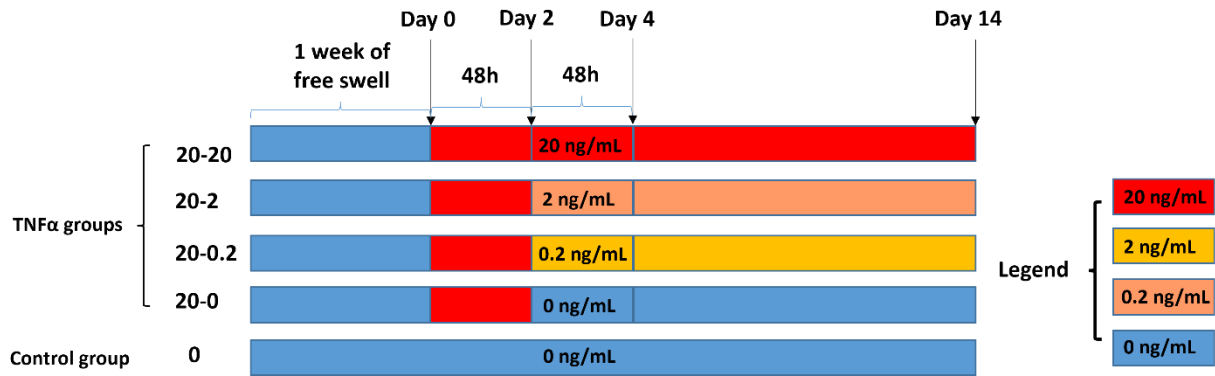


Fig. 7: Schematic of TNF α concentration usage in experiment two. Different colors represented the different concentrations of TNF α in medium. Blue: 0 ng/mL, Tangerine: 0.2 ng/mL, orange: 2 ng/mL, red: 20 ng/mL. 'Day0' marked the beginning of TNF α supplement. Day 2, Day 4, and Day 14 represented the second, fourth, and 14 days, respectively, following 'day0'.

Tab. 1: Details about the supplementation of different TNF α concentrations in Experiment one.

Experiment one		TNF α supplementation
Control group	0	0 ng/mL for 48 h
TNF α groups	0.1	0.1 ng/mL for 48 h
	1	1 ng/mL for 48 h
	10	10 ng/mL for 48 h
	20	20 ng/mL for 48 h
	50	50 ng/mL for 48 h
	100	100 ng/mL for 48 h

Tab. 2: Details about the supplementation of different TNF α concentrations in experiment two.

Experiment two		TNF α supplement
Control group	0	0 ng/mL for 14 days
TNF α groups	20-0	20 ng/mL for 48 h, followed by 0 ng/mL for next 12 days
	20-0.2	20 ng/mL for 48 h, followed by 0.2 ng/mL for next 12 days
	20-2	20 ng/mL for 48 h, followed by 2 ng/mL for next 12 days
	20-20	20 ng/mL for 48 h, followed by 20 ng/mL for next 12 days

2.3 Chondrocyte Isolation

In a sterile setting, the skin of the bovine fetlock joint was aseptically incised, followed by an arthrotomy of bovine specimens aged between 4 and 6 months. These animals were slaughtered by a local butcher for food production and the fetlock joints were regarded as waste byproducts, obtaining approval from the local ethical committee was not required.

Afterwards, the articular cartilage was aseptically cut into small fragments, approximately 10 to 25 mm² in size (Ossendorff et al., 2024c). The cartilage pieces were weighed and then cleaned two times for fifteen minutes each with cartilage wash solution (PBS with 10 % Penicillin/Streptomycin).

After the cleaning operations, those fragments underwent digestion employing 0.1 % pronase for a total of 105 minutes at 37°C in a CO₂ laboratory incubator maintained at 5 % CO₂ and 95 % humidity.

Subsequent to pronase digestion, those fragments underwent three additional washes with 100 mL of PBS containing 1 % Penicillin/Streptomycin each time and was then subjected to overnight digestion (more than 12 hours) at 37°C, 5 % CO₂, and 95 % humidity in 600 U/mL of collagenase type II in 100mL of DMEM (Robinson et al., 2016). After a 7-minute centrifugation at 565 × g at 4°C, the chondrocyte suspension was resuspended in 40 mL of chondrocyte growth medium. This procedure was repeated once more. Subsequently, 20 μ L of the cell suspension was taken to count the chondrocytes

and evaluate their viability by adding 20 μ L of trypan blue staining, followed by counting using a hemocytometer under a microscope.

Approximately 2.5×10^6 chondrocytes were plated into a T175 culture flask containing 25 mL of chondrocyte growth medium.

2.4 Passaging of Chondrocytes

Once the cells reached approximately 80 % confluence, they were subcultured. To get rid of any remaining serum and calcium, the chondrocytes were rinsed twice with PBS wash solution. Following a 15-minute incubation period at 37°C, 5 % CO₂, and 95 % humidity, they were digested in 12 mL PBS containing 1 % Penicillin/Streptomycin and 300 U/mg of collagenase II. An additional 1.2 mL of Trypsin-EDTA at 0.5 mg/mL was added to the flask and incubated for another 20 minutes under the same conditions to facilitate detachment. The cell solution was then collected, diluted with 13 mL of chondrocyte growth medium to stop the digestion process, and centrifuged at 565 \times g for 7 minutes at 4°C. After removing the supernatant, the cells were resuspended and subjected to a second round of centrifugation. The cells were then counted, and their viability was evaluated with trypan blue same as described above. A part of the collected chondrocytes underwent additional in vitro expansion under the same density and circumstances as previously described. 3D chondrocyte pellets were created using remaining chondrocytes. Up until passage 3, this procedure was repeated and the culture medium was replaced every two days.

2.5 Establishment of a 3D Chondrocyte Inflammation Pellets Model

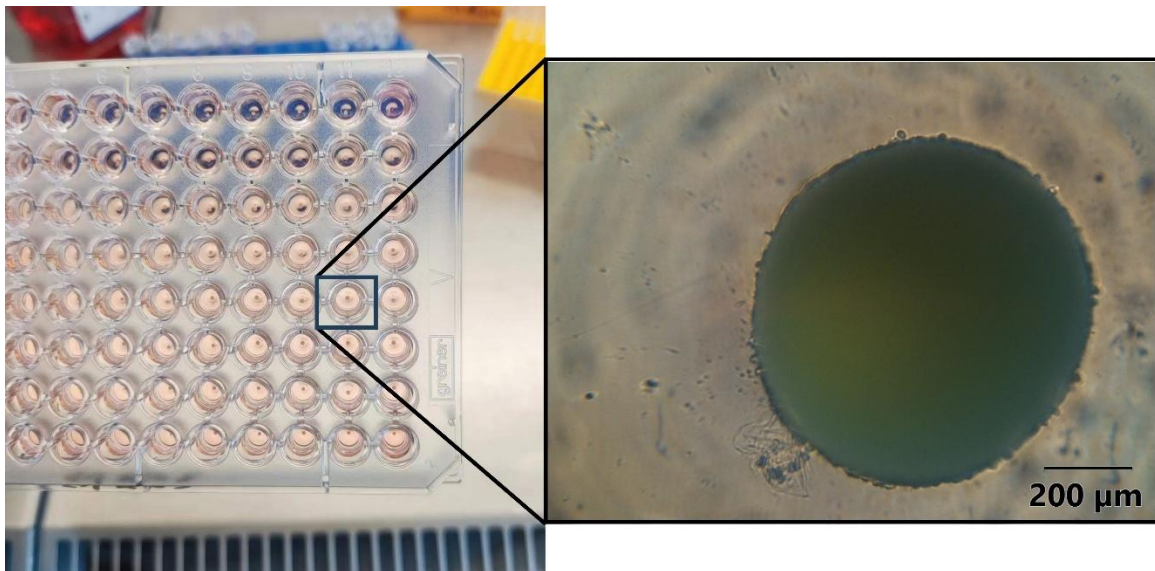


Fig. 8: Images of chondrocyte pellets in a 96-well V-bottom plate and a microscopic view of a representative chondrocyte spheroid (passage 3). The left panel displayed the aggregated chondrocyte pellets settling at the bottom of the V-shaped wells, demonstrating their compact and uniform formation. The right panel presented a magnified view of a macro photo of a single chondrocyte spheroid, showcasing its spherical morphology and dense cellular arrangement, characteristics of well-formed chondrocyte aggregates at that passage stage.

Separate 96-well V-bottom non-adherent plates were used to hold the chondrocytes from each passage (passages 1 through 3). 0.25 million chondrocytes were added in each well with 100 μ L of chondrogenic growth medium (see 2.1.3 Buffer and Solutions). After that, the plates were centrifuged for five minutes at $500 \times g$ to create pellets (Fig. 8). After that, they spent one week in an incubator set to 37 °C, 5 % CO₂, and 21 % O₂. Every two days, the medium was changed.

For experiment one, chondrocyte pellets from all three passages were divided into seven groups after one week of incubation, including six experimental groups and one control group (Fig. 5, Tab. 1). Cytokine stimulation was carried out for 48 hours, and the medium was changed every two days.

For experiment two, the chondrocyte pellet model was composed exclusively of chondrocytes from passage 3. After one week of free swelling in 96-well plates, pellets from the experimental groups were stimulated with recombinant bovine TNF α at a

concentration of 20 ng/mL for 48 hours. Subsequently, these pellets were exposed to varying concentrations of TNF α (ranging from 0.2 ng/mL to 20 ng/mL) for the following 12 days (Fig. 6, Fig. 7, Tab.2). The medium was changed every two days.

2.6 Analysis

2.6.1 RNA Extraction, Reverse Transcription and Real-Time PCR

Every four pellets collected from the same group were placed into an Eppendorf tube containing 1 mL of TRI reagent, 5 μ L of polyacrylate carrier, and a sterilized stainless-steel ball that could move freely within the tube, and the samples were then put into a tissuelyzer for 10 minutes at 30 Hz to release RNA from chondrocytes (Ossendorff et al., 2024c).

Phase separation was accomplished by adding 100 μ L of bromochloropropane for every 1 mL of TRI reagent, shaking the tubes violently for 15 second, and then setting them on an orbital shaker (no rack, set to around 20 rotations per minute). The tubes were then centrifuged for 15 minutes at 4 °C at 12000 x g. After carefully aspirating the aqueous phase into a fresh 1.5 mL Eppendorf tube, it was combined with an equivalent volume of 70 % ethanol and properly mixed using a pipette.

RNA was extracted using the RNeasy MINI kit following the manufacturer's instructions. RNA quantity and quality were assessed with the Nanophotometer N60 by measuring absorbance at A260, A280, and A230. The A260/A280 ratio for pure RNA should be between 1.9 and 2.0, while the A260/A230 ratio should be greater than 1.0.

Reverse transcription was performed by adding TaqMan® reverse transcription mix, 1 μ g of total RNA, and random hexamers into a 200 μ L tube, with a final reaction volume of 20 μ L. The reaction was conducted using the ProFlex PCR system under the following conditions: an initial primer incubation at 25°C for 10 minutes, reverse transcription at 37°C for 120 minutes, and inactivation of the reverse transcriptase at 85°C for 5 minutes. The resulting cDNA was then diluted with TE buffer and stored at -20°C.

Real-time PCR was conducted using the Applied Biosystems QuantStudio 5 Flex Real-Time PCR system on 384-well optical plates. Briefly, 8 μ L of master mix plus 2 μ L of cDNA sample were added to the wells. The plates were then covered with transparent film and centrifuged to mix the reagents and cDNA. The PCR was performed with an initial

incubation at 95°C for 10 minutes, followed by 40 cycles of dissociation at 95°C for 15 seconds and annealing/extension at 60°C for 1 minute.

The target genes were anabolic markers collagen 2 (Col2), proteoglycan gene aggrecan, glycoprotein gene cartilage oligomeric protein (COMP), and dedifferentiation gene collagen 1 (Col1); catabolic markers matrix metalloproteinases 3 (MMP3) and 13 (MMP13); inflammation markers interleukin-6 (IL-6), interleukin-8 (IL-8), nuclear factor kappa B 1 (NF κ B1), cyclooxygenase-2 (COX-2), and prostaglandin E synthase 2 (PTGES2); and the apoptosis marker caspase 3. And all those gene were defining bovine genes from Gene Bank (Grad et al., 2006). The human 18S ribosomal RNA gene was used as an internal control (Ossendorff et al., 2023). The threshold cycle (CT) values of the genes were first standardized to the average CT of the 18S gene (Δ CT), followed by the normalization to the CT value of day 0 ($\Delta\Delta$ CT). After that, the 2- $\Delta\Delta$ CT technique was used to determine relative gene expression levels.

2.6.2 Histology: Safranin-O Fast Green Staining

Samples prepared for histological assessment were initially fixed in 70 % methanol and stored at 4°C until analysis. Subsequently, pellets were dehydrated by immersion in increasing concentrations of ethanol, from 70 % to 100 %. Then pellets were embedded by paraffin, followed by cutting into 5 μ m sections in a microtome. Then staining by Safranin-O Fast Green to visualize the special deposition of collagens and proteoglycans in matrix. Safranin O Fast Green staining was an effective method for visualizing proteoglycans and collagen, two essential structural components of the extracellular matrix. In this staining process, proteoglycans were stained orange to red, collagen appeared green to light blue, and nuclei were stained dark purple to black.

To prepare the slides, they were placed on a hot plate (below 60°C) to allow the sections to flatten and adhere securely to the glass.

The slides were then submerged in xylene for two rounds, each lasting five minutes. After that, they spent two rounds of three minutes each in pure ethanol. The ethanol content was then progressively reduced from 96 % to 50 % by a series of hydration processes, each lasting two minutes. Following a 10-minute blue in tap water, the slides were washed with deionized water and stained with Weigert's Haematoxylin for 10 minutes to highlight

chondrocytes, which have a dark purple to black appearance. The slides were then differentiated in 1 % acetic acid for 20 seconds after being dyed with Fast Green (0.02 %) for 6 minutes. After that, they were dyed for ten minutes with 0.1 % Safranin O. Following a series of dehydration processes, the ethanol content increased from 70 % to 96 % (15–30 seconds) and then to absolute ethanol (4 minutes, twice). After that, the slides were submerged in xylene and covered with a coverslip and Eukitt. The staining images were then processed using cellSens (v4.3.1; Olympus Corporation, Tokyo, Japan) to generate quantitative data for further analysis (Fig. 21).

2.6.3 Enzyme-Linked Immunosorbent Assay (ELISA) of Pellet Medium

The Milliplex Bovine Cytokine/Chemokine Magnetic Beads Panel 1 kit was used to assess the cytokines and chemokines (IL-6, IL-8, MCP-1) produced into the cell supernatants. The assay was conducted in a 384-well format (Tang et al., 2016).

Preparation of the standard and control groups according to the manufacturer's instructions. First add 6 μ L of assay buffer to each 384-well, then add 6 μ L solutions of standard, control groups or experimental groups. 6 μ L of the magnetic bead mixture should then be added. The 384-well plate is then sealed to protect it from light and shaken at 400 rpm overnight in a low temperature (4°C) environment. The following day, a magnet was used to isolate all the magnetic beads, which were then washed twice using a BioTek 405 plate washer. Subsequently, the secondary antibody was added, and the reaction was carried out for 1 hour at room temperature in the dark. This was followed by the addition of the fluorescent detection reagent streptavidin-phycoerythrin, for 30 minutes incubation. After another round of bead washing, the beads were resuspended in 80 μ L sheath fluid to facilitate subsequent analysis using the FlexMap 3D instrument.

2.6.4 Biochemistry analysis

2.6.4.1 Nitric Oxide Quantification in Medium

The nitric oxide (NO) concentration in supernatants of both experiment one and experiment two was measured using a Griess diazotization reaction assay kit in a 96-well plate format. First, collect the culture medium from the experimental groups without centrifugation. Prepare a series of NO standard concentration solutions.

A standard nitrite solution was used to prepare a nitrite gradient concentration series. The nitrite gradient solution and the samples were added to separate wells of a 96-well plate. 50 μ L Sulfanilamide solution was then added to each well and incubated avoid light at room temperature for 10 minutes, followed by the addition 50 μ L of NED Solution, with the reaction continuing for another 10 minutes. Absorbance was subsequently measured at 540 nm using a spectrophotometer. Nitrite standard reference curves were generated based on the standard concentrations to determine the NO content in the samples.

2.6.4.2 Glycosaminoglycans Quantification

Glycosaminoglycans was quantified using the Blyscan™ assay kit. For this procedure, pellets (4 pellets per group) were transferred into tubes containing 1 mL of 0.5 mg/mL proteinase K. The tubes were then incubated overnight at 56°C on a shaker to facilitate digestion. After incubation, the samples were heat-inactivated at 95°C for 10 minutes and subsequently stored at -20°C. For the assay, 50 μ L of standard solutions with gradient concentrations and the samples were added to separate Eppendorf tubes. Then, 50 μ L of deionized water and 1000 μ L of dye reagent were added to each tube, followed by a 30-minute incubation. Following the incubation, the samples were centrifuged for 10 minutes at 12,100 g, and the supernatant was discarded. Next, 500 μ L of dissociation reagent was added to each tube, mixed thoroughly, and the samples were centrifuged again for 10 minutes at 12,100 g. The supernatant (200 μ L) was then transferred to a 96-well plate, and the absorbance was measured at 656 nm. A reference curve was generated using the standard solution, and the GAGs content in the samples was calculated based on this curve.

2.7 Statistics

Statistical analysis was performed using SPSS (v27; IBM, Armonk, USA). For continuous variables that followed a normal distribution, the independent t-test was used. The Mann-Whitney test was applied to continuous variables that did not follow a normal distribution. Statistical significance was set at $p < 0.05$. Graphical representation of the data was conducted using GraphPad Prism 8 (GraphPad Software Inc., San Diego, USA). Gene expression data were natural log transformed to avoid skewness.

3. Results

3.1 Results of Experiment One

Experiment one sought to determine whether the various passages had an impact on the chondrocyte inflammation pellet model and the concentration threshold of TNF α required. Above the concentration threshold (10 ng/mL), TNF α has generally been demonstrated a noticeable inflammatory response, which speeds up the cartilage matrix's breakdown while preventing the synthesis of matrix constituents. The fact that chondrocytes from various passages react differently to TNF α was also proved.

3.1.1 Gene Expression

3.1.1.1 Anabolic markers

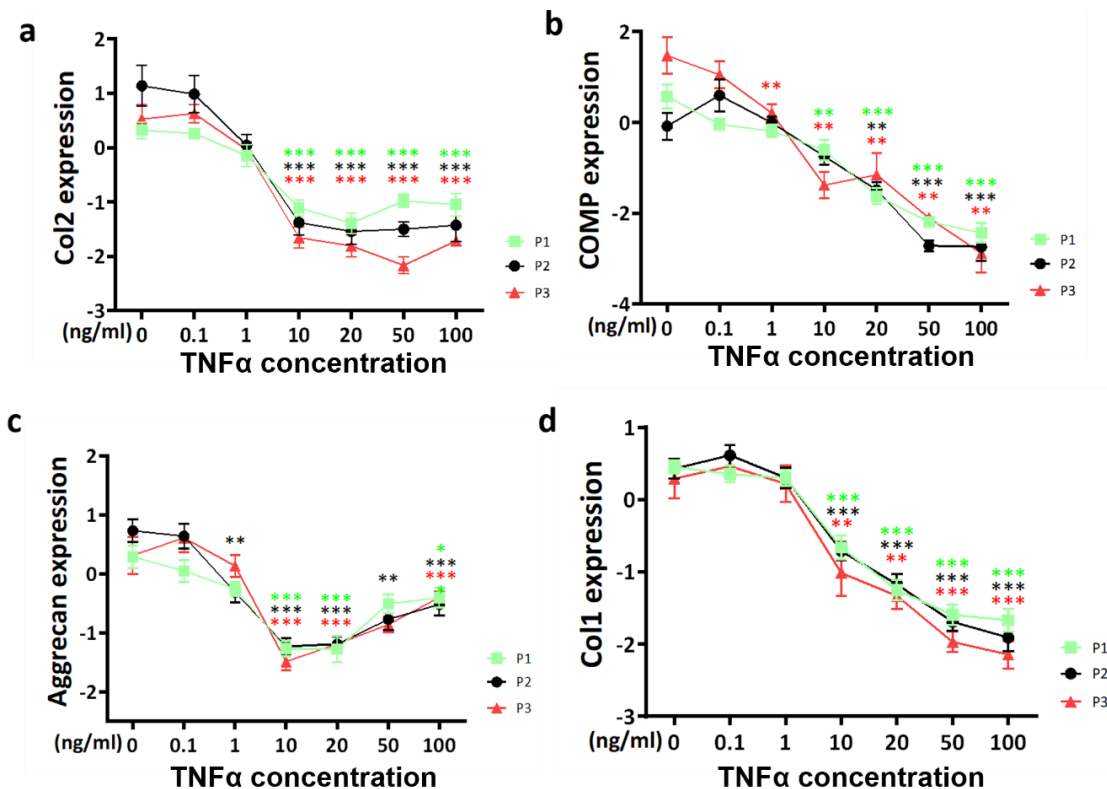


Fig. 9: Anabolic gene expression of experiment one. (a) collagen 2 (Col2), (b) cartilage oligomeric matrix protein (COMP), (c) aggrecan (AGN), and (d) collagen 1 (Col1). Pellets were treated by TNF α at different concentrations (0.1 ng/mL-100 ng/mL) for 48h. The results for chondrocyte-derived pellets from passages 1, 2, and 3 were represented by green, black, and red curves, respectively. Statistical comparisons to the control group for each passage were indicated by green, black, and red stars. For clarity, statistical significance between passages at the same cytokine concentration was not shown. *p < 0.05; **p < 0.01; ***p < 0.001. P1–P3: passages 1–3; '0': control (Ossendorff et al., 2024c).

Collagen 2 (Col2), as the most important component of the extracellular matrix in hyaline cartilage, is also the most critical collagen in healthy hyaline cartilage (Athanasou et al., 2017; Deshmukh and Nimni, 1973). TNF α suppressed Col2 expression level. A significant decrease in Col2 expression was only observed when the TNF α concentration reached a threshold of 10 ng/mL (Fig. 9a). And this trend was consistent across all three passages. When the TNF α concentration surpassed 10 ng/mL, the Col2 gene expression did not continue to decline significantly but instead stabilized at a relatively constant level.

Passage also influenced the response of the Col2 gene to TNF α . At a TNF α concentration of 0.1 ng/mL, the gene expression level of Col2 was lower in chondrocytes of passage 1, but when TNF α concentration continued to increase to 10 ng/mL, the chondrogenic expression level of passage 1 exceeded that of passage 3, and the gap widened and persisted when TNF α concentration continued to increase. (0.1ng/mL, p=0.039; 10ng/mL, p=0.023; 100ng/mL, p=0.023).

Cartilage oligomeric protein (COMP) is a glycoprotein which directly binds to collagens and other proteins, and plays an important role in the structural stabilization of the extracellular matrix, mechanical resistance, and assisting collagen fibre formation, is a marker of ECM turnover (Hecht et al., 2005; Haleem-Smith et al., 2012; Ossendorff et al., 2024b). TNF α had a negative effect on COMP expression and this effect showed concentration dependence, with this negative effect reaching significance at 1 ng/mL in Phase 3 (p = 0.005), 10 ng/mL in Phase 1 (p = 0.004) and 20 ng/mL in Phase 2 (Fig. 9b). Although the different Passages had different sensitivities to TNF α resulting in different concentrations at which this significance gap began, they all had significantly lower levels of gene expression in the face of stimulation with high concentrations of TNF α .

Aggrecan is a proteoglycan, mainly responsible for retaining water molecular within matrix and dispersing physical impact (Kiani et al., 2002). The expression level of aggrecan decreased in response to TNF α stimulation and reached its lowest point at 10 ng/mL of TNF α among all 3 passages (passage 1, p<0.001; passage 2, p<0.001; passage 3, p<0.001) (Fig. 9c). When the TNF α concentration exceeded 10 ng/mL, the gene expression level of aggrecan increased, and this trend continued until 100 ng/mL, and no significant difference was observed between passages.

Collagen 1 (Col1), located in the superficial zone of healthy hyaline cartilage, serves as a marker of chondrocyte dedifferentiation (Athanasou et al., 2017). Similar to Col2, TNF α also reduced the gene expression level of Col1 and the threshold concentration for this effect was 10 ng/mL. However, unlike the situation in Col2, the negative effect of TNF α on Col1 expression was concentration-dependent. No significant difference in Col1 expression was observed between different passages (Fig. 9d).

3.1.1.2 Catabolic Markers

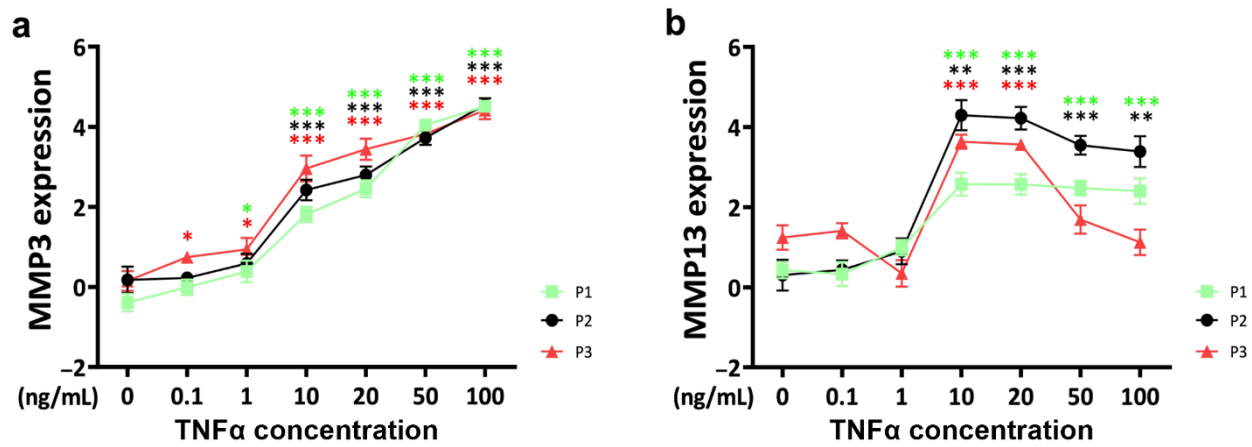


Fig. 10: Catabolic gene expression of experiment one. (a) Matrix metalloproteinase 3 (MMP3), (b) Matrix metalloproteinase 13 (MMP13). Pellets were treated by TNF α at different concentrations (0.1 ng/mL-100 ng/mL) for 48h. The results for chondrocyte-derived pellets from passages 1, 2, and 3 were represented by green, black, and red curves, respectively. Statistical comparisons to the control group for each passage were indicated by green, black, and red stars. To enhance interpretability and facilitate analysis, the gene expression data were natural log-transformed. For clarity, statistical significance between passages at the same cytokine concentration was not shown. * p < 0.05; ** p < 0.01; *** p < 0.001. P1: passage 1; P2: passage 2; P3: passage 3 and '0' represented control group (Ossendorff et al., 2024c).

Matrix metalloproteinases 3 (MMP3) and Matrix metalloproteinases 13 (MMP13) are enzymes for ECM degradation (Blasioli and Kaplan, 2014). TNF α increased MMP3 expression in a concentration-dependent manner (Fig. 10a). Passage 3 chondrocytes were the most sensitive to TNF α stimulation, showing a significant increase at a concentration of 0.1 ng/mL (p=0.015), followed by passage 1 (p =0.024). A common concentration threshold of 10 ng/mL was observed across all three passages (passage 1, p<0.000; passage 2, p<0.000; passage 3, p<0.000). At 20 ng/mL, expression levels began

to differ between passages (passage 1 vs. passage 3, $p = 0.024$); however, this difference gradually disappeared by 50 ng/mL.

MMP13 had the same TNF α concentration threshold as MMP3 (10 ng/mL) but differed in its response beyond this threshold (Fig. 10b). In chondrocytes from passage 1, MMP13 expression plateaued and persisted up to 100 ng/mL (10ng/mL, passage 1, $p<0.000$; 10ng/mL, passage 2, $p=0.002$; 10ng/mL, $p<0.000$). In contrast, expression levels in passage 2 and passage 3 initially increased with rising TNF α concentrations but later declined. Furthermore, at TNF α concentrations above 10 ng/mL, significant differences emerged between passages (10ng/mL, passage 1 vs. passage 3: $p=0.008$, passage 1 vs. passage 2: $p=0.139$, passage2 vs. passage3: $p=0.011$; 20ng/mL, passage 1 vs. passage 3: $p=0.004$, passage 1 vs. passage 2: $p=0.002$, passage2 vs. passage3: $p=0.094$; 50ng/mL, passage 1 vs. passage 3: $p=0.161$, passage 1 vs. passage 2: $p=0.002$, passage2 vs. passage3: $p=0.002$; 100ng/mL, passage 1 vs. passage 3: $p=0.011$, passage 1 vs. passage 2: $p=0.2$, passage2 vs. passage3: $p=0.001$).

3.1.1.3 Inflammation

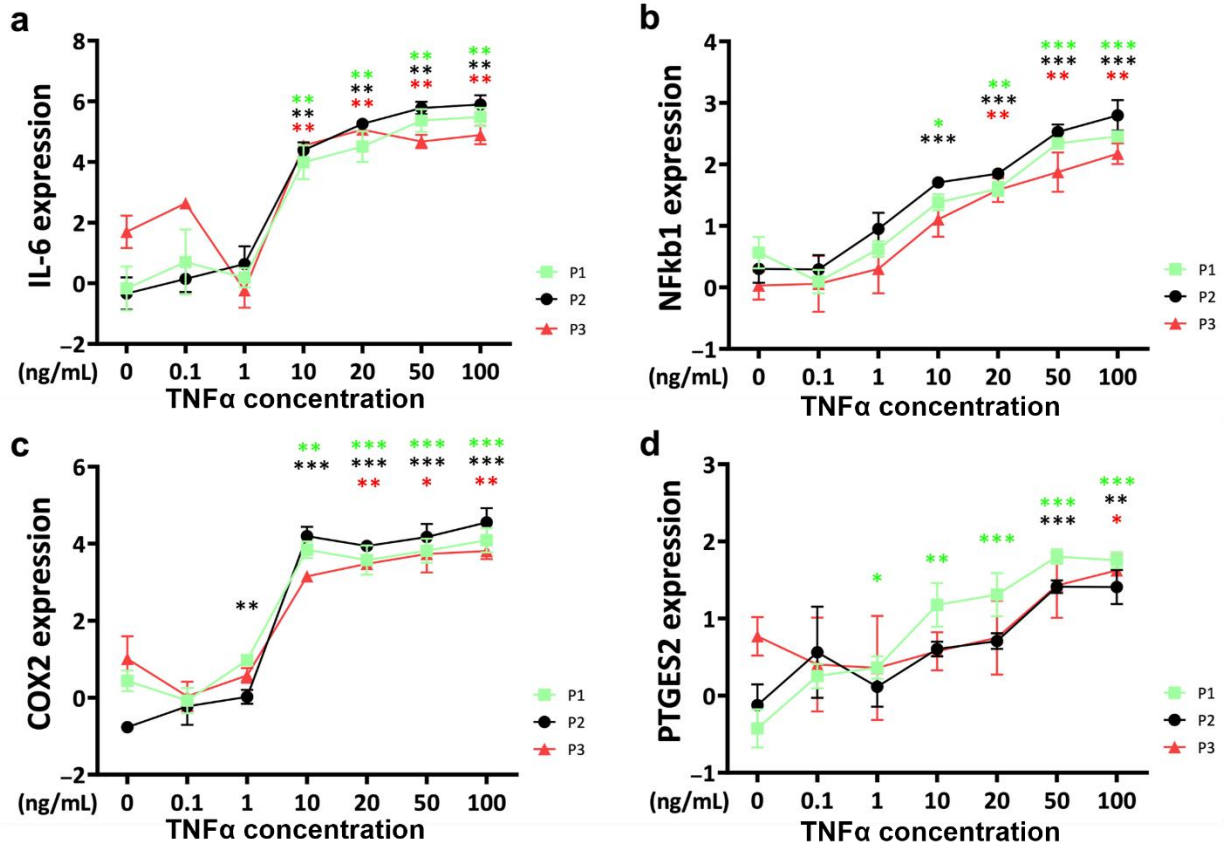


Fig. 11: Inflammation gene expression of experiment one. (a) Interleukin-6 (IL-6), (b) Nuclear Factor kappa-light-chain-enhancer of activated B cells 1 (NFkb1), (c) Cyclooxygenase 2 (COX2), (d) Prostaglandin E Synthase 2. Pellets were treated by TNF α at different concentrations (0.1 ng/mL-100 ng/mL) for 48h. The results for chondrocyte pellets from passages 1, 2, and 3 were represented by green, black, and red curves, respectively. Statistical comparisons to the control group for each passage were indicated by green, black, and red stars. To enhance interpretability and facilitate analysis, the gene expression data were natural log-transformed. For clarity, statistical significance between passages was not shown. * p < 0.05; ** p < 0.01; *** p < 0.001. P1: passage 1; P2: passage 2; P3: passage 3 and '0' represented control group (Ossendorff et al., 2024c).

Interleukin-6 (IL-6) is a multifunctional cytokine that plays a crucial role in immune responses, inflammation, and tissue repair (Pearson et al., 2017). At a TNF α concentration of 10 ng/mL, IL-6 gene expression increased rapidly, reaching significant levels in all three passages (passage1, p=0.003; passage 2, p=0.009; passage3, p=0.001), and this elevated expression persisted (Fig. 11a). Interestingly, chondrocytes in passage 3 exhibited higher IL-6 expression at low TNF α concentrations (0.1ng/mL) compared with

passage 1 (passage 1 vs. passage 3, $p=0.043$); however, this difference quickly diminished as TNF α concentrations increased. By 50 ng/mL, and even at 100 ng/mL, IL-6 expression in passage 3 chondrocytes fell below that of passage 1 or passage 2 (50ng/m, passage1 vs. passage3: $p =0.046$; 100ng/mL, passage2 vs. passage3: $p=0.024$).

Nuclear Factor kappa-light-chain-enhancer of activated B cells 1 (NFkb1) is a key component of the NFkb pathway which is crucial for regulating immune response, inflammation (Choi et al., 2019; Goldring and Otero, 2011). TNF α increased NFkb1 expression in a concentration-dependent manner, although individual passages differed in their sensitivity to TNF α ($p=0.001$). Passage 3 was the least sensitive, showing no significant increase in expression until TNF α reached 20 ng/mL (Fig. 11b). The lowest expression levels were observed in passage 3 compared with passage 2 and passage 1, but this difference was not always significant (100ng/mL, passage 1 vs. passage3: $p=0.047$, passage 2 vs. passage3, $p=0.024$; 50ng/mL, passage1 vs. passage3: $p=0.222$, passage2 vs. passage3: $p=0.136$; 20ng/mL, passage1 vs. passage3: $p=0.627$, passage2 vs. passage3: $p=0.34$; 10ng/mL, passage1 vs. passage3: $p=0.965$, passage2 vs. passage3: $p=0.05$; 1ng/mL, passage1 vs. passage3: $p=0.791$, passage2 vs. passage3: $p=0.397$; 0.1ng/mL, passage1 vs. passage3: $p=0.408$, passage2 vs. passage3: $p=0.383$;).

Cyclooxygenase 2 (COX2) is an enzyme involved to the synthesis of prostaglandins and related to inflammation, pain, and fever (Lianxu et al., 2006; Ulivi et al., 2008). The common TNF α threshold for different passages was 20 ng/mL, beyond which the increase in COX2 gene expression gradually slowed (passage1, $p<0.000$; passage2, $p<0.000$; passage3, $p=0.007$) (Fig. 11c). Additionally, COX2 expression in the control group of passage 2 was lower than that in passage 1 and passage 3 (passage 1 vs. passage 2, $p=0.004$; passage 2 vs. passage 3, $p=0.001$), leading to a significant increase in COX2 expression at 1 ng/mL TNF α stimulation ($p=0.008$).

TNF α supplementation induced an upregulation of PTGES2 gene expression, with varying concentration thresholds across passages (passage 1, 1ng/mL, $p=0.015$; passage 2, 50ng/mL, $p<0.001$; passage 3, 100ng/mL, $p=0.031$) (Fig. 11d). Notably, no significant differences in gene expression levels between passages were observed except in the control group, where PTGES2 expression in passage 3 was higher than in the other two passages (passage 1 vs. passage 3, $p=0.004$; passage 2 vs. passage 3, $p=0.038$).

3.1.1.4 Apoptosis

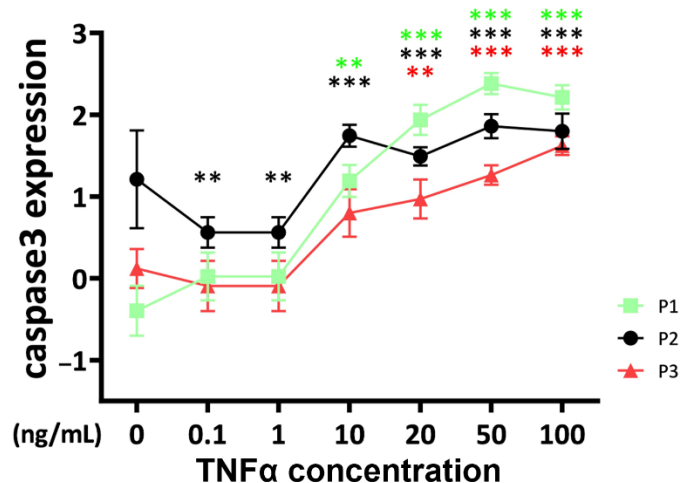


Fig. 12: Apoptosis gene expression of experiment one. Pellets were treated by TNF α at different concentrations (0.1 ng/mL-100 ng/mL) for 48h. The results for chondrocyte pellets from passages 1, 2, and 3 were represented by green, black, and red curves, respectively. Statistical comparisons to the control group for each passage were indicated by green, black, and red stars. To enhance interpretability and facilitate analysis, the gene expression data were natural log-transformed. For clarity, statistical significance between passages was not shown. * $p < 0.05$; ** $p < 0.01$; *** $p < 0.001$. P1: passage 1; P2: passage 2; P3: passage 3 and '0' represented control group (Ossendorff et al., 2024c).

Caspase 3 is a key enzyme in chondrocytes apoptosis (Porter and Jänicke, 1999). Taken together, TNF α application increased caspase-3 expression, but the response of chondrocytes varied slightly between passages (Fig. 12). Chondrocytes in passage 2 exhibited a significant increase in gene expression after stimulation with 10 ng/mL TNF α ($p < 0.000$), whereas at 0.1–1 ng/mL, expression levels were even lower than in the control group (0.1 ng/mL, $p = 0.008$; 1 ng/mL, $p = 0.008$). In contrast, a TNF α concentration of 20 ng/mL was required to induce a response in passages 1 and 3 (passage 1, $p < 0.000$; passage 3, $p = 0.008$). Notably, caspase-3 expression in passage 3 was lower than in passages 1 and 2, particularly at TNF α concentrations of 20 ng/mL and 50 ng/mL (20ng/mL, passage 1 vs. passage 3: $p = 0.014$, passage 2 vs. passage 3: $p = 0.161$; 50ng/mL, passage 1 vs. passage 3: $p < 0.000$, passage 2 vs. passage 3: $p = 0.006$).

3.1.2 Analysis of Glycosaminoglycans and ELISA

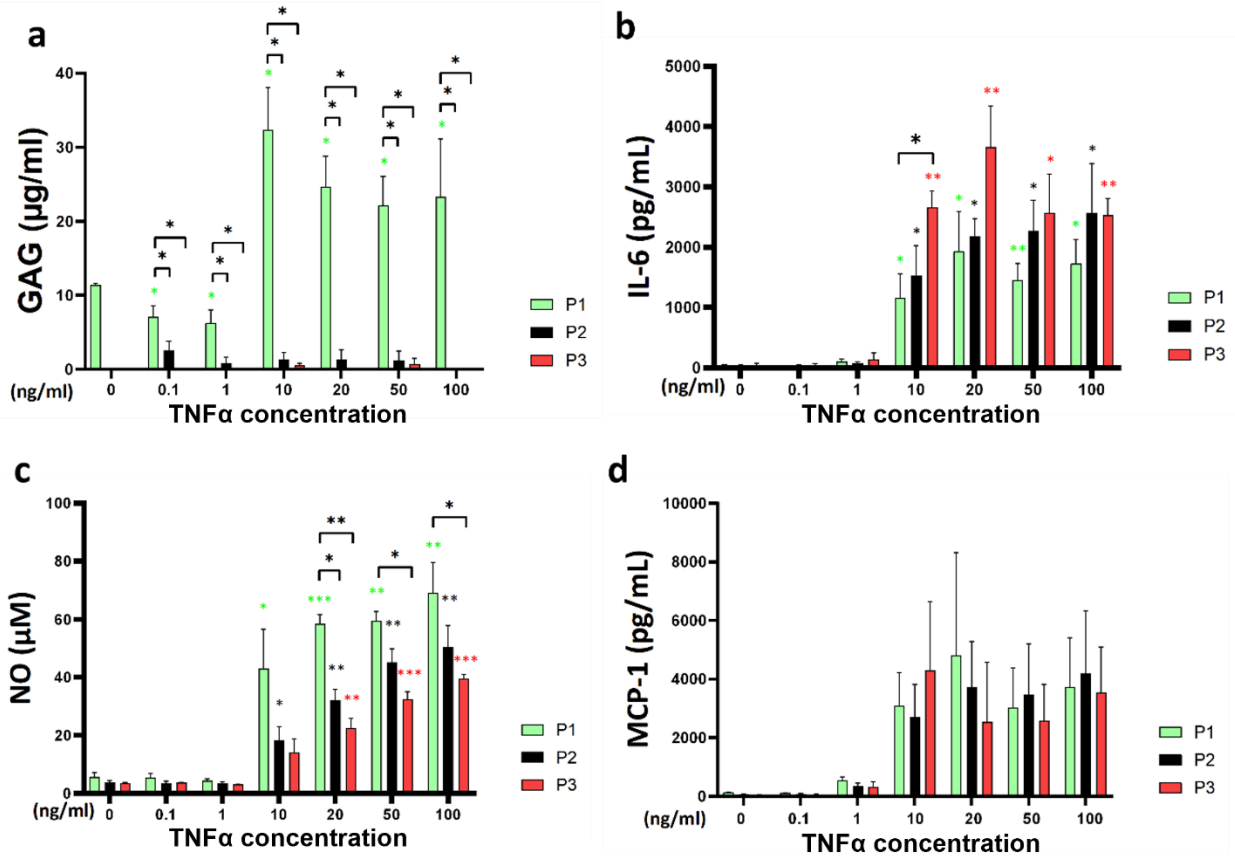


Fig. 13: Analysis of proteoglycan and inflammation related molecules. (a) Glycosaminoglycans (GAG; μ g/mL), nitric oxide (NO; μ M), interleukin-6 (IL-6; pg/mL), monocyte chemoattractant protein-1 (MCP-1; pg/mL). Pellets were treated by TNF α at different concentrations (0.1 ng/mL-100 ng/mL) for 48h. Comparisons with the relevant control group were shown by the green, black, and red stars, respectively. * $p < 0.05$; ** $p < 0.01$; *** $p < 0.001$. P1: passage 1; P2: passage 2; P3: passage 3 and '0' represented control group (Ossendorff et al., 2024c).

The amount of glycosaminoglycans (GAGs) released into the medium was significantly affected by TNF α and varied markedly between passages, with this difference observed at a TNF α concentration of 0.1 ng/mL (passage 1 vs. passage 2: $p = 0.049$; passage 1 vs. passage 3: $p = 0.037$) (Fig. 13a). Interestingly, at 0.1 ng/mL TNF α , GAG release was lower than in the control group ($p = 0.049$); however, this trend reversed at 10 ng/mL TNF α stimulation ($p=0.035$). At higher TNF α concentrations, GAG release remained relatively stable in passage 1.

Similar to IL-6 gene expression result, IL-6 in the medium were significantly elevated when TNF α reached 10 ng/mL, with the highest IL-6 concentration observed in passage 3 ($p=0.049$) (Fig. 13b). Beyond this point, increasing TNF α concentration did not consistently raise IL-6 levels, which was consistent with the gene expression results.

Overall, NO release increased with increasing TNF α concentration, but the TNF α concentration required to stimulate NO production varied across chondrocyte passages (Fig. 13c). Notably, chondrocytes in passage 1 released the highest amount of NO at a TNF α concentration of 20 ng/mL (passage 1 vs. passage 3: $p=0.001$, passage 1 vs. passage 2: $p=0.006$), and this trend persisted even under higher TNF α stimulation.

Monocyte Chemoattractant Protein-1 (MCP-1) is a chemokine related to chondrocyte immune responses and ECM degradation (Akagi et al., 2009). TNF α supplementation resulted in an increase in MCP-1 production; however, these differences did not reach statistical significance, and no substantial differences were observed between passages (Fig. 13d).

3.2 Results of Experiment Two

Overall, the application of TNF α exerted a negative impact on chondrocyte pellets by reducing the expression of anabolic genes while increasing the expression of catabolic, apoptosis and inflammatory genes. The results indicate that on day 4, most genes were more sensitive to TNF α stimulation compared to day 14, as evidenced by a more rapid change in expression at lower concentrations of TNF α (like group 20-0 and 20-0.2). Certain genes, such as COMP, Collagen 1, MMP13, and Caspase-3, showed significant changes in expression at lower concentrations of TNF α on Day 4, but increasing the TNF α concentration did not elicit a stronger response. In contrast, other genes, such as MMP3, IL6, and COX2, exhibited different patterns of expression. For some genes, including MMP3, COX2, IL6, and NF κ B1, the responses to the same TNF α concentration were markedly different between Day 4 and Day 14.

3.2.1 Gene Expression

3.2.1.1 Anabolic Markers

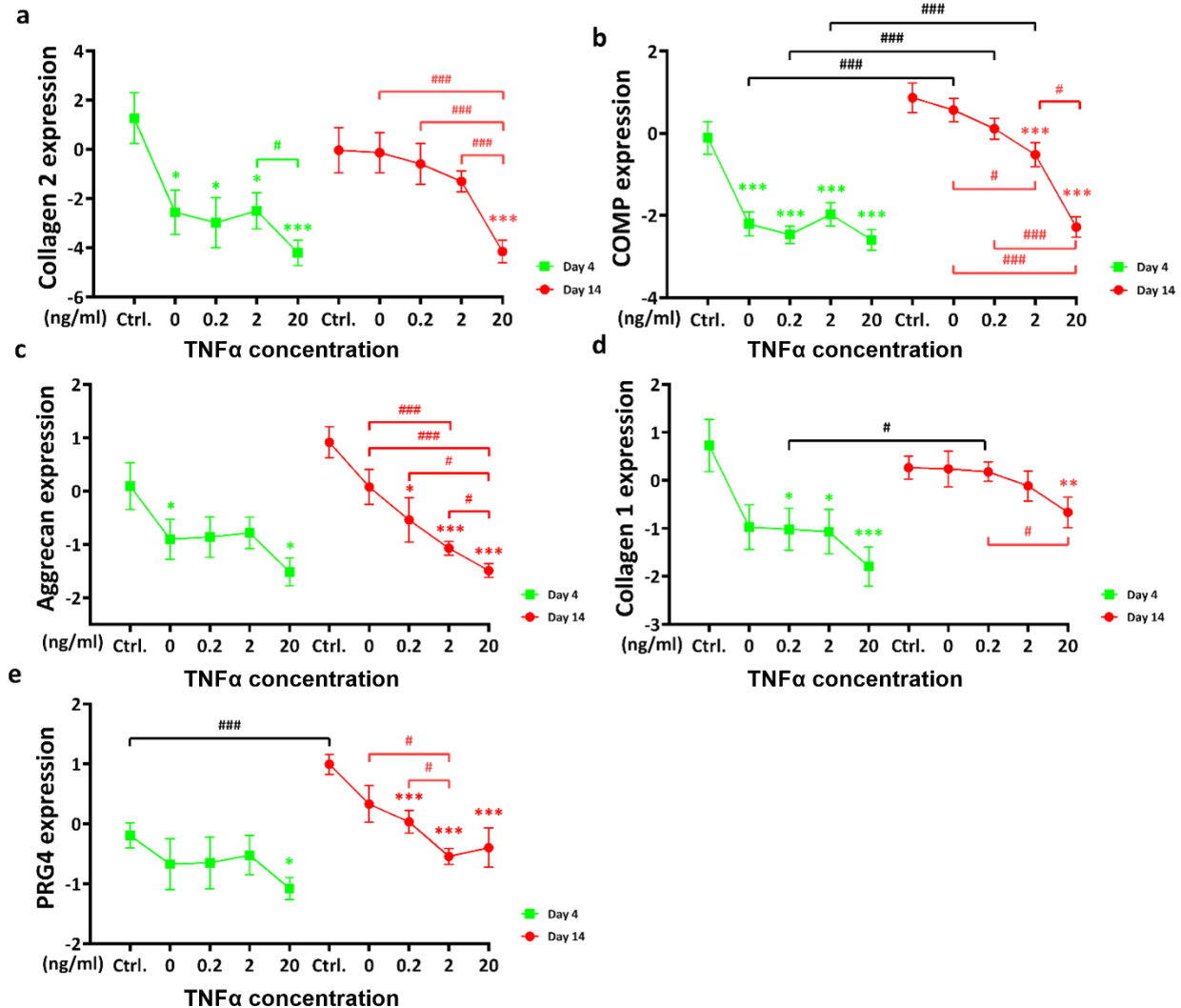


Fig. 14: Gene expression of anabolic markers in experiment two. (a) Collagen 2 (Col2), (b) Cartilage oligomeric matrix protein (COMP), (c) Aggrecan (AGN), and (d) Collagen 1 (Col1), (e) Proteoglycan 4 (PRG4). 'Ctrl.' represented the control group, while 0, 0.2, 2, and 20 indicated experimental groups exposed to different TNF α concentrations. Specifically, bovine chondrocyte pellets were initially treated with 20 ng/mL of TNF α for 48 hours, followed by exposure to varying TNF α doses (0 ng/mL, 0.2 ng/mL, 2 ng/mL, or 20 ng/mL) for 12 days. Gene expression data were normalized to day 0 and natural log transformed. *p < 0.05; **p < 0.01; ***p < 0.001. #p < 0.05; ##p < 0.01; ###p < 0.001. Stars in different colors indicate comparisons with the control group on day 4 and day 14, respectively.

Collagen 2 gene expression was reduced by TNF α supplementation on both day 4 and day 14 (Fig. 14a). For result of day 4, stimulation with 20 ng/mL TNF α for 48 hours caused a significant decrease in Collagen 2 expression (day 4, 20-0 vs. 0, p=0.039). However, subsequent treatment with 0.2 ng/mL or 2 ng/mL TNF α for the following 2 days did not result in a further decrease in gene expression. When the TNF α concentration was increased to 20 ng/mL for the subsequent 2 days, although gene expression levels decreased further, the change was not statistically significant (day 4, 20-0 vs. 20-20, p=0.153). Interestingly, the difference in gene expression levels between the 20-2 group and the 20-20 group on day 4 was significant (day 4, 20-2 vs. 20-20, p=0.047).

For day 14, stimulation with 20 ng/mL TNF α just for the first 48 hours alone did not reduce Collagen 2 gene expression level. However, a significant decrease in expression was observed when TNF α was maintained at the highest concentration of 20 ng/mL for the subsequent 12 days. Notably, when 20 ng/mL TNF α was used to stimulate chondrocytes for either 4 days or 14 days, the final Collagen 2 gene expression levels were similar (20-20, day 4 vs. day 14, p=0.825).

COMP gene expression was negatively affected by TNF α on both day 4 and day 14 (Fig. 14b). On day 4, stimulation with 20 ng/mL TNF α for 48 hours caused a significant decrease in COMP expression (day 4, 20-0 vs. 0, p=0.004). After this initial decrease, the effect appeared to plateau, as higher concentrations of TNF α (0.2 ng/mL to 20 ng/mL) applied over the next 2 days did not produce a stronger effect. On day 14, the effect of TNF α on COMP expression was concentration-dependent. However, following the initial 20 ng/mL TNF α stimulation for 48 hours, subsequent TNF α concentrations below 2 ng/mL over the next 12 days failed to sustain the suppressive effect. When TNF α was maintained at 20 ng/mL for the full 14 days, the suppressive effect was enhanced, the difference was statistically significant (day 14, 20-2 vs. 20-20, p=0.001). Interestingly, apart from the 20-20 group, all other groups showed higher COMP gene expression levels on day 14 compared to day 4 (20-0, day 4 vs. day 14, p=0.002; 20-0.2, day 4 vs. day 14, p=0.002; 20-2, day 4 vs. day 14, p=0.005). For the 20-20 group, gene expression levels between day 4 and day 14 remained similar (20-20, day 4 vs. day 14, p=0.402).

Aggrecan expression was decreased by the effect of TNF α (Fig. 14c). Interestingly, on day 4, a significant reduction in aggrecan levels was observed when cells were stimulated

with TNF α at a concentration of 20 ng/mL for just two days (day 4, 20-0 vs. 0, p=0.039). However, if the subsequent supplementation was at a lower concentration (0.2 ng/mL or 2 ng/mL), the change in gene expression was not significant. A significant reduction was only observed when TNF α concentration was maintained at 20 ng/mL for an additional 48 h (day 4, 20-20 vs. 0, p=0.024). The negative impact of TNF α on aggrecan expression was concentration-dependent by day 14. The concentration of TNF α during the subsequent 12 days played a critical role in influencing aggrecan gene expression, with higher concentrations exerting a stronger negative effect (day 14, 20-20 vs. 20-2, p=0.046; day 14, 20-20 vs. 20-0.2, p=0.049). A significant difference was first noted in the 20-0.2 group (day 14, 20-0.2, p=0.037). It is noteworthy that, although the gene expression patterns differed between day 4 and day 14, the differences in gene expression levels within each concentration group did not reach statistical significance.

Collagen 1 gene expression was negatively impacted by the addition of TNF α (Fig. 14d). Notably, on day 4, collagen 1 expression sharply declined following stimulation with 20 ng/mL of TNF α for two days (day 4, 20-0 vs. 0, p=0.05). Subsequent supplementation with lower concentrations did not result in a noticeable further reduction in gene expression. However, an additional 48 h stimulation with 20 ng/mL of TNF α further suppressed collagen 1 expression, although the difference was not statistically significant (day 4, 20-20 vs. 20-2, p=0.171). On day 14, TNF α continued to reduce collagen 1 expression, with the highest concentration group (20-20) showing a significant decrease (day 14, 20-20 vs. 0, p=0.011). Although the decline in gene expression on day 14 was more gradual compared to day 4, there was no significant difference in gene expression level on these two time point especially between the highest concentration groups (20-20, day 4 vs. day 14, p=0.153).

PRG4 expression was suppressed by TNF α supplementation at both day 4 and day 14 (Fig. 14e). At lower concentrations (day 4: 20-0, 20-0.2, and 20-2 groups), TNF α treatment over four days did not result in a strong inhibitory effect. A significant reduction in PRG4 expression was observed only in the highest concentration group (20-20), where cells were stimulated with 20 ng/mL TNF α for four days (day 4, 20-20 vs. 0, p=0.015). By day 14, a remarkable decrease in PRG4 was evident in the 20-0.2 group (day 14, 20-0.2 vs. 0, p=0.004). After an initial 48 h stimulation with 20 ng/mL TNF α , PRG4 expression

became more sensitive to subsequent $\text{TNF}\alpha$ exposure over the following 12 days compared to the results on day 4. Interestingly, the inhibitory effect seemed to reach saturation at a concentration of 2 ng/mL, as higher concentrations did not result in further suppression of PRG4 expression (day 14, 20-20 vs. 20-2, $p=0.315$).

Notably, PRG4 expression levels in the control groups differed significantly between the two time points (0, day 4 vs. day 14, $p<0.001$). This difference may be attributed to PRG4's role as a surface matrix marker. On day 4, the extracellular matrix produced by chondrocytes was likely less mature, resulting in lower baseline PRG4 expression. By day 14, as the matrix matured, chondrocytes likely upregulated PRG4 expression to further develop surface markers. This progression may also explain why the decline in PRG4 expression on day 14 was more pronounced; the increased abundance of surface markers rendered the cells more sensitive to $\text{TNF}\alpha$ -induced suppression.

3.2.1.2 Catabolic Markers

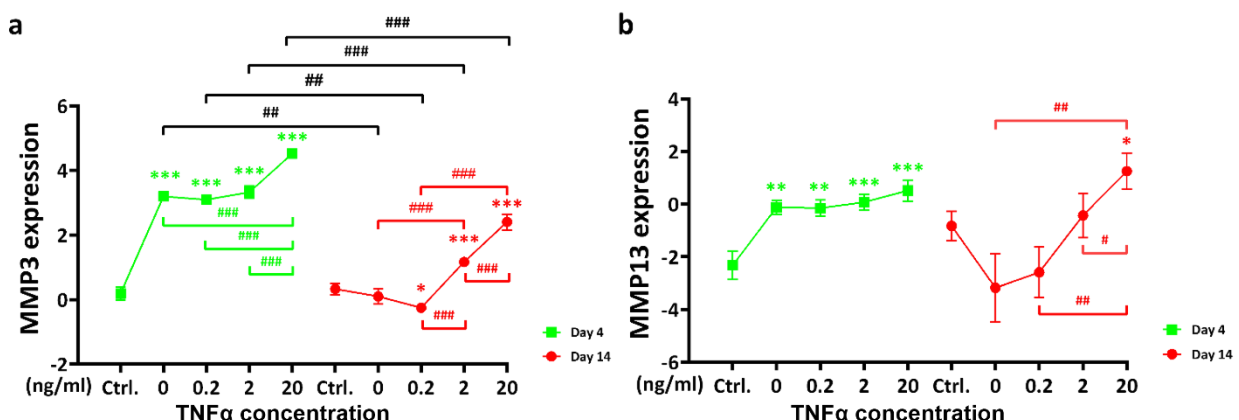


Fig. 15: Gene expression of catabolic markers in experiment two. (a) Matrix metalloproteinase 3 (MMP3), (b) Matrix metalloproteinase 13 (MMP13). 'Ctrl.' represented the control group, while 0, 0.2, 2, and 20 indicated experimental groups exposed to different $\text{TNF}\alpha$ concentrations. Specifically, bovine chondrocyte pellets were initially treated with 20 ng/mL of $\text{TNF}\alpha$ for 48 hours, followed by exposure to varying $\text{TNF}\alpha$ doses (0 ng/mL, 0.2 ng/mL, 2 ng/mL, or 20 ng/mL) for 12 days. Gene expression data were normalized to day 0 and natural log transformed. * $p < 0.05$; ** $p < 0.01$; *** $p < 0.001$. # $p < 0.05$; ## $p < 0.01$; ### $p < 0.001$. Stars in different colors indicate comparisons with the control group on day 4 and day 14, respectively.

MMP3 expression was markedly increased by the supplementation of TNF α on day 4 (Fig. 15a), with a statistically significant difference observed starting from the 20-0 group (day 4, 20-0 vs. 0, p<0.001). Subsequent lower concentrations, such as 0.2 ng/mL and 2 ng/mL, showed minimal effects on gene expression. However, a further increase in TNF α concentration to 20 ng/mL significantly enhanced MMP3 expression (day 4, 20-20 vs. 20-2, p<0.001). By day 14, MMP3 gene expression exhibited a slight reduction in the 20-0 group, and this decrease reached statistical significance in the 20-0.2 group (day 14, 20-0.2 vs. 0, p=0.028). Interestingly, the gene expression level began to rise instead of decline when subsequent concentrations reached 2 ng/mL or higher, surpassing the control group levels in the 20-2 group (day 14, 20-2 vs. 0, p<0.001). Notably, the gene expression patterns differed between the two time points. Additionally, expression levels were consistently lower on day 14 compared to day 4 across all groups (20-0, day 4 vs. day 14, p=0.001; 20-0.2, day 4 vs. day 14, p=0.001; 20-2, day 4 vs. day 14, p<0.001; 20-20, day 4 vs. day 14, p<0.001).

TNF α also increased MMP13 expression on day 4 (Fig. 15b). This effect was observed as early as the 20-0 group (day 4, 20-0 vs. 0, p<0.001), while subsequent lower concentrations showed no remarkable additional effect. By day 14, MMP13 expression levels decreased in the lower concentration groups (20-0 and 20-0.2), although these reductions were not statistically significant. Interestingly, when TNF α concentration was increased to 2 ng/mL for the subsequent 12 days, it appeared to counteract the potential negative feedback adjustments caused by the initial 48-hour stimulation, bringing MMP13 expression back to control level. Continuous stimulation with TNF α at 20 ng/mL over the entire 14 days period significantly increased MMP13 gene expression (day 14, 20-20 vs. 0, p=0.031). This effect was also significant compared to the other treatment groups (day 14, 20-20 vs. 20-2, p=; day 14, 20-20 vs. 20-0.2, p=; day 14, 20-20 vs. 20-0, p=).

Notably, continuous stimulation with 20 ng/mL TNF α for 14 days not only significantly elevated MMP13 expression compared to the control group but also when compared to other groups (day 14, 20-20 vs. 20-2, p=0.047; 20-20 vs. 20-0.2, p=0.004; 20-20 vs. 20-0, p=0.005). In particular, although the gene responses to stimulation with different concentrations of TNF α varied at the two time points, there were no significant differences in gene expression levels within the same concentration groups.

3.2.1.3 Inflammatory Makers

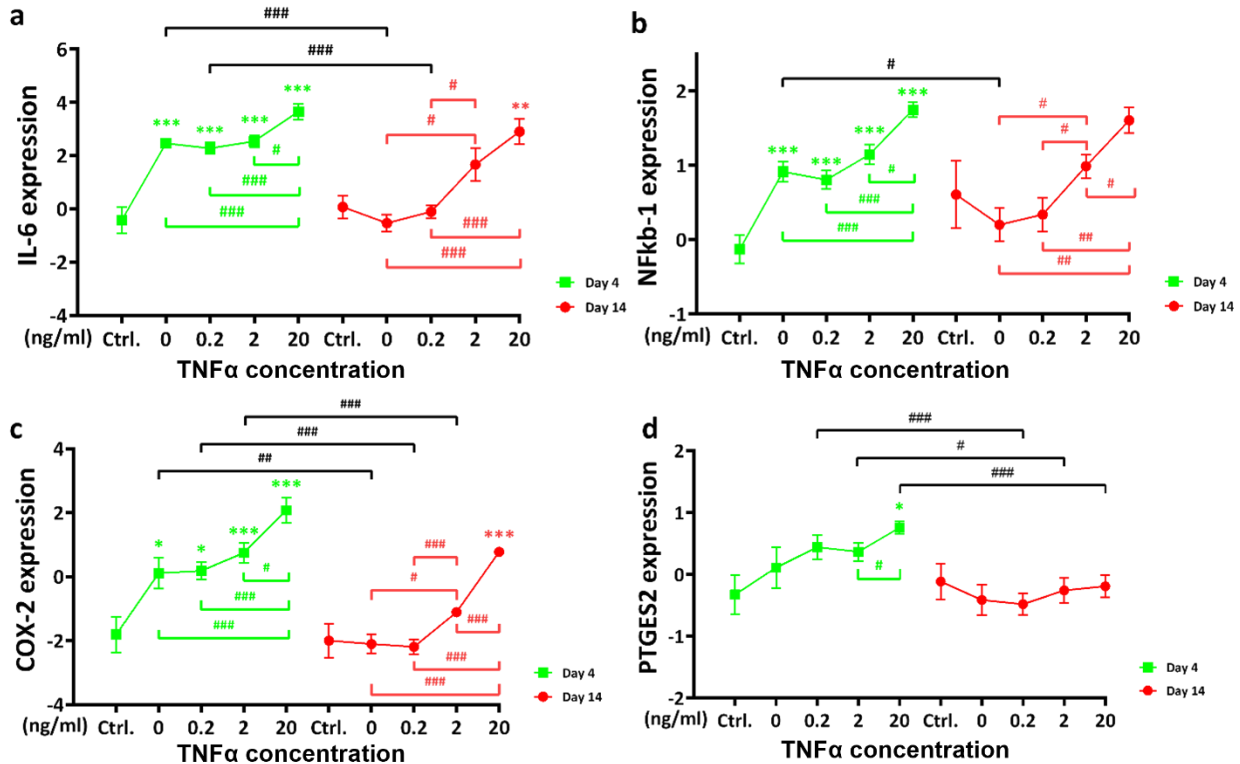


Fig. 16: Gene expression of inflammatory markers in experiment two. (a) Interleukin-6 (IL-6), (b) Nuclear Factor kappa-light-chain-enhancer of activated B cells 1 (NFkb1), (c) Cyclooxygenase-2 (COX2), and (d) Prostaglandin E Synthase 2 (PTGES2). ‘Ctrl.’ represented the control group, while 0, 0.2, 2, and 20 indicated experimental groups exposed to different TNF α concentrations. Specifically, bovine chondrocyte pellets were initially treated with 20 ng/mL of TNF α for 48 hours, followed by exposure to varying TNF α doses (0 ng/mL, 0.2 ng/mL, 2 ng/mL, or 20 ng/mL) for 12 days. Gene expression data were normalized to day 0 and natural log transformed. *p < 0.05; **p < 0.01; ***p < 0.001. #p < 0.05; ##p < 0.01; ###p < 0.001. Stars in different colors indicate comparisons with the control group on day 4 and day 14, respectively.

IL-6 expression was sharply increased following TNF α supplementation (Fig. 16a, day 4). A 48 h stimulation with TNF α at 20 ng/mL significantly induced IL-6 expression (day 4, 20-0 vs. 0, p<0.001). Subsequent supplementation at a lower concentration (0.2 ng/mL) did not result in any obvious substantial further increase. When the concentration was raised to 2 ng/mL, IL-6 expression increased slightly, but the difference was not statistically significant (day 4, 20-2 vs. 20-0.2, p=0.328; day 4, 20-2 vs. 20-0, p=0.758). Continued

stimulation with 20 ng/mL for another 48 h further elevated IL-6 expression to a significant degree (day 4, 20-20 vs. 20-2, $p=0.014$). By day 14, lower concentrations (20-0 and 20-0.2 groups) did not show a noticeable effect on IL-6 expression (day 14, 20-0.2 vs. 0, $p=0.959$; day 14, 20-0 vs. 0, $p=0.247$). The medium concentration group (20-2, day 14) induced an increase, but it was not statistically significant yet (day 14, 20-2 vs. 0, $p=0.083$). Only the highest concentration group (20-20) significantly elevated IL-6 expression (day 14, 20-20 vs. 0, $p=0.004$). Remarkably, while the lower concentration groups (20-0 and 20-0.2) on day 14 had a weaker effect compared to IL-6 respective levels on day 4 (20-0, day 4 vs. day 14, $p<0.001$; 20-0.2, day 4 vs. day 14, $p<0.001$), the highest concentration group (20-20) was able to restore IL-6 expression to the same level observed on day 4 (20-20, day 4 vs. day 14, $p=0.34$).

NF κ B1 expression levels were rapidly upregulated by TNF α supplementation across all groups on day 4 (Fig. 16b). This effect was evident starting from the 20-0 group (day 4, 20-0 vs. 0, $p=0.002$). Increasing the TNF α concentration of the next two days did not show a significantly stronger effect until it reached 20 ng/mL (day 4, 20-20 vs. 20-2, $p=0.011$; day 4, 20-20 vs. 20-0.2, $p<0.001$; day 4, 20-20 vs. 20-0, $p<0.001$). At day 14, stimulating chondrocytes with TNF α at 20 ng/mL for just two days initially reduced NF κ B1 expression levels, although this decrease was not statistically significant. Continuous exposure to increasing TNF α concentrations over the subsequent 12 days gradually elevated NF κ B1 expression (day 14, 20-20 vs. 20-2, $p=0.014$; day 14, 20-20 vs. 20-0.2, $p=0.003$; day 14, 20-20 vs. 20-0, $p=0.001$; day 14, 20-2 vs. 20-0.2, $p=0.047$; day 14, 20-2 vs. 20-0, $p=0.031$). Notably, after an initial two days stimulation with TNF α at 20 ng/mL, if no further TNF α supplementation was provided, NF κ B1 expression levels eventually declined by day 14 (20-0, day 4 vs. day 14, $p=0.024$). This reduction may be attributed to a negative feedback mechanism leading to downregulation of expression.

COX-2 expression was upregulated by TNF α stimulation (Fig. 16c). At the day 4 time point, this effect was evident starting with the 20-0 group (day 4, 20-0 vs. 0, $p=0.024$), with the strongest upregulation observed in the 20-20 group (day 4, 20-20 vs. 0, $p<0.001$). At the day 14 time point, lower concentrations of TNF α (20-0 and 20-0.2 groups) did not produce a significant increasing on COX-2 expression (Fig. 16c, day 14) However, an increase in expression was observed in the 20-2 group, with statistically significant upregulation

occurring in the 20-20 group (day 14, 20-20 vs. 0, $p<0.001$). Notably, COX-2 expression levels on day 14 were significantly lower compared to day 4 across all groups respectively, except for the control and 20-20 groups (20-0, day 4 vs. day 14, $p=0.004$; 20-0.2, day 4 vs. day 14, $p<0.001$; 20-2, day 4 vs. day 14, $p<0.001$).

3.2.1.4 Apoptosis

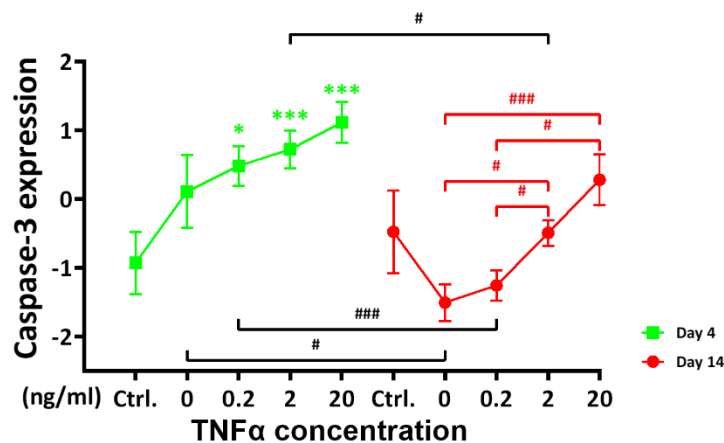


Fig. 17: Gene expression of apoptosis marker in experiment two. ‘Ctrl.’ represented the control group, while 0, 0.2, 2, and 20 indicated experimental groups exposed to different TNF α concentrations. Specifically, bovine chondrocyte pellets were initially treated with 20 ng/mL of TNF α for 48 hours, followed by exposure to varying TNF α doses (0 ng/mL, 0.2 ng/mL, 2 ng/mL, or 20 ng/mL) for 12 days. Gene expression data were normalized to day 0 and natural log transformed. * $p < 0.05$; ** $p < 0.01$; *** $p < 0.001$. # $p < 0.05$; ## $p < 0.01$; ### $p < 0.001$. Stars in different colors indicate comparisons with the control group on day 4 and day 14, respectively.

Caspase-3 expression was upregulated by TNF α stimulation in a concentration-dependent manner on day 4 (Fig. 17). A significant increase was observed in the 20-0.2 group (day 4, 20-0.2 vs. 0, $p=0.024$). At the day 14 time point, TNF α supplementation initially reduced caspase-3 expression (day 14, 20-0 vs. 0, $p=0.161$). However, as the concentration increased over the subsequent 12 days, caspase-3 expression gradually rose, reaching control group levels in the 2 ng/mL group. In the 20-20 group, expression levels exceeded those of the control group, with significant differences observed when compared to lower concentration groups (day 14, 20-20 vs. 20-0.2, $p=0.04$; day 14, 20-20 vs. 20-0, $p=0.008$), although the difference was not significant when compared to the

control group itself (day 14, 20-20 vs. 0, $p=0.133$). Furthermore, with the exception of the control group and 20-20 group, caspase-3 expression levels in all other groups on day 14 were lower than those on day 4 (20-0, day 4 vs. day 14, $p=0.047$; 20-0.2, day 4 vs. day 14, $p<0.001$; 20-2, day 4 vs. day 14, $p=0.019$; 20-20, day 4 vs. day 14, $p=0.133$).

3.2.2 Medium analysis of IL-6, nitric oxide and MCP-1

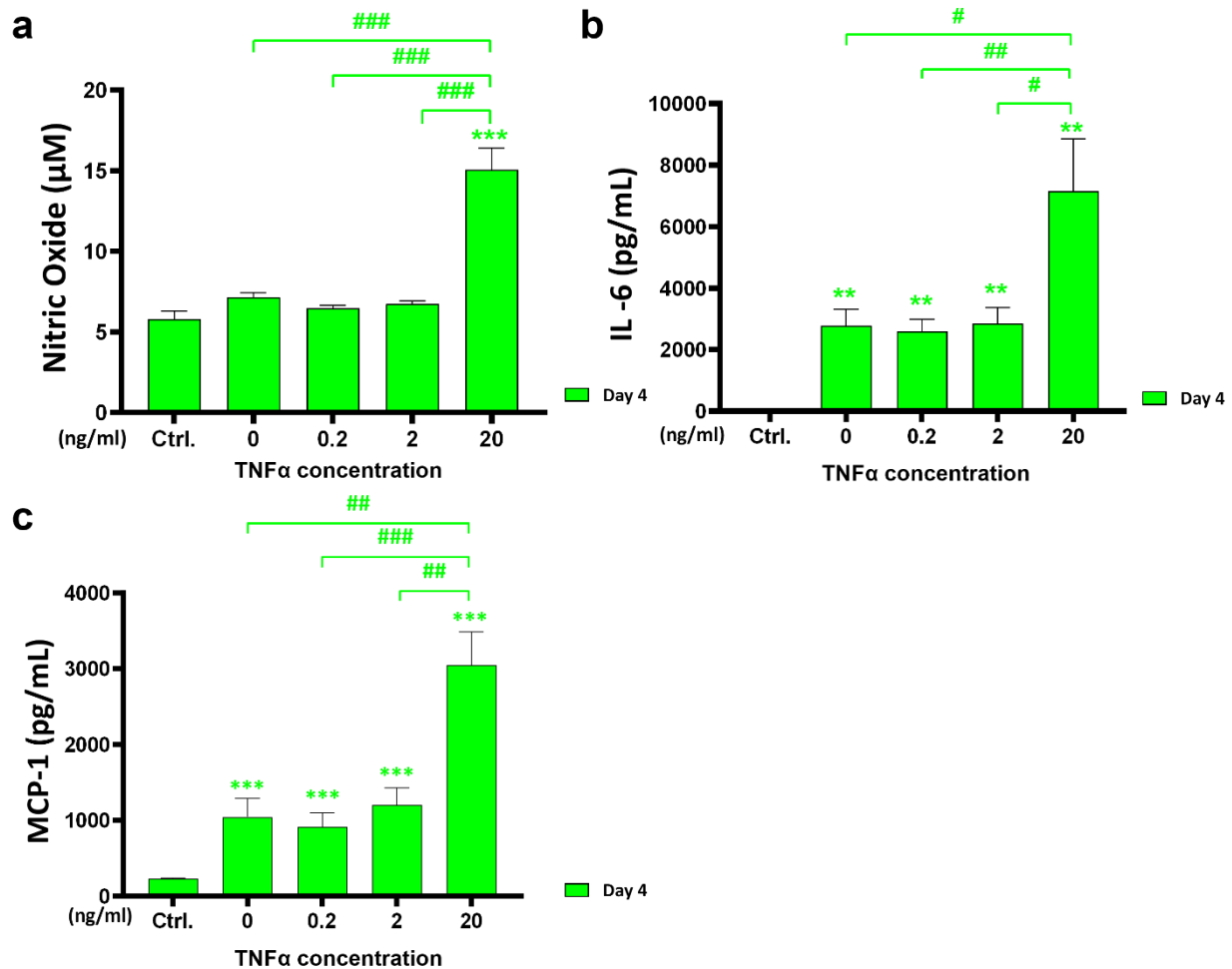


Fig. 18: The analysis of inflammation-related molecules released into the medium. (a) Inflammatory mediator: nitric oxide (NO; μ M); (b) Pro-inflammatory cytokine: interleukin-6 (IL-6; pg/mL); (c) Chemokine: monocyte chemoattractant protein-1 (MCP-1; pg/mL). The medium was collected at day 4. The pellets were initially treated with TNF α at 20 ng/mL for 48 hours, followed by treatment with different concentrations of TNF α (0 ng/mL, 0.2 ng/mL, 2 ng/mL, and 20 ng/mL) for the next 48 hours. 'Ctrl.' stands for the control group. * $p < 0.05$, ** $p < 0.01$, and *** $p < 0.001$; ## $p < 0.01$, and ### $p < 0.001$.

IL-6 released into the medium on day 4 was significantly upregulated by TNF α stimulation (Fig. 18a). In the control group, IL-6 concentration was very low, but stimulation just with TNF α at 20 ng/mL for the first two days caused a significant increase in IL-6 production (20-0 vs. 0, p=0.003), that was consistent with result of experiment one (Fig. 18c). The use of relatively lower doses of TNF α in the following two days did not markedly influence IL-6 production. However, when the TNF α concentration was increased to 20 ng/mL for the subsequent two days, IL-6 production showed a further significant upregulation (20-20 vs. 20-2, p=0.024; 20-20 vs. 20-0.2, p=0.008; 20-20 vs. 20-0, p=0.031), which was consistent with the gene expression results (Fig. 18a).

NO was significantly increased by TNF α stimulation in the 20-20 group (20-20 vs. 0, p<0.001) (Fig. 18b). In contrast, the other groups maintained gene expression levels comparable to the control group. This indicates that after stimulating chondrocytes with TNF α at 20 ng/mL for 48 hours, NO production would return to control group levels if the subsequent TNF α concentration was not sufficiently high.

MCP-1 released into medium showed the supplementation of TNF α of only 48 h could increase its releasement (20-0 vs. 0, p<0.001), and then the releasement reached a plateau, unless TNF α reached 20 ng/mL for the next 2 days could further increase its releasement (20-20 vs. 20-0, p=0.002).

3.2.3 Histology Analysis: Safranin-O Fast Green Staining

Native bovine cartilage, stained with Safranin-O Fast Green, revealed distinct tissue features that highlight the key components of the cartilage matrix. The collagen fibres, which are an essential part of cartilage structure, are stained light blue (Fig. 19). Additionally, the cartilage matrix contains a high content of proteoglycans, which are seen in orange to red areas in the image (Fig. 19). The chondrocytes, marked by black arrows (Fig. 19) are typically arranged either individually or in clusters within lacunae. In healthy cartilage, the distribution of these chondrocytes within the matrix is relatively sparse and uniformly distributed. This uniformity is characteristic of normal cartilage, where the cells are surrounded by a translucent, homogeneous matrix. The even distribution of the matrix and the orderly arrangement of the cells are considered hallmark features of healthy, well-maintained cartilage tissue (Lotz et al., 2010).

In this experiment, bovine chondrocyte pellet sections stained with Safranin-O Fast Green showed a similar pattern, further validating that this in vitro model successfully replicates the key characteristics of normal cartilage (Fig. 19, Fig. 20). To achieve this, we first centrifuged bovine chondrocytes into pellets and allowed them to undergo a one-week period of free swelling. After this, the chondrocyte pellets exhibited a matrix rich in collagen fibers, as indicated by the light blue staining, along with a lower but noticeable presence of proteoglycans, which appeared as orange-red staining (Fig. 19). The development of these matrix components in the pellet was observed even at the initial stage, showing the potential of this model to replicate the tissue-specific characteristics of cartilage. When comparing day 0 to the control group, we observed that after extending the culture period of the chondrocyte pellet to two weeks, the amount of proteoglycans in the matrix increased, reflecting the development of a more mature cartilage structure that was similar to normal cartilage tissue (Fig. 19).

However, based on the quantitative analysis, when comparing the control group with the 20-0 group, we found that TNF α -stimulated pellets (just for 2 days) exhibited both a larger size and a significantly higher proteoglycan content than the control group (Fig. 20, Fig. 21, Fig. 22). But as the TNF α concentration continued to rise, the proteoglycan content decreased rapidly, and the intensity of Safranin-O staining gradually diminished. Further quantitative analysis revealed that increasing TNF α concentrations over the following 12 days led to a further decline in proteoglycan production (Fig. 20, Fig. 22). The significant differences in pellet diameter between experimental groups provide strong evidence that higher TNF α concentrations impair matrix production and compromise the overall structural integrity of the pellet. Overall, this pellet model successfully replicated the fundamental structure of hyaline cartilage (Fig. 3.11). Moreover, as TNF α concentration increased over the subsequent 12 days, the suppression of proteoglycan production became more pronounced, accompanied by a marked reduction in pellet diameter (Fig. 22).

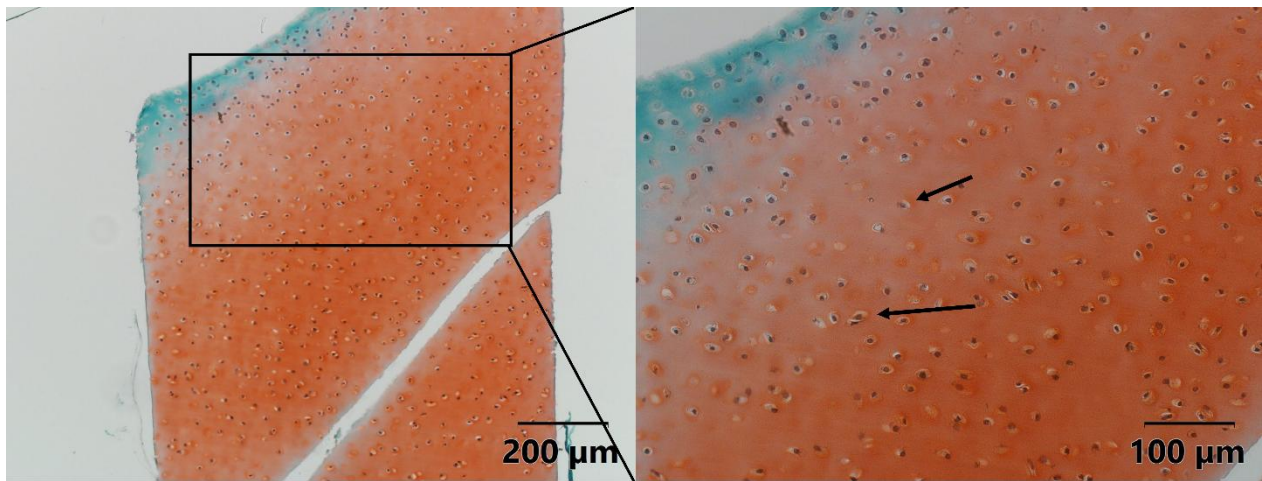


Fig. 19: Safranin-O Fast Green stained slide of normal bovine cartilage. Orange areas represented proteoglycans, and green to light blue areas represented collagen fibers. Chondrocytes were arranged either individually or in clusters within lacunae, as indicated by the black arrows.

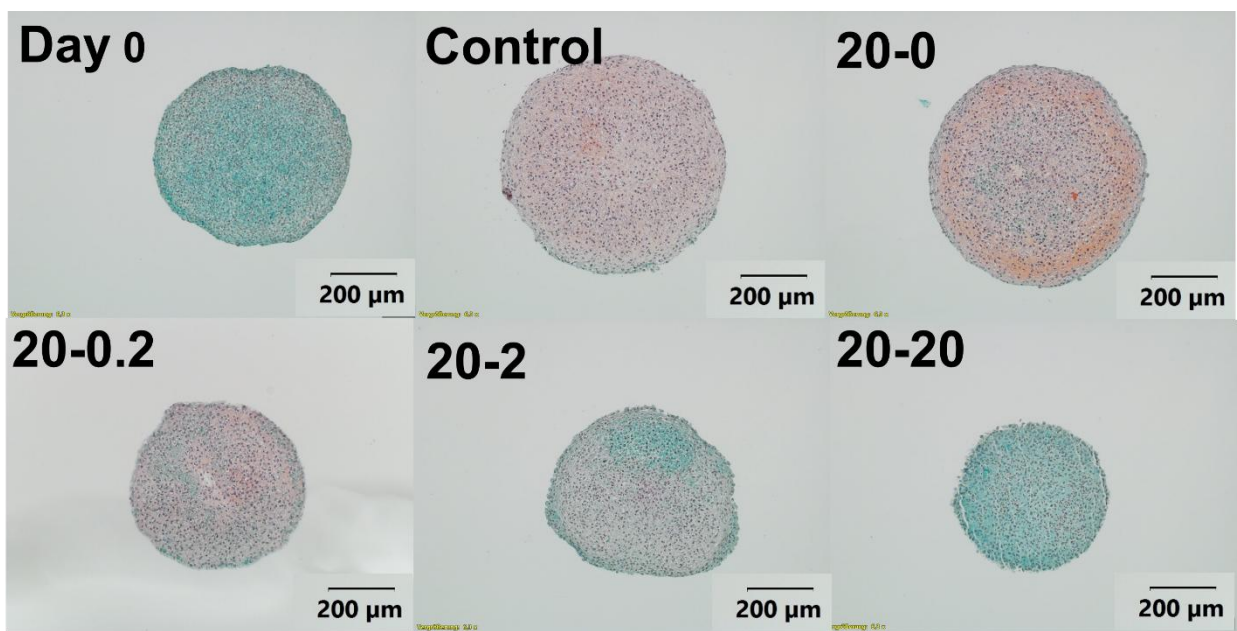


Fig. 20: Safranin-O Fast Green stained slides of chondrocyte pellets. 'Day 0' represented the pellet before TNF α stimulation. 'Control' represented the chondrocyte pellets treated with chondrogenic growth medium without TNF α for 14 days, while '20-0', '20-0.2', '20-2', and '20-20' represented experimental groups stimulated by different TNF α concentrations. Specifically, chondrocyte pellets were initially treated with 20 ng/mL of TNF α for 48 hours, followed by treatment with varying TNF α doses (0 ng/mL, 0.2 ng/mL, 2 ng/mL, or 20 ng/mL) for 12 days.

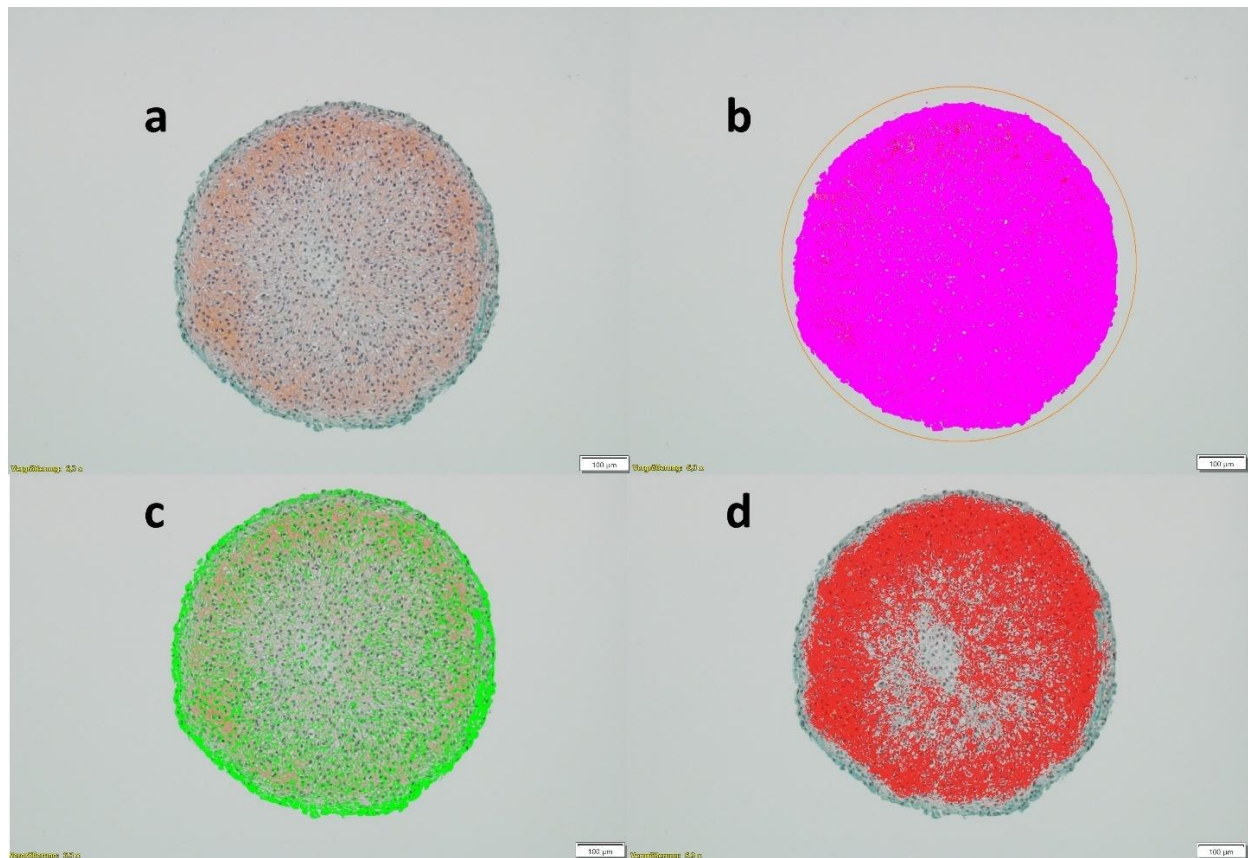


Fig. 21: Example images illustrating the quantitative analysis of a chondrocyte pellet slide using Cell Sense software. (a) Unprocessed Safranin O Fast Green stained slide. (b) The purple area represents the total pellet size. (c) The green area represents the Fast Green stained region, indicating collagen distribution within the chondrocyte pellet. (d) The red area represents the Safranin O-stained region, indicating proteoglycans distribution within the chondrocyte pellet.

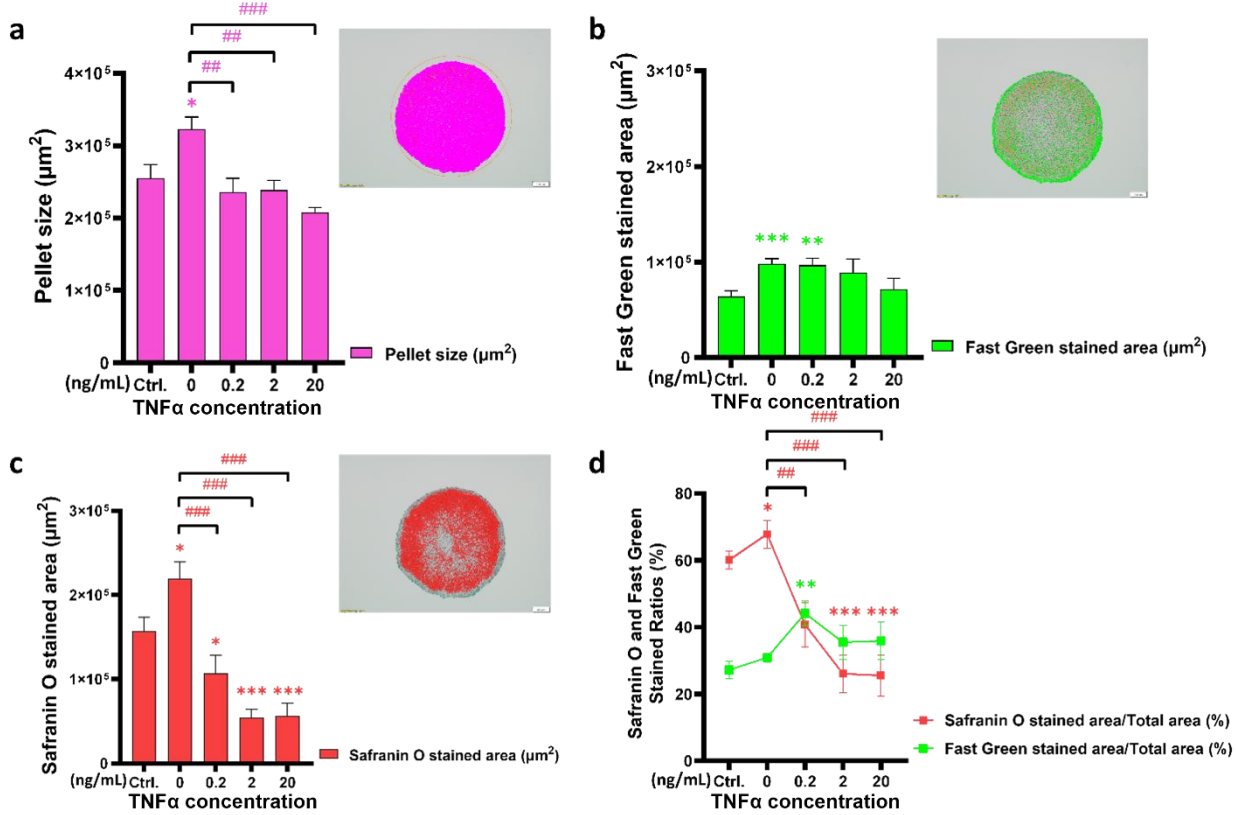


Fig. 22: Quantitative analysis of pellet size, collagens, and proteoglycans content of the pellets. (a) Pellet size analysis. (b) Collagens content analysis. (c) Proteoglycans content analysis. (d) Safranin O staining ratio and Fast Green staining ratio. Stars indicated comparison with the corresponding control group. 'Ctrl.' represented the control group, while 0, 0.2, 2, and 20 indicate experimental groups exposed to different TNF α concentrations. Specifically, bovine chondrocyte pellets were initially treated with 20 ng/mL of TNF α for 48 hours, followed by exposure to varying TNF α doses (0 ng/mL, 0.2 ng/mL, 2 ng/mL, or 20 ng/mL) for 12 days. All data were obtained from pellets at day 14. *p < 0.05, **p < 0.01, ***p < 0.001, #p < 0.05, ##p < 0.01, ###p < 0.001.

4. Discussion

Summary

This study investigated the concentration-dependent effects of TNF α and the influence of chondrocyte expansion in establishing a standardized chondrocyte pellet inflammation model. Additionally, it explored the response of chondrocyte pellets to dynamic TNF α concentrations over time, simulating the natural inflammatory process observed *in vivo*. The goal was to provide a standardized platform for chondrocyte-related research and the development of new therapeutic drugs.

The study identified a concentration threshold of TNF α at 10 ng/mL, beyond which significant inflammatory responses were observed. Passage was found to be a factor influencing chondrocyte reactions to TNF α and should be considered when interpreting related experimental results. Furthermore, dynamic TNF α stimulation successfully mimicked the physiological inflammatory response. Gene expression, protein analysis, and histological assessments confirmed that after inducing inflammation with 20 ng/mL TNF α , a much lower concentration of 0.2 ng/mL was sufficient to sustain the inflammatory state. Overall, TNF α exerted detrimental effects on chondrocytes, and the study revealed that different genes exhibited distinct responses at the early and later stages of inflammation.

4.1 TNF α Concentration Dependent Effect and Stimulation Duration

Many studies have shown that TNF α has detrimental effects on chondrocytes; however, there is a lack of relevant research investigating the concentration threshold at which these effects occur (Caramés et al., 2008; Schuerwagh et al., 2003; Westacott et al., 2000). Besides that, due to variations in study models and their TNF α requirements, comparing results across studies is challenging (Wang et al., 2024). Therefore, a systematic investigation of TNF α concentration and its effects is urgently needed.

According to experiment one, TNF α stimulation of chondrocyte pellets successfully demonstrated its detrimental effects. Meanwhile, we observed that the effects of TNF α were influenced by its concentration.

In experiment one, the results indicated that when TNF α concentration reached 10 ng/mL, chondrocytes exhibited a distinct pathological pattern characteristic of OA, including a

decrease in anabolic activity and an increase in catabolic and inflammatory responses. Therefore, 10 ng/mL of recombinant bovine TNF α can be considered a threshold concentration capable of inducing an inflammatory response. This finding was consistent with previous studies, where TNF α at 10 ng/mL successfully triggered similar inflammatory effects (Caramés et al., 2008; Djouad et al., 2009; Xiang et al., 2019; Campbell et al., 2013).

Beyond identifying the concentration threshold of TNF α , this study also revealed that the response pattern of some genes to TNF α stimulation were concentration-related. Collagen 2 gene expression level varied with different TNF α concentrations. Before reaching the threshold, gene expression declined, although without statistical significance. However, at 10 ng/mL, the reduction in gene expression became significantly different from the control group. When the concentration exceeded the threshold, Collagen 2 gene expression plateaued, showing no further decline even at 100 ng/mL, maintaining a level similar to that observed at 10 ng/mL. This phenomenon was also observed in the expression of MMP13, COX2, as well as in IL-6 secretion. These findings may explain why different studies, despite using varying TNF α concentrations, reported similar experimental outcomes (Ding et al., 2017b; López-Armada et al., 2006; Mohanraj et al., 2018; Malemud et al., 2012).

Interestingly, aggrecan gene expression exhibited a distinct response, showing a significant decline around the threshold concentration. However, beyond this threshold, its expression partially recovered, which may have resulted from negative feedback regulation within chondrocytes.

Experiment one demonstrated that other genes, including COMP, Collagen 1, MMP-3, and NFkb1, exhibited a clear concentration-dependent response to TNF α , with the threshold concentration for significant changes consistently at 10 ng/mL. Tilwani et al. stimulated chondrocytes cultured in agarose with TNF α at concentrations ranging from 0.1 ng/mL to 100 ng/mL and found that 10 ng/mL TNF α significantly increased NO and Prostaglandin E₂ release. Additionally, MMP activity was shown to be concentration-dependent with TNF α stimulation (Tilwani et al., 2017).

Findings from experiment one indicated that constructing an inflammatory chondrocyte model required the cytokine concentration to reach at least the threshold level to

effectively induce an inflammatory response. Furthermore, before and after the concentration threshold, the response of the same gene can be either similar or different. Specifically, COMP showed the same response both before and after the TNF α concentration threshold. In contrast, Collagen 2 exhibited a different response, while MMP-13 demonstrated the opposite response. Therefore, these factors should be considered when comparing results from different studies.

Notably, under physiological conditions, the concentration of TNF α in synovial fluid is significantly lower than the concentrations used in this study. However, based on the results of this study, TNF α must reach a specific threshold to induce a significant inflammatory response in chondrocytes. One possible explanation is the presence of multiple cytokines in the body, and complex interactions, which may demand lower TNF α concentration. Additionally, although TNF α level is lower under physiological conditions, the duration of TNF α exposure *in vivo* is significantly longer than in this experimental setup, which may also influence the inflammatory response.

Under physiological conditions, the concentration of TNF α in synovial fluid is not constant and may vary according to disease severity (Bertuglia et al., 2016; Leung et al., 2017; Ren et al., 2018; Yang et al., 2021). In cases of cartilage trauma such as anterior cruciate ligament rupture or intra-articular fractures, TNF α level transiently rise before gradually decreasing during the subsequent osteoarthritis (Bertuglia et al., 2016; Pham et al., 2021; Khella et al., 2021). Experiment two was designed to better simulate this scenario and investigate the effects of dynamic TNF α concentration and varying culture durations.

In experiment two, the expression of all selected genes was significantly influenced by TNF α stimulation. Compared to the control group, 20 ng/mL TNF α induced a clear inflammatory response, and even after TNF α was removed, gene expression changes remained significant on Day 4. This also confirmed the concentration threshold identified in experiment one.

For most of the genes examined, continuous exposure to 20 ng/mL TNF α for four days produced the strongest and most evident pro-inflammatory effect, which remained significant on day 14. This trend was particularly evident in anabolic genes such as aggrecan and COMP, showing a concentration-dependent inflammatory response.

The results from experiment two revealed that certain genes, such as MMP3, MMP13, IL6, and COX2, exhibited a transient increase in expression following TNF α stimulation, which was subsequently followed by a decline. Although increasing TNF α concentration over the next 12 days led to an upregulation of their expression, the expression levels of some genes, such as MMP3 and IL6, remained lower on day 14 compared to day 4.

The possible explanation could be that the chondrocyte repair process was activated in response to TNF α stimulation or that negative feedback regulation occurred. Further studies are required to elucidate the molecular mechanisms underlying these responses.

This phenomenon may also explain why, in quantitative histological analysis, the expression levels of anabolic-related genes were lower in the 2-day TNF α stimulation group (group '20-0') compared to the control group, while the proteoglycans and collagens content in chondrocyte pellets were higher than in the control group (Fig. 22). Histological results also indicated that proteoglycan content was highly sensitive to TNF α concentration, providing insight into potential TNF α inhibitor treatments. This suggests that reducing TNF α levels after the initial inflammatory phase may help mitigate proteoglycan loss. Many studies have already demonstrated that TNF α inhibitors can slow OA progression (Catrina et al., 2002; Kawaguchi et al., 2009; Žigon-Branc et al., 2018; Zhang et al., 2012).

According to the results from experiment two, including gene expression and histological analysis, an initial stimulation with 20 ng/mL TNF α followed by subsequent exposure to 0.2 ng/mL TNF α was sufficient to replicate OA-like conditions, such as reduced anabolic activity, cartilage degradation, and persistent cartilage inflammation, albeit at a lower level compared to the early stages of the disease. As the disease progresses and inflammation persists, TNF α concentration increases, leading to further cartilage degradation (Kapoor et al., 2011). Similarly, in the experiment, when TNF α concentration exceeded 0.2 ng/mL, its detrimental effects on chondrocytes became concentration-dependent.

Besides, the duration of TNF α stimulation also influenced chondrocyte responses. For example, in experiment two, COMP and MMP3 were particularly sensitive to time, with significant differences observed between the results at day 14 and those at day 4.

The time course of gene expression in chondrocyte inflammation models has not been thoroughly investigated. In this study, overall, prolonged culture periods led to a partial

"recovery" in the expression of certain genes, particularly in groups exposed to lower TNF α concentrations (e.g., COMP and COX2). However, this recovery was not always statistically significant. This phenomenon may be attributed to changes in TNF α receptor expression after prolonged TNF α exposure, resulting in reduced sensitivity, where only high concentrations can exert significant effects on chondrocytes. However, the detailed underlying mechanisms require further investigation.

Additionally, experiment two demonstrated that even in the absence of TNF α stimulation, the expression levels of some genes, such as PRG4, COL2, COMP, and MMP13, fluctuated over time, though these differences were not always statistically significant. This may be related to chondrocyte physiological activity changes due to ECM turnover and maturation.

4.2 TNF α Effects on Chondrocyte 3D model

4.2.1 Anabolic Aspect

This study demonstrated that TNF α significantly reduced anabolic activity in chondrocytes, like collagen 2, collagen 1, aggrecan, COMP which are very important on ECM formation.

Collagen 2 is the most important and core collagen in hyaline cartilage (Athanasou et al., 2017; Deshmukh and Nimni, 1973). This study demonstrated that TNF α significantly reduced collagen synthesis. In experiment one, after 48 hours of stimulation, Collagen 2 showed a rapid decrease, and its expression level then reached a plateau. In other words, the negative effect of TNF α on collagen 2 expression is not concentration-dependent. In experiment two, TNF α also inhibited collagen II expression in a similar manner, particularly in the later stages of the experiment. This study successfully replicated the scenario observed in osteoarthritis, where collagen synthesis is reduced (Kleemann et al., 2005; Tschaikowsky et al., 2022). Seguin and Bernier et al. investigated the signaling pathways underlying inflammation by using 30 ng/mL TNF α to stimulate rat chondrocytes (monolayer), which suppressed collagen 2 synthesis (Séguin and Bernier, 2003). Klooster and Bernier et al. used a similar process and proved that TNF α inhibited collagen 2 expression at both the gene and protein levels (Klooster and Bernier, 2005). Mohanraj et al. demonstrated that using agarose as a scaffold for chondrocytes, TNF α inhibits collagen 2 synthesis and that chondrocytes derived from mesenchymal stem cells were more

susceptible to TNF α effects than primary chondrocytes from cartilage (Mohanraj et al., 2018). Those studies are consistent with this experiment.

Collagen 1 serves as a marker of dedifferentiation in expanded chondrocytes (Athanasios et al., 2017). It is well established that chondrocytes lose their unique phenotype during in vitro expansion (Athanasios et al., 2017; Benya et al., 1978). Numerous studies have explored strategies to maintain the phenotype, among which providing a 3D culture environment and increasing cell density have been shown to effectively mitigate dedifferentiation (Carballo et al., 2017; Watt, 1988). This study demonstrated that TNF α supplementation could inhibit collagen1 expression. Additionally, experimental results indicated that this inhibitory effect was TNF α concentration-dependent. However, the expression pattern of collagen 2 exhibited a distinct response. Notably, under inflammatory conditions, the extent of collagen 1 gene suppression was significantly lower than that of collagen 2. This phenomenon aligns with clinical observations, where repaired cartilage predominantly consists of fibrocartilage rich in collagen 1. Further investigations are required to elucidate the underlying mechanisms.

Aggrecan is a key component of the extracellular matrix and is responsible for retaining water molecules within the matrix to maintain its physical properties (Carballo et al., 2017; Kiani et al., 2002). Klooster et al. demonstrated that TNF α supplementation resulted in the decrease of aggrecan expression, which aligns with our experiment (Klooster and Bernier, 2005). Interestingly, we observed that during short-term (48-hour) stimulation, the effect of TNF- α on chondrocytes was not concentration-dependent. However, when the stimulation period was extended to two weeks, its detrimental effects became concentration-dependent. Stevens et al. found aggrecan degradation in bovine cartilage induced by TNF α could be enhanced by nitric oxide (Stevens et al., 2008). This study observed a similar trend in both experiment one and two, but further studies are needed to determine whether the same mechanism is responsible.

COMP is associated with cartilage matrix turnover, stabilizes the cartilage matrix by interacting with other collagens, and has been identified in a recent study as a potential marker for early OA (Boeth et al., 2017; Das et al., 2015; Hecht et al., 2005; Ossendorff et al., 2024b). This study demonstrated that TNF α stimulation negatively affected COMP expression in a concentration-dependent manner. Notably, short-term (48h) TNF α

exposure caused a rapid decrease in COMP expression. However, as the duration of stimulation increased, this effect gradually weakened, requiring higher concentrations of TNF α to replicate the reduction in COMP observed in OA conditions.

PRG4, or lubricin, is a proteoglycan mainly expressed in the synovial lining and articular cartilage (Alquraini et al., 2017; Iqbal et al., 2016). Studies show that PRG 4 plays an important anti-inflammatory role and reduces expression of proinflammatory cytokines (Alquraini et al., 2017; Iqbal et al., 2016). We observed that TNF α suppressed the expression of PRG4 on both day 4 and day 14. Interestingly, the expression level of PRG4 was higher on day 14 compared to day 4, and chondrocytes on day 14 exhibited greater sensitivity to TNF α -induced suppression than those on day 4. This variation may be attributed to differences in the maturity of the extracellular matrix over time. On day 4, the ECM produced by chondrocytes was likely less mature, resulting in a lower baseline expression of PRG4. By day 14, the ECM had likely become more developed, prompting chondrocytes to upregulate PRG4 expression as part of their role in advancing the matrix's structural and functional properties. The pronounced decline in PRG4 expression observed on day 14 may also be linked to this increased matrix maturity. The abundance of surface markers on more developed ECM might have heightened the chondrocytes' responsiveness to TNF α , thereby intensifying its suppressive effects on PRG4 expression.

4.2.2 Catabolic aspect

Matrix metalloproteinases (MMPs) are enzymes that degrade extracellular matrix components, including collagen, elastin, and proteoglycans (Hey and Linder, 2024; Laronha and Caldeira, 2020; Nicodemus and Bryant, 2010). It is widely accepted that proinflammatory cytokines play a central role in the upregulation of these catabolic factors (Blasioli and Kaplan, 2014; Malemud, 2017).

Results confirmed that TNF α supplementation led to increased levels of MMP3 and MMP13 at both day 4 and day 14 time points. This finding is consistent with the results of other studies (Bevill et al., 2014; Kunisch et al., 2016; Tilwani et al., 2017).

We also found that the effect of TNF α on these two genes differed. For MMP-3, the effect was concentration-dependent, while for MMP-13, expression levels reached saturation after 10 ng/mL. For chondrocytes from passage 3, the expression level of MMP-13 even decreased, returning to normal control levels. In experiment two, on day 4, chondrocytes

showed sensitivity to TNF α stimulation for both MMP-3 and MMP-13, after which a saturation point was reached. By day 14, the expression of MMP-3 was significantly lower than on day 4. This may be due to a decrease in the rate of matrix turnover over time. Additionally, on day 14, low concentrations of TNF α stimulation led to a decrease in the gene expression of MMP-3 and MMP-13, rather than an increase. This might be due to a negative feedback regulation resulting from the prior 20 ng/mL TNF α stimulation.

4.2.3 Inflammation

Interleukin-6 (IL-6) is a pro-inflammatory cytokine involved in chondrocyte inflammation and OA pathogenesis, promoting cartilage degradation and joint inflammation (Nishimoto and Kishimoto, 2006; Wojdasiewicz et al., 2014). This study showed that TNF α could induce IL-6 production at both the gene and protein levels. This finding is consistent with previous reports by Ossendorff et al., who demonstrated that TNF α supplementation resulted in catabolic stimulation with increased levels of NO and IL-6 (Ossendorff et al., 2024a). In experiment one, 10 ng/mL was identified as the threshold concentration for TNF α . As the concentration of TNF α increased further, the rate of IL-6 production gradually slowed down. However, in experiment two, the opposite trend was observed, where the rate of IL-6 production increased progressively with higher TNF α concentrations.

NFkb1, a key transcription factor, plays a significant role in chondrocyte inflammation and cartilage degradation (Roman-Blas and Jimenez, 2006). Activation of NFkb1 in chondrocytes leads to the expression of pro-inflammatory cytokines and matrix-degrading enzymes, contributing to the pathogenesis of OA (Jimi et al., 2019; Roman-Blas and Jimenez, 2006). This study showed that TNF α supplementation resulted in an increase in NFkb1 expression. And in experiment one, this increase appeared to be concentration-dependent. In contrast, in experiment two, although TNF α supplementation still led to an increase in NFkb1 expression, the final level of increase was not significantly different from the control group. Interestingly, in experiment two, lower concentrations of TNF α even resulted in a decrease in NFkb1 gene expression. This may be due to negative feedback regulation caused by the earlier use of 20 ng/mL TNF α .

COX2 and PTGES2 are both enzymes involved in the biosynthesis of prostaglandins, which are important mediators of inflammation and pain (Simon, 1999; Murakami et al., 2003). Experiment one demonstrated that COX2 expression was upregulated by TNF α ,

with a concentration threshold observed at 10 ng/mL. In experiment two, it was shown that a TNF α concentration of 20 ng/mL was required for continuous stimulation to induce a significant increase in COX2 expression. The possible reason may be due to a longer period (14 days) might lead to receptor downregulation. Cells may become less responsive to lower concentrations of TNF α due to the prolonged presence of the cytokine. Higher concentrations, such as 20 ng/mL, could overcome this desensitization and maintain a significant activation of signaling pathways leading to COX2 expression.

Sakai et al. reported that just 6 h incubation with TNF α markedly induced the expression of MMP-3 and COX-2 genes in human chondrocytes through NF κ b pathway (Sakai et al., 2001). This finding is consistent with our results. After 14 days of stimulation, a TNF α concentration of 20 ng/mL led to upregulation of PTGES2, and different passage had different thresholds (experiment one). For 14 days stimulation of TNF α , there was no significant difference in gene expression compared with control group. The possible reason could be post-transcriptional regulation or activated compensatory mechanisms that counteract the effects of TNF α . Further experiments are needed to clarify this.

This study also demonstrated that nitric oxide (NO) concentration was significantly higher after TNF α supplementation. Additionally, different cell passages exhibited varying sensitivity to TNF α . NO is controversial now, as it exhibits both pro-inflammatory and anti-inflammatory effects. (Sharma et al., 2007). Schuerwagh et al. investigated the effects of TNF α at concentrations ranging from 0.1 to 100 ng/mL on bovine chondrocytes in monolayer culture over 72 hours (Schuerwagh et al., 2003). They observed a concentration-dependent increase in NO production (Schuerwagh et al., 2003). Tilwani et al. demonstrated that TNF α stimulation led to increased production of NO, prostaglandin E2 (PGE2) (Tilwani et al., 2017). These findings are consistent with the results observed in this study, further reinforcing the understanding of TNF α 's role in driving inflammatory and degradative processes in chondrocytes.

In this study, the gene expression of caspase 3, a key marker of apoptosis, was significantly upregulated in TNF α -treated chondrocytes, with a threshold concentration of 10 ng/mL. Interestingly, passage 3 chondrocytes exhibited lower caspase 3 expression compared to chondrocytes from other passages. Despite these variations in gene expression, no significant differences in cell viability were found between the treatment

groups. By day 14, caspase 3 gene expression in the treated groups was not significantly different from the control group and was notably lower than at day 4.

4.2.4 Histology

Histological analysis revealed that the 3D pellets successfully mimicked the structure of hyaline cartilage, similar to the control group. TNF α was shown to influence matrix production in articular chondrocytes, as indicated by changes in both gene expression and protein levels. Higher concentrations of TNF α had a more significant impact on reducing matrix synthesis. Additionally, chondrocyte pellets exhibited a similar matrix distribution pattern to normal cartilage, with more collagen present on the surface and abundant proteoglycan within the pellet's interior. Ossendorff et al. successfully demonstrated the spatial distribution of collagen 1 and collagen 2 using immunohistochemistry (Ossendorff et al., 2023). Their findings align with the results observed in this study. Moreover, this experiment confirmed from a macroscopic perspective that TNF α does not need to maintain a consistently high concentration to induce and sustain an inflammatory response. Dynamic fluctuations in TNF α concentration can also maintain the inflammatory response, which is consistent with earlier gene expression analysis results. This mirrors the natural pathological process of cartilage inflammation induced by trauma.

4.3 Passage

Wang et al. reported differences in the functional phenotype of passaged and non-passaged chondrocytes in a comparative study of 3D chondrocyte culture (Wang et al., 2013). Dehne et al. observed that passaged osteoarthritic and healthy chondrocytes produced more collagen 1 in scaffolds than in pellet culture (Dehne et al., 2009). In this study, we found that the passage of chondrocytes significantly impacted gene expression. Notably, key inflammatory markers, such as IL-6, NFkb1, COX2, PTGES2, and NO, exhibited notable differences in both gene and protein levels across passages. This underscores the importance of specifying passage when comparing results between different experiments. Our results revealed that chondrocytes at passage 3 showed the greatest sensitivity to higher concentrations of TNF α (ranging from 10–100 ng/mL), especially regarding the anabolic marker collagen 2. In contrast, passage 2 chondrocytes were more responsive to TNF α in terms of the catabolic marker MMP13. At lower TNF α

concentrations (0.1–20 ng/mL), chondrocytes from passage 3 demonstrated the highest sensitivity, particularly in the expression of MMP3. However, for MMP13, passage 2 chondrocytes showed heightened sensitivity at concentrations between 10 and 20 ng/mL, which is consistent with previous studies (Ossendorff et al., 2024a). We also observed that gene expression of the inflammatory marker COX2 was lower in passage 3 compared to the other passages. At the protein level, IL-6 release from passage 3 chondrocyte spheroids was elevated when exposed to 10 ng/mL TNF α . These findings suggest that the variations observed between passages may be due to differences in NF κ b1 expression, potentially stemming from a reduced TNF α receptor affinity in passage 3. Interestingly, NO production was significantly higher in passage 1 chondrocytes compared to those from passages 2 and 3. Additionally, we found that gene expression of caspase 3, a marker of apoptosis, was notably upregulated in TNF α -treated chondrocytes at a concentration threshold of 10 ng/mL. However, passage 3 chondrocytes displayed lower caspase 3 expression compared to the other passages, suggesting a potential cell culture-adapted effect.

4.4 Clinical relevance

4.4.1 Cartilage Regenerative Therapy

Autologous chondrocyte implantation (ACI) is a promising treatment for cartilage defects larger than 2 cm² (Brittberg et al., 1994; Liu et al., 2021). It is usually indicated in cases of large cartilage defects or failed microfracture surgery (Guillén-García et al., 2023). The ACI procedure consists of two main steps: the first step is to obtain autologous healthy cartilage from the patient's own body (in a nonweight-bearing area) and to expand the chondrocytes *in vitro*. The second step is to implant the expanded chondrocytes into the defect site (Brittberg et al., 1994; Gikas et al., 2009). Niemeyer et al. reported that more than half of all ACI surgeries would implant chondrocytes into an inflammatory degraded environment (Niemeyer et al., 2010; Niemeyer et al., 2016). TNF α plays an important role in the inflammatory response of cartilage. Cartilage itself has a poor repair ability, and TNF α interferes with the synthesis of cartilage matrix and accelerates its decomposition, which not only leads to the degradation of the original cartilage, but also affects the newly implanted chondrocytes, thus affecting the results of the ACI surgery, and even leading to graft failure (Angele et al., 2015; Maldonado and Nam, 2013; Mabey and Honsawek,

2015). Therefore, some studies have been conducted to reduce the inflammation of cartilage tissue through the use of TNF α antagonists to mitigate the effects of ACI (Ossendorff et al., 2018).

In addition to autologous chondrocyte implantation (ACI), microfracture is a surgical technique commonly used to treat small cartilage defects (Steadman et al., 2002). This procedure involves drilling small holes into the articular surface to access the bone marrow cavity, thereby allowing bone marrow-derived mesenchymal stem cells (MSCs) to migrate into the defect area (Erggelet and Vavken, 2016; Steadman et al., 2002). However, it has been shown that inflammation in the focal region of the microfracture site can negatively affect the outcome of the procedure (Danilkowicz et al., 2021). Moreover, a study has demonstrated that TNF α can impair the quality of ECM produced by chondrocytes derived from mesenchymal stem cells (Mohanraj et al., 2018).

Therefore, there is an urgent need for drugs or therapies that can effectively control or slow down inflammation. To support this goal, the establishment of a standardized inflammatory model may serve as a novel platform that not only reduces the learning curve and experimental costs, but also harmonizes data across different studies and research groups, thereby accelerating the pace of drug development. Addressing this need was the primary objective of the present study.

4.4.2 Osteoarthritis

Since cartilage has a very limited capacity for self-repair and is unable to recover from accidental injuries such as intra-articular fractures, which ultimately lead to OA, and the current treatment for OA is mainly based on symptomatic therapy, and arthroplasty is usually the only option for end-stage OA, there is a strong need for an effective treatment for cartilage injuries (Dainese et al., 2022; Glyn-Jones et al., 2015; Liu et al., 2021; Man and Mologhianu, 2014; Siddiq et al., 2022). In addition to traumatic injuries, there are also ligament and meniscal injuries, which, although not immediately leading to cartilage injuries, can disrupt the normal structure of the joint. These injuries often result in increased cartilage wear, triggering inflammatory responses that ultimately lead to OA (Jacobs et al., 2020).

Lohmander et al. conducted a review indicating that a significant number of patients with an ACL tear will eventually develop OA (Lohmander et al., 2007). Ding et al. and Bigoni et al. reported that after meniscal injury, TNF α levels within the joint capsule remain elevated, and these levels are correlated with the severity of the disease (Bigoni et al., 2017; Ding et al., 2017a). Therefore, controlling TNF α levels and managing inflammation are crucial for improving the outcomes of cartilage repair treatments and preventing further joint damage in OA patients.

This study demonstrated that TNF α exerts concentration-dependent effects on chondrocytes, with a threshold concentration of 10 ng/mL required to induce a significant inflammatory response. Below this level, TNF α had minimal impact, whereas sustained inflammation could be maintained with a much lower concentration of 0.2 ng/mL after initial stimulation with 20 ng/mL TNF α . This experiment emphasizes the importance of controlling cytokine concentration levels in managing cartilage inflammation. The results also suggest that early inhibition of TNF α could be a viable strategy for slowing the progression of OA. In the analysis of genes involved in cartilage inflammation, a detailed examination revealed that these genes are closely associated with the level and duration of inflammation. This finding may enhance the effectiveness of drugs targeting specific genes related to inflammatory responses.

The mouse inflammation model established by Keffer et al. has been used in the development and testing of anti-TNF α drugs (Keffer et al., 1991). Liao et al. reported that a TNF α -induced inflammation model showed Haidalimumab effectively improved cartilage quality (Liao et al., 2021). The chondrocyte pellet model developed in this study could also be used for testing new drugs.

4.4.3 Rheumatoid arthritis

Unlike OA, rheumatoid arthritis (RA) is a chronic autoimmune disease characterized by persistent synovial inflammation, progressive cartilage and bone destruction (Alivernini et al., 2022; Harris, 1990). RA disproportionately affects women, and its high disability rate underscores the importance of early diagnosis and effective treatment (Alivernini et al., 2022; Harris, 1990; Koch et al., 1994). Extensive studies have demonstrated that the synovial fluid of RA patients contains elevated concentrations of pro-inflammatory cytokines such as TNF α , IL-1 β , and IL-6. Additionally, synovial membranes in RA joints

exhibit an increased capacity to synthesize TNF α , further amplifying the inflammatory response (Cheon et al., 2002; Feldmann et al., 1996).

Research by Elliott et al. has shown that TNF α blockade can significantly alleviate clinical symptoms in RA patients (Elliott et al., 1994). Other studies revealed that combined therapy involving anti-CD4 and anti-TNF α agents exerts a synergistic effect, leading to sustained improvements in cartilage integrity and joint function (Maini et al., 1998; Marinova-Mutafchieva et al., 2000; Williams et al., 1994; Williams et al., 2000). Although anti-TNF α biologics have improved quality of life and slowed disease progression in RA patients, their efficacy remains limited in some cases. Therefore, new therapeutic strategies are still urgently needed (Constantin et al., 2023; Feldmann, 2002; Smolen, 2009).

The study's findings on the concentration-dependent effects of TNF α on chondrocytes provided crucial insights into RA related cartilage damage. Based on our experimental data, a relatively high concentration of TNF α was required to trigger a marked inflammatory response in chondrocytes. Moreover, the extent of cartilage matrix degradation was found to be strongly correlated with TNF α levels. This observation is consistent with the pathological environment of RA, where elevated TNF α concentrations in the synovial fluid contribute significantly to progressive joint erosion (Altobelli et al., 2017; Fong et al., 1994; Neidel et al., 1995; Schlaak et al., 1996). This suggests that, in the context of RA, the therapeutic efficacy of anti-TNF α agents may depend not only on the timing of administration but also on the local concentration of TNF α at the time of treatment.

Furthermore, the inflammatory model established in this study provides a reproducible platform for simulating cartilage inflammation *in vitro*. This model could be readily integrated into the development of RA-related therapeutics. For example, Parmentier et al. utilized a similar inflammatory model to evaluate the efficacy of upadacitinib in the treatment of RA (Parmentier et al., 2018).

Overall, these findings underscore the therapeutic importance of TNF α inhibition in RA management. Additionally, the application of dynamic inflammatory model may enhance our mechanistic understanding of inflammation in RA and support the development of more targeted and effective drugs.

4.4.4 Origin of Chondrocyte

Obtaining sufficient cartilage tissue from small animals is challenging, often requiring multiple passages or expansions to obtain an adequate number of chondrocytes (Chu et al., 2010). The process of constructing these models is time-consuming and prone to higher variability, which leads to increased costs due to prolonged animal housing and the need for larger sample sizes to ensure statistical power in studies (Lampropoulou-Adamidou et al., 2014; Teeple et al., 2013; Vincent et al., 2012). Although human cartilage is larger, it is often more difficult to obtain because the majority of accessible cartilage is from end-stage OA patients and that unhealthy cartilage is likely to be exhausted and may not respond to external stimuli in the same way as healthy cartilage (Wang et al., 2024). This may cause significant diversity in the specific functional phenotype, making standardization of the inflammatory model challenging and adding difficulty to the interpretation of experimental results. Furthermore, factors such as chondrocyte vitality may differ between various sources, depending on patient-specific variables and comorbidities (Chu et al., 2010; Lampropoulou-Adamidou et al., 2014; McCoy, 2015; Kuyinu et al., 2016; Teeple et al., 2013; Wang et al., 2024). In such cases, using animal cartilage becomes a valuable alternative.

In addition to differences between species, there are also variations in methods for obtaining cartilage within the same species. Typically, cartilage cells are obtained by providing cartilage tissue, which is then enzymatically digested to release chondrocytes from the cartilage matrix (Yan et al., 2021). Alternatively, mesenchymal stem cells (MSCs), which are multipotent, can differentiate into chondrocytes under specific conditions. These stem cells can be isolated from various tissues, including bone marrow and adipose tissue, and can be induced to differentiate into chondrocytes under appropriate culture conditions (Boeuf and Richter, 2010; Chung and Burdick, 2008; Mohanraj et al., 2018). The main advantage of directly isolating chondrocytes is the preservation of their native phenotype and function. This method, used in this experiment, ensures that the cells retain high cartilage specificity, including the expression of key genes such as collagen 2 and aggrecan. These chondrocytes also maintain the ability to secrete cartilage matrix proteins, such as proteoglycans and glycosaminoglycans, which closely resemble native cartilage characteristics. Furthermore, Mohanraj et al. found that chondrocytes derived from MSCs

are more sensitive to inflammatory stimuli compared to primary chondrocytes (Mohanraj et al., 2018). However, this method limits the quantity of cells that can be obtained, especially obtaining sufficient quantities of chondrocytes directly from clinical or animal models is challenging due to the limited availability of cartilage tissue, which restricts the number of cells that can be harvested for research and therapeutic applications (Al-Masawa et al., 2020; Nordberg et al., 2022; Lampropoulou-Adamidou et al., 2014). Therefore, in some applications, inducing MSCs to differentiate into chondrocytes remains a valuable alternative (Lampropoulou-Adamidou et al., 2014; Schwarzl et al., 2023). Moreover, Voskamp et al. found that TNF α exposure during MSC expansion increased the chondrogenic differentiation capacity. Interestingly, pre-treatment with another pro-inflammatory cytokine, IL-1 β , did not enhance the chondrogenic potential of MSCs, suggesting that the pro-chondrogenic effect is specific to TNF α (Voskamp et al., 2020).

Additionally, the quality of cartilage can vary depending on the site from which it is collected (Akens and Hurtig, 2005). Bevil et al. found that chondrocytes from different regions of the porcine tibial plateau express mRNA for structural proteins at varying levels and respond to equivalent in vitro mechanical loading with distinct changes in gene expression (Bevill et al., 2014).

Compared to smaller animals, the bovine fetlock joint provides larger cartilage samples, which are essential for experiments requiring more tissue or for scaling up studies. Furthermore, cartilage from these joints can be easily sourced from slaughterhouses, ensuring a consistent and readily available supply without ethical concerns. Ossendorff et al. used chondrocytes from this joint to investigate how TNF α can negatively affect chondrogenesis under simulated autologous chondrocyte implantation (ACI) conditions (Ossendorff et al., 2018).

Many studies currently use human cells obtained incidentally during surgeries, without requiring additional surgical procedures (Cheung et al., 2013; Sato et al., 2011; Ridky et al., 2010; Dönges et al., 2024). These human cells can be utilized to construct organoids, which, when derived from specific patients, are valuable for testing novel therapeutic strategies, guiding the selection of personalized treatments, or generating replacement cells or tissues from the patient's own cells. Additionally, organoids can be analysed to evaluate their dynamic molecular responses to standardized cellular and molecular stimuli

(Dönges et al., 2024; Liu et al., 2004; Schwank et al., 2013). In this study, we successfully modelled 3D cartilage tissue using only bovine chondrocytes, which also serve as a form of organoid. This approach provides valuable experience for future efforts to construct organoids using human chondrocytes.

4.5 Limitations

Immunohistochemistry (IHC) is a useful technique for examining the distribution and content of various collagen fibers by using specific antibodies against different types of collagens (Horton et al., 1983). However, this technique was not used in our experiment.

This experiment did not involve mechanical stimulation of chondrocytes.

Our experiment only established an inflammation model as a platform, but no related drugs or treatment interventions were tested.

It is important to acknowledge that inflammation is a complex, chronic condition. A two-week incubation period remains insufficient to replicate the full progression of chondrocyte inflammation. Therefore, the experimental model cannot fully capture the pathophysiological processes involved. In addition, the inclusion of additional sampling time points during culture would allow for a more detailed assessment of chondrocyte development over time.

While the experiment successfully mimicked cartilage tissue formation and induced an inflammatory response, it is crucial to recognize that an *in vitro* model couldn't fully replicate the *in vivo* environment. Thus, *in vivo* studies remain necessary for a more comprehensive understanding of chondrocyte inflammation.

This experiment used only one cytokine to induce an inflammatory response, whereas in reality, multiple cytokines, chemokines, and other molecules exist in the joint, with complex regulatory relationships among them. Consequently, the findings may only reflect a partial view of chondrocyte inflammation. Therefore, the results of this experiment have certain limitations. Further studies are essential to explore the interactions between various cytokines involved in disease progression.

Moreover, bovine chondrocytes were used in this study. Given the potential species-specific differences, the results may not be entirely transferable to humans. Therefore,

additional validation using human chondrocytes is necessary to enhance the clinical relevance of the findings.

4.6 Conclusion and Future Perspective

This study provides a detailed analysis of the dynamics in multi-phase models, examining the effects of chondrocyte passage and TNF α concentration. In the TNF α chondrocyte inflammation model, TNF α has a negative effect on chondrocytes. There was a clear threshold for the induction of inflammation (10 ng/mL). The effects of TNF α were concentration-dependent for selected genes. Passage could also affect chondrocyte gene expression. In experiment two, TNF α required a concentration threshold of 0.2 ng/mL to induce a significant catabolic and inflammatory response. Future research could utilize this model to explore potential treatments and drugs for cartilage-related inflammatory diseases. Furthermore, developing models that incorporate mechanical stimuli could enhance the understanding of how mechanical forces influence chondrocyte behavior and inflammation, mimicking the complex environment of native cartilage. Imaging in 3D cultures is also a promising approach, as it enables continuous cellular and molecular analysis of tissue development over extended periods, from days to weeks. The use of human chondrocytes could further refine the model, offering more possibilities for understanding disease pathogenesis and developing therapeutic strategies.

5. Summary

Current inflammation models lack uniformity making comparisons difficult. This study aimed to develop a standardized chondrocyte inflammation model by evaluating the effects of TNF α concentration and cell passage, and to further refine it into a dynamic model that more accurately reflects pathological inflammatory conditions.

To establish a standardized chondrocyte inflammation model, bovine chondrocytes at different passages (P1-P3) were cultured as pellets and stimulated with TNF α at different concentrations (0.1 ng/mL to 100 ng/mL) for 48 h. To refine this into a dynamic model, passage 3 chondrocyte pellets were initially stimulated with 20 ng/mL TNF α for 48 h, followed by exposure to different concentrations of TNF α (0.2 ng/mL to 20 ng/mL) for the next 12 days. Gene expression (collagen 1, collagen 2, aggrecan, COMP, PRG4, MMP3, MMP13, IL-6, IL-8, NFkb1, COX2, PTGES2, Caspase-3) was determined. IL-6, MCP-1, nitric oxide and GAG released into the medium were measured. Histology staining was performed on pellets. Statistical analysis was performed using the independent t-test and Mann-Whitney U test. The statistical significance was defined as $p<0.05$.

This study showed that TNF α supplementation caused a decrease of anabolic gene expression in 48h pellet culture and this detrimental effect had a concentration threshold. Cell passage also affected the gene expression. Certain genes (COMP, collagen 1, MMP13, and Caspase-3) showed significant changes at lower concentrations of TNF α on day 4, but increasing the TNF α concentration did not elicit a stronger response. In contrast, other genes (MMP3, IL6, and COX2) exhibited different patterns. The responses of gene expression to the TNF α stimulation could be markedly different between day 4 and day 14. Protein analysis and histology results were in line with PCR results.

Overall, TNF α exhibited a detrimental effect on chondrocytes. A clear threshold for the induction of inflammation was identified at 10 ng/mL. Following inflammation induction, TNF α at 0.2 ng/mL could maintain the inflammation process. Cell passage had an effect on model construction. This dynamic model can reproduce key pathological features of OA and may serve as a platform for drug development and the testing of potential therapies.

6. List of figures

Figure 1: A schematic illustration of the the four zones of articular cartilage, the distribution and morphology of chondrocytes, and the arrangement of collagen.	8
Figure 2: A schematic illustration of the basic components of aggrecan monomer and how they connect to form a macromolecular structure. GAGs: glycosaminoglycans.	9
Figure 3: TNF α inflammation models categories (in vitro).	12
Figure 4: Summary pie chart showing the utilization of chondrocytes at different passages in inflammation model construction.	13
Figure 5: Flowchart of experiment one design.	19
Figure 6: Flowchart of experiment two design.	19
Figure 7: Schematic of TNF α concentration usage in experiment two.	20
Figure 8: Images of chondrocyte pellets in a 96-well V-bottom plate and a microscopic view of a representative chondrocyte spheroid (passage 3).	23
Figure 9: Anabolic gene expression of experiment one.	28
Figure 10: Catabolic gene expression of experiment one.	30
Figure 11: Inflammation gene expression of experiment one.	32
Figure 12: Apoptosis gene expression of experiment one.	34
Figure 13: Analysis of proteoglycan and inflammation related molecules.	35
Figure 14: Gene expression of anabolic markers in Experiment two.	37
Figure 15: Gene expression of catabolic markers in Experiment two.	40
Figure 16: Gene expression of inflammatory markers in Experiment two.	42
Figure 17: Gene expression of apoptosis marker in Experiment two..	44
Figure 18: The analysis of inflammation-related molecules released into the medium.	45
Figure 19: Safranin-O Fast Green stained slide of normal bovine cartilage.	48
Figure 20: Safranin-O Fast Green stained slides of chondrocyte pellets.	48

Figure 21: Example images illustrating the quantitative analysis of a chondrocyte pellet slide using Cell Sense software. 49

Figure 22: Quantitative analysis of pellet size, collagens, and proteoglycans content of the pellets. (a) Pellet size analysis. (b) Collagens content analysis1. 50

7. List of tables

Table 1: Details about the supplementation of different TNF α concentrations in Experiment one.	20
Table 2: Details about the supplementation of different TNF α concentrations in Experiment two.	21

8. References

Akagi M, Ueda A, Teramura T, Kanata S, Sawamura T, Hamanishi C. Oxidized LDL binding to LOX-1 enhances MCP-1 expression in cultured human articular chondrocytes. *Osteoarthritis Cartilage*. 2009; 17: 271–275

Akens MK, Hurtig MB. Influence of species and anatomical location on chondrocyte expansion. *BMC Musculoskelet Disord*. 2005; 6: 23

Alivernini S, Firestein GS, McInnes IB. The pathogenesis of rheumatoid arthritis. *Immunity*. 2022; 55: 2255–2270

Allen KD, Thoma LM, Golightly YM. Epidemiology of osteoarthritis. *Osteoarthritis Cartilage*. 2022; 30: 184–195

Al-Masawa M-E, Wan Kamarul Zaman, Wan Safwani, Chua K-H. Biosafety evaluation of culture-expanded human chondrocytes with growth factor cocktail: a preclinical study. *Sci Rep*. 2020; 10: 21583

Alquraini A, Jamal M, Zhang L, Schmidt T, Jay GD, Elsaid KA. The autocrine role of proteoglycan-4 (PRG4) in modulating osteoarthritic synoviocyte proliferation and expression of matrix degrading enzymes. *Arthritis Res Ther*. 2017; 19: 89

Altobelli E, Angeletti PM, Piccolo D, Angelis R de. Synovial Fluid and Serum Concentrations of Inflammatory Markers in Rheumatoid Arthritis, Psoriatic Arthritis and Osteoarthritis: A Systematic Review. *Curr Rheumatol Rev*. 2017; 13: 170–179

Angele P, Fritz J, Albrecht D, Koh J, Zellner J. Defect type, localization and marker gene expression determines early adverse events of matrix-associated autologous chondrocyte implantation. *Injury*. 2015; 46: S2-S9

Athanasiou KA, Darling EM, DuRaine GD, Hu JC, Reddi AH. Articular cartilage. Boca Raton, London, New York: CRC Press Taylor & Francis Group , 2017

Bartolotti I, Roseti L, Petretta M, Grigolo B, Desando G. A Roadmap of In Vitro Models in Osteoarthritis: A Focus on Their Biological Relevance in Regenerative Medicine. *J Clin Med.* 2021; 10

Bendele AM. Animal models of osteoarthritis. *J Musculoskelet Neuronal Interact.* 2001; 1: 363–376

Benya PD, Padilla SR, Nimni ME. Independent regulation of collagen types by chondrocytes during the loss of differentiated function in culture. *Cell.* 1978; 15: 1313–1321

Bertuglia A, Pagliara E, Grego E, Ricci A, Brkljaca-Bottegaro N. Pro-inflammatory cytokines and structural biomarkers are effective to categorize osteoarthritis phenotype and progression in Standardbred racehorses over five years of racing career. *BMC Vet Res.* 2016; 12: 246

Bevill SL, Boyer KA, Andriacchi TP. The regional sensitivity of chondrocyte gene expression to coactive mechanical load and exogenous TNF- α stimuli. *J Biomech Eng.* 2014; 136: 91005

Bigoni M, Turati M, Sacerdote P, ..., Torsello A. Characterization of synovial fluid cytokine profiles in chronic meniscal tear of the knee. *J. Orthop. Res.* 2017; 35: 340–346

Blasioli DJ, Kaplan DL. The Roles of Catabolic Factors in the Development of Osteoarthritis. *Tissue Eng Part B Rev.* 2014; 20: 355–363

Boeth H, MacMahon A, Poole AR, Buttgereit F, Önnerfjord P, Lorenzo P, Klint C, Pramhed A, Duda GN. Differences in biomarkers of cartilage matrix turnover and their changes over 2 years in adolescent and adult volleyball athletes. *J Exp Orthop.* 2017; 4: 7

Boeuf S, Richter W. Chondrogenesis of mesenchymal stem cells: role of tissue source and inducing factors. *Stem Cell Res Ther.* 2010; 1: 31

Brittberg M, Lindahl A, Nilsson A, Ohlsson C, Isaksson O, Peterson L. Treatment of deep cartilage defects in the knee with autologous chondrocyte transplantation. *N Engl J Med.* 1994; 331: 889–895

Buckwalter JA, Mankin HJ, Grodzinsky AJ. Articular cartilage and osteoarthritis. *Instr Course Lect.* 2005; 54: 465–480

Campbell KA, Minashima T, Zhang Y, Hadley S, Lee YJ, Giovinazzo J, Quirno M, Kirsch T. Annexin A6 interacts with p65 and stimulates NF- κ B activity and catabolic events in articular chondrocytes. *Arthritis Rheum.* 2013; 65: 3120–3129

Caramés B, López-Armada MJ, Cillero-Pastor B, Lires-Dean M, Vaamonde C, Galdo F, Blanco FJ. Differential effects of tumor necrosis factor-alpha and interleukin-1beta on cell death in human articular chondrocytes. *Osteoarthritis Cartilage.* 2008; 16: 715–722

Carballo CB, Nakagawa Y, Sekiya I, Rodeo SA. Basic Science of Articular Cartilage. *Clin Sports Med.* 2017; 36: 413–425

Caron MMJ, Emans PJ, Coolsen MME, Voss L, Surtel DAM, Cremers A, van Rhijn LW, Welting TJM. Redifferentiation of dedifferentiated human articular chondrocytes: comparison of 2D and 3D cultures. *Osteoarthritis Cartilage.* 2012; 20: 1170–1178

Catrina AI, Lampa J, Ernestam S, Klint E af, Bratt J, Klareskog L, Ulfgren A-K. Anti-tumour necrosis factor (TNF)-alpha therapy (etanercept) down-regulates serum matrix metalloproteinase (MMP)-3 and MMP-1 in rheumatoid arthritis. *Rheumatology (Oxford, England).* 2002; 41: 484–489

Chen T, Weng W, Liu Y, Aspera-Werz RH, Nüssler AK, Xu J. Update on Novel Non-Operative Treatment for Osteoarthritis: Current Status and Future Trends. *Front Pharmacol.* 2021; 12: 755230

Cheon H, Yu S-J, Yoo DH, Chae IJ, Song GG, Sohn J. Increased expression of pro-inflammatory cytokines and metalloproteinase-1 by TGF-beta1 in synovial fibroblasts from rheumatoid arthritis and normal individuals. *Clin Exp Immunol.* 2002; 127: 547–552

Cheung KJ, Gabrielson E, Werb Z, Ewald AJ. Collective invasion in breast cancer requires a conserved basal epithelial program. *Cell*. 2013; 155: 1639–1651

Choi M-C, Jo J, Park J, Kang HK, Park Y. NF-κB Signaling Pathways in Osteoarthritic Cartilage Destruction. *Cells*. 2019; 8: 734

Chu CR, Szczerdy M, Bruno S. Animal models for cartilage regeneration and repair. *Tissue Eng Part B Rev*. 2010; 16: 105–115

Chung C, Burdick JA. Engineering cartilage tissue. *Adv Drug Deliv Rev*. 2008; 60: 243–262

Constantin A, Caporali R, Edwards CJ, ..., Yoo DH. Efficacy of subcutaneous vs intravenous infliximab in rheumatoid arthritis: a post-hoc analysis of a randomized phase III trial. *Rheumatology (Oxford, England)*. 2023; 62: 2838–2844

Cope PJ, Ourradi K, Li Y, Sharif M. Models of osteoarthritis: the good, the bad and the promising. *Osteoarthritis Cartilage*. 2019; 27: 230–239

Cui J, Zhang J. Cartilage Oligomeric Matrix Protein, Diseases, and Therapeutic Opportunities. *Int J Mol Sci*. 2022; 23

Dainese P, Wyngaert KV, Mits S de, Wittoek R, van Ginckel A, Calders P. Association between knee inflammation and knee pain in patients with knee osteoarthritis: a systematic review. *Osteoarthritis Cartilage*. 2022; 30: 516–534

Danilkowicz RM, Allen NB, Grimm N, Nettles DL, Nunley JA, Easley ME, Adams SB. Histological and Inflammatory Cytokine Analysis of Osteochondral Lesions of the Talus After Failed Microfracture: Comparison With Fresh Allograft Controls. *Orthop J Sports Med*. 2021; 9: 23259671211040535

Darling EM, Athanasiou KA. Articular Cartilage Bioreactors and Bioprocesses. *Tissue Eng*. 2003; 9: 9–26

Das BR, Roy A, Khan FR. Cartilage oligomeric matrix protein in monitoring and prognostication of osteoarthritis and its utility in drug development. *Perspect Clin Res.* 2015; 6: 4–9

Dehne T, Karlsson C, Ringe J, Sittinger M, Lindahl A. Chondrogenic differentiation potential of osteoarthritic chondrocytes and their possible use in matrix-associated autologous chondrocyte transplantation. *Arthritis Res Ther.* 2009; 11: R133

Deshmukh K, Nimni ME. Isolation and characterization of cyanogen bromide peptides from the collagen of bovine articular cartilage. *Biochem J.* 1973; 133: 615–622

Di Chen, Shen J, Zhao W, Wang T, Han L, Hamilton JL, Im H-J. Osteoarthritis: toward a comprehensive understanding of pathological mechanism. *Bone Res.* 2017; 5: 16044

Ding J, Niu X, Su Y, Li X. Expression of synovial fluid biomarkers in patients with knee osteoarthritis and meniscus injury. *Exp Ther Med.* 2017a; 14: 1609–1613

Ding L, Buckwalter JA, Martin JA. DAMPs Synergize with Cytokines or Fibronectin Fragment on Inducing Chondrolysis but Lose Effect When Acting Alone. *Mediators Inflamm.* 2017b; 2017: 2642549

Djouad F, Rackwitz L, Song Y, Janjanin S, Tuan RS. ERK1/2 activation induced by inflammatory cytokines compromises effective host tissue integration of engineered cartilage. *Tissue Eng Part A.* 2009; 15: 2825–2835

Dönges L, Damle A, Mainardi A, Bock T, Schönenberger M, Martin I, Barbero A. Engineered human osteoarthritic cartilage organoids. *Biomaterials.* 2024; 308: 122549

Elliott MJ, Maini RN, Feldmann M, Long-Fox A, Charles P, Bijl H, Woody JN. Repeated therapy with monoclonal antibody to tumour necrosis factor alpha (cA2) in patients with rheumatoid arthritis. *Lancet.* 1994; 344: 1125–1127

Erggelet C, Vavken P. Microfracture for the treatment of cartilage defects in the knee joint – A golden standard? *J Clin Orthop Trauma.* 2016; 7: 145–152

Eschweiler J, Horn N, Rath B, Betsch M, Baroncini A, Tingart M, Migliorini F. The Biomechanics of Cartilage—An Overview. *Life (Basel)*. 2021; 11: 302

Feldmann M. Development of anti-TNF therapy for rheumatoid arthritis. *Nat Rev Immunol*. 2002; 2: 364–371

Feldmann M, Brennan FM, Maini RN. Role of cytokines in rheumatoid arthritis. *Annu Rev Immunol*. 1996; 14: 397–440

Fernandes JC, Martel-Pelletier J, Pelletier J-P. The role of cytokines in osteoarthritis pathophysiology. *Biorheology*. 2002; 39: 237–246

Fong KY, Boey ML, Koh WH, Feng PH. Cytokine concentrations in the synovial fluid and plasma of rheumatoid arthritis patients: correlation with bony erosions. *Clin Exp Rheumatol*. 1994; 12: 55–58

Freed LE, Vunjak-Novakovic G, Langer R. Cultivation of cell-polymer cartilage implants in bioreactors. *J Cell Biochem*. 1993; 51: 257–264

Gikas PD, Bayliss L, Bentley G, Briggs TWR. An overview of autologous chondrocyte implantation. *J Bone Joint Surg Br*. 2009; 91: 997–1006

Glyn-Jones S, Palmer AJR, Agricola R, Price AJ, Vincent TL, Weinans H, Carr AJ. Osteoarthritis. *Lancet*. 2015; 386: 376–387

Goldring MB, Otero M. Inflammation in osteoarthritis. *Curr Opin Rheumatol*. 2011; 23: 471–478

Grad S, Gogolewski S, Alini M, Wimmer MA. Effects of simple and complex motion patterns on gene expression of chondrocytes seeded in 3D scaffolds. *Tissue Eng*. 2006; 12: 3171–3179

Guillén-García P, Guillén-Vicente I, Rodríguez-Iñigo E, Guillén-Vicente M, Fernández-Jaén TF, Navarro R, Aboli L, Torres R, Abelow S, López-Alcorocho JM. Cartilage Defect Treatment Using High-Density Autologous Chondrocyte Implantation (HD-ACI). *Bioengineering (Basel)*. 2023; 10

Haleem-Smith H, Calderon R, Song Y, Tuan RS, Chen FH. Cartilage oligomeric matrix protein enhances matrix assembly during chondrogenesis of human mesenchymal stem cells. *J Cell Biochem*. 2012; 113: 1245–1252

Harris ED. Rheumatoid arthritis. Pathophysiology and implications for therapy. *N Engl J Med*. 1990; 322: 1277–1289

Hecht JT, Hayes E, Haynes R, Cole WG. COMP mutations, chondrocyte function and cartilage matrix. *Matrix Biol*. 2005; 23: 525–533

Hey S, Linder S. Matrix metalloproteinases at a glance. *J Cell Sci*. 2024; 137: jcs261898

Horton WA, Dwyer C, Goering R, Dean DC. Immunohistochemistry of types I and II collagen in undecalcified skeletal tissues. *J Histochem Cytochem*. 1983; 31: 417–425

Iqbal SM, Leonard C, Regmi SC, ..., Krawetz RJ. Lubricin/Proteoglycan 4 binds to and regulates the activity of Toll-Like Receptors In Vitro. *Sci Rep*. 2016; 6: 18910

Jacobs CA, Hunt ER, Conley CE-W, Johnson DL, Stone AV, Huebner JL, Kraus VB, Lattermann C. Dysregulated Inflammatory Response Related to Cartilage Degradation after ACL Injury. *Med Sci Sports Exerc*. 2020; 52: 535–541

Jimi E, Huang F, Nakatomi C. NF-κB Signaling Regulates Physiological and Pathological Chondrogenesis. *Int J Mol Sci*. 2019; 20: 6275

Johnson CI, Argyle DJ, Clements DN. In vitro models for the study of osteoarthritis. *Veterinary Journal (London, England: 1997)*. 2016; 209: 40–49

Kapoor M, Martel-Pelletier J, Lajeunesse D, Pelletier J-P, Fahmi H. Role of proinflammatory cytokines in the pathophysiology of osteoarthritis. *Nat Rev Rheumatol*. 2011; 7: 33–42

Kawaguchi A, Nakaya H, Okabe T, Tensho K, Nawata M, Eguchi Y, Imai Y, Takaoka K, Wakitani S. Blocking of tumor necrosis factor activity promotes natural repair of osteochondral defects in rabbit knee. *Acta Orthop*. 2009; 80: 606–611

Keffer J, Probert L, Cazlaris H, Georgopoulos S, Kaslaris E, Kioussis D, Kollias G. Transgenic mice expressing human tumour necrosis factor: a predictive genetic model of arthritis. *EMBO J.* 1991; 10: 4025–4031

Khella CM, Asgarian R, Horvath JM, Rolauffs B, Hart ML. An Evidence-Based Systematic Review of Human Knee Post-Traumatic Osteoarthritis (PTOA): Timeline of Clinical Presentation and Disease Markers, Comparison of Knee Joint PTOA Models and Early Disease Implications. *Int J Mol Sci.* 2021; 22

Kiani C, Chen L, Wu YJ, Yee AJ, Yang BB. Structure and function of aggrecan. *Cell Res.* 2002; 12: 19–32

Kleemann RU, Krock D, Cedraro A, Tuischer J, Duda GN. Altered cartilage mechanics and histology in knee osteoarthritis: relation to clinical assessment (ICRS Grade). *Osteoarthritis Cartilage.* 2005; 13: 958–963

Klooster AR, Bernier SM. Tumor necrosis factor alpha and epidermal growth factor act additively to inhibit matrix gene expression by chondrocyte. *Arthritis Res Ther.* 2005; 7: R127-38

Koch AE, Harlow LA, Haines GK, Amento EP, Unemori EN, Wong WL, Pope RM, Ferrara N. Vascular endothelial growth factor. A cytokine modulating endothelial function in rheumatoid arthritis. *J Immunol.* 1994; 152: 4149–4156

Koelling S, Clauditz TS, Kaste M, Miosge N. Cartilage oligomeric matrix protein is involved in human limb development and in the pathogenesis of osteoarthritis. *Arthritis Res Ther.* 2006; 8: R56

Kunisch E, Kinne RW, Alsalameh RJ, Alsalameh S. Pro-inflammatory IL-1beta and/or TNF-alpha up-regulate matrix metalloproteases-1 and -3 mRNA in chondrocyte subpopulations potentially pathogenic in osteoarthritis: in situ hybridization studies on a single cell level. *Int J Rheum Dis.* 2016; 19: 557–566

Kuyinu EL, Narayanan G, Nair LS, Laurencin CT. Animal models of osteoarthritis: classification, update, and measurement of outcomes. *J Orthop Surg Res.* 2016; 11: 19

Lampropoulou-Adamidou K, Lelovas P, Karadimas EV, Liakou C, Triantafillopoulos IK, Dontas I, Papaioannou NA. Useful animal models for the research of osteoarthritis. *Eur J Orthop Surg Traumatol.* 2014; 24: 263–271

Laronha H, Caldeira J. Structure and Function of Human Matrix Metalloproteinases. *Cells.* 2020; 9: 1076

Leung YY, Huebner JL, Haaland B, Wong SBS, Kraus VB. Synovial fluid pro-inflammatory profile differs according to the characteristics of knee pain. *Osteoarthritis Cartilage.* 2017; 25: 1420–1427

Lianxu C, Hongti J, Changlong Y. NF-kappaBp65-specific siRNA inhibits expression of genes of COX-2, NOS-2 and MMP-9 in rat IL-1beta-induced and TNF-alpha-induced chondrocytes. *Osteoarthritis Cartilage.* 2006; 14: 367–376

Liao X, Liang H, Pan J, Zhang Q, Niu J, Xue C, Ni J, Cui D. Preparation and characterization of a fully human monoclonal antibody specific for human tumor necrosis factor alpha. *Bioengineered.* 2021; 12: 10821–10834

Liu S, Deng Z, Chen K, Jian S, Zhou F, Yang Y, Fu Z, Xie H, Xiong J, Zhu W. Cartilage tissue engineering: From proinflammatory and anti-inflammatory cytokines to osteoarthritis treatments (Review). *Mol Med Rep.* 2022; 25

Liu Y, Shah KM, Luo J. Strategies for Articular Cartilage Repair and Regeneration. *Front Bioeng Biotechnol.* 2021; 9

Liu Y, Stein E, Oliver T, Li Y, Brunkin WJ, Koch M, Tessier-Lavigne M, Hogan BLM. Novel role for Netrins in regulating epithelial behavior during lung branching morphogenesis. *Curr Biol.* 2004; 14: 897–905

Loeser RF. Molecular mechanisms of cartilage destruction: mechanics, inflammatory mediators, and aging collide. *Arthritis Rheum.* 2006; 54: 1357–1360

Loeser RF, Goldring SR, Scanzello CR, Goldring MB. Osteoarthritis: a disease of the joint as an organ. *Arthritis Rheum.* 2012; 64: 1697–1707

Lohmander LS, Englund PM, Dahl LL, Roos EM. The Long-term Consequence of Anterior Cruciate Ligament and Meniscus Injuries: Osteoarthritis. *Am J Sports Med.* 2007; 35: 1756–1769

López-Armada MJ, Caramés B, Lires-Deán M, Cillero-Pastor B, Ruiz-Romero C, Galdo F, Blanco FJ. Cytokines, tumor necrosis factor-alpha and interleukin-1beta, differentially regulate apoptosis in osteoarthritis cultured human chondrocytes. *Osteoarthritis Cartilage.* 2006; 14: 660–669

Lotz MK, Otsuki S, Grogan SP, Sah R, Terkeltaub R, D'Lima D. CARTILAGE CELL CLUSTERS. *Arthritis Rheum.* 2010; 62: 2206–2218

Mabey T, Honsawek S. Cytokines as biochemical markers for knee osteoarthritis. *World J Orthop.* 2015; 6: 95–105

Maini RN, Breedveld FC, Kalden JR, ..., Feldmann M. Therapeutic efficacy of multiple intravenous infusions of anti-tumor necrosis factor ? monoclonal antibody combined with low-dose weekly methotrexate in rheumatoid arthritis. *Arthritis Rheum.* 1998; 41: 1552–1563

Maldonado M, Nam J. The Role of Changes in Extracellular Matrix of Cartilage in the Presence of Inflammation on the Pathology of Osteoarthritis. *Biomed Res Int.* 2013; 2013: 284873

Malemud CJ. Matrix Metalloproteinases and Synovial Joint Pathology. *Prog Mol Biol Transl Sci.* 2017; 148: 305–325

Malemud CJ, Sun Y, Pearlman E, Ginley NM, Awadallah A, Wisler BA, Dennis JE. Monosodium Urate and Tumor Necrosis Factor- α Increase Apoptosis in Human Chondrocyte Cultures. *Rheumatology (Sunnyvale).* 2012; 2: 113

Man GS, Mologhianu G. Osteoarthritis pathogenesis – a complex process that involves the entire joint. *J Med Life.* 2014; 7: 37–41

Marinova-Mutafchieva L, Williams RO, Mauri C, Mason LJ, Walmsley MJ, Taylor PC, Feldmann M, Maini RN. A comparative study into the mechanisms of action of anti-

tumor necrosis factor α , anti-CD4, and combined anti-tumor necrosis factor α /anti-CD4 treatment in early collagen-induced arthritis. *Arthritis Rheum.* 2000; 43: 638

Martin JA, Brown T, Heiner A, Buckwalter JA. Post-traumatic osteoarthritis: the role of accelerated chondrocyte senescence. *Biorheology.* 2004; 41: 479–491

McCoy AM. Animal Models of Osteoarthritis: Comparisons and Key Considerations. *Vet Pathol.* 2015; 52: 803–818

Mohanraj B, Huang AH, Yeger-McKeever MJ, Schmidt MJ, Dodge GR, Mauck RL. Chondrocyte and mesenchymal stem cell derived engineered cartilage exhibits differential sensitivity to pro-inflammatory cytokines. *J. Orthop. Res.* 2018; 36: 2901–2910

Murakami M, Nakashima K, Kamei D, Masuda S, Ishikawa Y, Ishii T, Ohmiya Y, Watanabe K, Kudo I. Cellular prostaglandin E2 production by membrane-bound prostaglandin E synthase-2 via both cyclooxygenases-1 and -2. *J Biol Chem.* 2003; 278: 37937–37947

Neidel J, Schulze M, Lindschau J. Association between degree of bone-erosion and synovial fluid-levels of tumor necrosis factor alpha in the knee-joints of patients with rheumatoid arthritis. *Inflamm Res.* 1995; 44: 217–221

Nicodemus GD, Bryant SJ. Mechanical loading regimes affect the anabolic and catabolic activities by chondrocytes encapsulated in PEG hydrogels. *Osteoarthritis Cartilage.* 2010; 18: 126–137

Niemeyer P, Feucht MJ, Fritz J, Albrecht D, Spahn G, Angele P. Cartilage repair surgery for full-thickness defects of the knee in Germany: indications and epidemiological data from the German Cartilage Registry (KnorpelRegister DGOU). *Arch Orthop Trauma Surg.* 2016; 136: 891–897

Niemeyer P, Salzmann G, Steinwachs M, Südkamp NP, Schmal H, Lenz P, Köstler W. Presence of subchondral bone marrow edema at the time of treatment represents a

negative prognostic factor for early outcome after autologous chondrocyte implantation. Arch Orthop Trauma Surg. 2010; 130: 977–983

Nishimoto N, Kishimoto T. Interleukin 6: from bench to bedside. Nat Clin Pract Rheumatol. 2006; 2: 619–626

Nordberg RC, Otarola GA, Wang D, Hu JC, Athanasiou KA. Navigating regulatory pathways for translation of biologic cartilage repair products. Sci Transl Med. 2022; 14: eabp8163

Oliveria SA, Felson DT, Reed JI, Cirillo PA, Walker AM. Incidence of symptomatic hand, hip, and knee osteoarthritis among patients in a health maintenance organization. Arthritis Rheum. 1995; 38: 1134–1141

Ossendorff R, Grad S, Stoddart MJ, Alini M, Schmal H, Südkamp N, Salzmann GM. Autologous Chondrocyte Implantation in Osteoarthritic Surroundings: TNF α and Its Inhibition by Adalimumab in a Knee-Specific Bioreactor. Am J Sports Med. 2018; 46: 431–440

Ossendorff R, Grad S, Tertel T, Wirtz DC, Giebel B, Börger V, Schildberg FA. Immunomodulatory potential of mesenchymal stromal cell-derived extracellular vesicles in chondrocyte inflammation. Front Immunol. 2023; 14: 1198198

Ossendorff R, Grede L, Scheidt S, Strauss AC, Burger C, Wirtz DC, Salzmann GM, Schildberg FA. Comparison of Minced Cartilage Implantation with Autologous Chondrocyte Transplantation in an In Vitro Inflammation Model. Cells. 2024a; 13: 546

Ossendorff R, Kurth S, Wang S, ..., Schildberg FA. Comparison of Concentration- and Homology-Dependent Effects of the Proinflammatory Cytokine Interleukin-1 β (IL-1 β) in a Bovine Chondrocyte Inflammation Model. Cells. 2024b; 14

Ossendorff R, Wang S, Kurth S, ..., Schildberg FA. TNF α -Induced Inflammation Model-Evaluation of Concentration and Passage-Dependent Effects on Bovine Chondrocytes. Int J Mol Sci. 2024c; 25

Parmentier JM, Voss J, Graff C, ..., Long AJ. In vitro and in vivo characterization of the JAK1 selectivity of upadacitinib (ABT-494). *BMC Rheumatol.* 2018; 2: 23

Pearson MJ, Herndler-Brandstetter D, Tariq MA, Nicholson TA, Philp AM, Smith HL, Davis ET, Jones SW, Lord JM. IL-6 secretion in osteoarthritis patients is mediated by chondrocyte-synovial fibroblast cross-talk and is enhanced by obesity. *Sci Rep.* 2017; 7: 3451

Pham TM, Erichsen JL, Kowal JM, Overgaard S, Schmal H. Elevation of Pro-Inflammatory Cytokine Levels Following Intra-Articular Fractures-A Systematic Review. *Cells.* 2021; 10

Porter AG, Jänicke RU. Emerging roles of caspase-3 in apoptosis. *Cell Death Differ.* 1999; 6: 99–104

Ren G, Lutz I, Railton P, Wiley JP, McAllister J, Powell J, Krawetz RJ. Serum and synovial fluid cytokine profiling in hip osteoarthritis: distinct from knee osteoarthritis and correlated with pain. *BMC Musculoskelet Disord.* 2018; 19: 39

Ridky TW, Chow JM, Wong DJ, Khavari PA. Invasive three-dimensional organotypic neoplasia from multiple normal human epithelia. *Nat Med.* 2010; 16: 1450–1455

Robinson WH, Lepus CM, Wang Q, Raghu H, Mao R, Lindstrom TM, Sokolove J. Low-grade inflammation as a key mediator of the pathogenesis of osteoarthritis. *Nat Rev Rheumatol.* 2016; 12: 580–592

Roman-Blas JA, Jimenez SA. NF- κ B as a potential therapeutic target in osteoarthritis and rheumatoid arthritis. *Osteoarthritis Cartilage.* 2006; 14: 839–848

Roughley PJ, Lee ER. Cartilage proteoglycans: structure and potential functions. *Microsc Res Tech.* 1994; 28: 385–397

Sakai T, Kambe F, Mitsuyama H, Ishiguro N, Kurokouchi K, Takigawa M, Iwata H, Seo H. Tumor Necrosis Factor α Induces Expression of Genes for Matrix Degradation in Human Chondrocyte-like HCS-2/8 Cells Through Activation of NF- κ B: Abrogation of the

Tumor Necrosis Factor α Effect by Proteasome Inhibitors. *J Bone Miner Res.* 2001; 16: 1272–1280

Sato T, Stange DE, Ferrante M, ..., Clevers H. Long-term expansion of epithelial organoids from human colon, adenoma, adenocarcinoma, and Barrett's epithelium. *Gastroenterology.* 2011; 141: 1762–1772

Schlaak JF, Pfers I, zum Meyer Büschenfelde KH, Märker-Hermann E. Different cytokine profiles in the synovial fluid of patients with osteoarthritis, rheumatoid arthritis and seronegative spondylarthropathies. *Clin Exp Rheumatol.* 1996; 14: 155–162

Schuerwagh AJ, Dombrecht EJ, Stevens WJ, van Offel JF, Bridts CH, Clerck LS de. Influence of pro-inflammatory (IL-1 α , IL-6, TNF- α , IFN- γ) and anti-inflammatory (IL-4) cytokines on chondrocyte function. *Osteoarthritis Cartilage.* 2003; 11: 681–687

Schwank G, Koo B-K, Sasselli V, ..., Clevers H. Functional repair of CFTR by CRISPR/Cas9 in intestinal stem cell organoids of cystic fibrosis patients. *Cell Stem Cell.* 2013; 13: 653–658

Schwarzl T, Keogh A, Shaw G, Krstic A, Clayton E, Higgins DG, Kolch W, Barry F. Transcriptional profiling of early differentiation of primary human mesenchymal stem cells into chondrocytes. *Sci Data.* 2023; 10: 758

Séguin CA, Bernier SM. TNFalpha suppresses link protein and type II collagen expression in chondrocytes: Role of MEK1/2 and NF-kappaB signaling pathways. *J Cell Physiol.* 2003; 197: 356–369

Sharma JN, Al-Omran A, Parvathy SS. Role of nitric oxide in inflammatory diseases. *Inflammopharmacology.* 2007; 15: 252–259

Siddiq MAB, Clegg D, Jansen TL, Rasker JJ. Emerging and New Treatment Options for Knee Osteoarthritis. *Curr Rheumatol Rev.* 2022; 18: 20–32

Simon LS. Role and regulation of cyclooxygenase-2 during inflammation. *Am J Med.* 1999; 106: 37S-42S

Smolen JS. Ten years of infliximab: insights from clinical trials in rheumatoid arthritis. *Eur J Pharmacol.* 2009; 623 Suppl 1: S5-9

Sophia Fox AJ, Bedi A, Rodeo SA. The Basic Science of Articular Cartilage: Structure, Composition, and Function. *Sports Health.* 2009; 1: 461–468

Steadman JR, Rodkey WG, Briggs KK. Microfracture to treat full-thickness chondral defects: surgical technique, rehabilitation, and outcomes. *J Knee Surg.* 2002; 15: 170–176

Stevens AL, Wheeler CA, Tannenbaum SR, Grodzinsky AJ. Nitric oxide enhances aggrecan degradation by aggrecanase in response to TNF-alpha but not IL-1beta treatment at a post-transcriptional level in bovine cartilage explants. *Osteoarthritis Cartilage.* 2008; 16: 489–497

Tang H, Panemangalore R, Yarde M, Zhang L, Cvijic ME. 384-Well Multiplexed Luminex Cytokine Assays for Lead Optimization. *J Biomol Screen.* 2016; 21: 548–555

Teeple E, Jay GD, Elsaid KA, Fleming BC. Animal models of osteoarthritis: challenges of model selection and analysis. *AAPS J.* 2013; 15: 438–446

Tilwani RK, Vessillier S, Pinguan-Murphy B, Lee DA, Bader DL, Chowdhury TT. Oxygen tension modulates the effects of TNF α in compressed chondrocytes. *Inflamm Res.* 2017; 66: 49–58

Tschaikowsky M, Brander S, Barth V, Thomann R, Rolauffs B, Balzer BN, Hugel T. The articular cartilage surface is impaired by a loss of thick collagen fibers and formation of type I collagen in early osteoarthritis. *Acta Biomater.* 2022; 146: 274–283

Ulivi V, Giannoni P, Gentili C, Cancedda R, Descalzi F. p38/NF- κ B-dependent expression of COX-2 during differentiation and inflammatory response of chondrocytes. *J Cell Biochem.* 2008; 104: 1393–1406

Vanlauwe J, Saris DBF, Victor J, Almqvist KF, Bellemans J, Luyten FP. Five-year outcome of characterized chondrocyte implantation versus microfracture for

symptomatic cartilage defects of the knee: early treatment matters. *Am J Sports Med.* 2011; 39: 2566–2574

Vincent TL, Williams RO, Maciewicz R, Silman A, Garside P. Mapping pathogenesis of arthritis through small animal models. *Rheumatology (Oxford, England).* 2012; 51: 1931–1941

Voskamp C, Koevoet, Wendy J. L. M., Somoza RA, Caplan AI, Lefebvre V, van Osch GJVM, Narcisi R. Enhanced Chondrogenic Capacity of Mesenchymal Stem Cells After TNF α Pre-treatment. *Front Bioeng Biotechnol.* 2020; 8: 658

Wang N, Grad S, Stoddart MJ, Niemeyer P, Südkamp NP, Pestka J, Alini M, Chen J, Salzmann GM. Bioreactor-Induced Chondrocyte Maturation Is Dependent on Cell Passage and Onset of Loading. *Cartilage.* 2013; 4: 165–176

Wang S, Kurth S, Burger C, Wirtz DC, Schildberg FA, Ossendorff R. TNF α -Related Chondrocyte Inflammation Models: A Systematic Review. *Int J Mol Sci.* 2024; 25: 10805

Watt FM. Effect of seeding density on stability of the differentiated phenotype of pig articular chondrocytes in culture. *J Cell Sci.* 1988; 89 (Pt 3): 373–378

Westacott CI, Barakat AF, Wood L, Perry MJ, Neison P, Bisbinas I, Armstrong L, Millar AB, Elson CJ. Tumor necrosis factor alpha can contribute to focal loss of cartilage in osteoarthritis. *Osteoarthritis Cartilage.* 2000; 8: 213–221

Williams RO, Marinova-Mutafchieva L, Feldmann M, Maini RN. Evaluation of TNF-alpha and IL-1 blockade in collagen-induced arthritis and comparison with combined anti-TNF-alpha/anti-CD4 therapy. *J Immunol.* 2000; 165: 7240–7245

Williams RO, Mason LJ, Feldmann M, Maini RN. Synergy between anti-CD4 and anti-tumor necrosis factor in the amelioration of established collagen-induced arthritis. *PNAS.* 1994; 91: 2762–2766

Wojdasiewicz P, Poniatowski ŁA, Szukiewicz D. The role of inflammatory and anti-inflammatory cytokines in the pathogenesis of osteoarthritis. *Mediators Inflamm.* 2014; 2014: 561459

Xiang X, Zhou Y, Sun H, Tan S, Lu Z, Huang L, Wang W. Ivabradine abrogates TNF- α -induced degradation of articular cartilage matrix. *Int Immunopharmacol*. 2019; 66: 347–353

Yan Y, Fu R, Liu C, Yang J, Li Q, Huang R-L. Sequential Enzymatic Digestion of Different Cartilage Tissues: A Rapid and High-Efficiency Protocol for Chondrocyte Isolation, and Its Application in Cartilage Tissue Engineering. *Cartilage*. 2021; 13: 1064S-1076S

Yang L, Chen Z, Guo H, ..., Jin Q. Extensive cytokine analysis in synovial fluid of osteoarthritis patients. *Cytokine*. 2021; 143: 155546

Zhang Q, Lv Hh, Chen A, Liu F, Wu X. Efficacy of infliximab in a rabbit model of osteoarthritis. *Connect Tissue Res*. 2012; 53: 355–358

Žigon-Branc S, Barlič A, Knežević M, Jeras M, Vunjak-Novakovic G. Testing the potency of anti-TNF- α and anti-IL-1 β drugs using spheroid cultures of human osteoarthritic chondrocytes and donor-matched chondrogenically differentiated mesenchymal stem cells. *Biotechnol Prog*. 2018; 34: 1045–1058

9. Statement on personal contributions

I declare that the conceptualization of this experimental dissertation originated from my supervisors, Prof. Frank A. Schildberg and Dr. Robert Ossendorff. The adaptation of already established methodology was carried out by myself under supervision of Prof. Schildberg and Dr. Ossendorff as well as after initial training by Sarah Kurth and Werner Masson. Data collection and data analysis were carried out by myself in close collaboration with Dr. Ossendorff and under the supervision of Prof. Schildberg. The writing of this dissertation was performed by myself under the supervision of Dr. Ossendorff and Prof. Schildberg. Additionally, DeepL and ChatGPT are used to identify and correct grammatical errors in this dissertation, thereby enhancing readability. Furthermore I confirm that I have reviewed the contents of this dissertation and take full responsibility for it. Some of the histological samples were generated in the histology platform of the ImmunoSensation² Cluster of Excellence and evaluated by myself, Prof. Schildberg, and Dr. Ossendorff. Damien Bertheloot performed the Luminex analyses. The statistical evaluation was carried out independently under the guidance of Prof. Schildberg and Dr. Ossendorff. The results were interpreted and discussed jointly by myself, Prof. Schildberg, and Dr. Ossendorff. In selected cases, datasets were discussed, analyzed, and placed in a clinical context with Sarah Kurth, PD Dr. Max Jaenisch, Dr. Elio Assaf, PD Dr. Andreas C. Strauss, Dr. Damien Bertheloot, PD Dr. Kristian Welle, Prof. Dr. Christof Burger and Prof. Dr. Dieter C. Wirtz.

I confirm that I have written this dissertation independently and have not used any sources or aids other than those mentioned.

10. Publications

Parts of this thesis were published in International Journal of Molecular Sciences (IJMS) with the title “TNF α -Induced Inflammation Model—Evaluation of Concentration and Passage-Dependent Effects on Bovine Chondrocytes”. In addition, the following papers were generated in the context of my dissertation and were subsequently published in the International Journal of Molecular Sciences (IJMS). The titles of these articles are: “Comparison of Concentration- and Homology-Dependent Effects of the Proinflammatory Cytokine Interleukin-1 β (IL-1 β) in a Bovine Chondrocyte Inflammation Model” and “TNF α -Related Chondrocyte Inflammation Models: A Systematic Review.”

Ossendorff R, Kurth S, Wang S, Jaenisch M, Assaf E, Scheidt S, Welle K, Burger C, Wirtz DC, Strauss AC, Schildberg FA. Comparison of Concentration- and Homology-Dependent Effects of the Proinflammatory Cytokine Interleukin-1 β (IL-1 β) in a Bovine Chondrocyte Inflammation Model. *Cells* 2024b; 14

<https://doi.org/10.3390/cells14010030>

Ossendorff R, Wang S, Kurth S, Jaenisch M, Assaf E, Strauss AC, Bertheloot D, Welle K, Burger C, Wirtz DC, Schildberg FA. TNF α -Induced Inflammation Model—Evaluation of Concentration and Passage-Dependent Effects on Bovine Chondrocytes. *International Journal of Molecular Sciences* 2024c; 25

<https://doi.org/10.3390/ijms25179136>

Wang S, Kurth S, Burger C, Wirtz DC, Schildberg FA, Ossendorff R. TNF α -Related Chondrocyte Inflammation Models: A Systematic Review. *International Journal of Molecular Sciences* 2024; 25: 10805

<https://doi.org/10.3390/ijms251910805>

11. Acknowledgments

I am grateful to my family for their support and to the members of the laboratory at the University of Bonn, Germany, for their support and understanding. Love you all.